Methodological Considerations Of Microdialysis Sampling For Determination Of Cerebral Basal Glucose Concentration In Extracellular Space of Freely Moving Rat

By

Vrushali Tembe

B.Sc. (Chemistry), University of Bombay, 1991

B.Sc. (Pharmaceutical Technology), University of Bombay, 1994

Submitted to the department of Chemistry and the Faculty of the Graduate School of the University of Kansas in partial fulfillment of the requirements for the degree of

Master of Science

Date Defended: February 18, 1998

We dance around in a ring and suppose,

But the Secret sits in the middle and knows

- Robert Frost

Acknowledgements

I wish to thank all those who, in one way or another, kept me on the road, without whom this work would be incomplete.

My advisor, Professor George S. Wilson for his continuous support, help and guidance throughout the completion of this work. Thank you for helping me build confidence in my scientific endeavors.

My committee, Professor Craig Lunte and Associate Professor Marylee Southard for their time and invaluable suggestions.

Special thanks to Drs. Yibai Hu, Alexander Faibushevich and Michael Gilinsky for the stimulating discussions and help.

My friends, Amrita and Deepak, for showing me that life away from home is not so bad after all.

My friends, Vishal, Joe, Amy, Stan, Sandra and Doug for wacky conversations. Special thanks to Joe and Amy for providing me with a comfortable abode during the last two months and Vishal for making my stay in Lawrence thoroughly enjoyable.

Members of the Wilson and Lunte group for keeping me sane during the lengthy animal experiments.

Mom, Dad, Manjiri and Rishikesh, for their love and understanding through all these years.

Finally, to my husband, Vinay, for being there when I needed most.

Table of Contents

Chapter 3: Quantitative Microdialysis Using Zero Net Flux Approach for the Determination of Basal Glucose Levels in the Brain of Freely Moving Rat

Chapter 4: Effects of Sodium Channel Blockers and Transport Inhibitors on Brain Glucose Levels and Development of a Mathematical Model to describe Extraction Efficiencies

Abstract

In the recent past there has been a controversy about the basal glucose levels in the brain of freely moving rats. Kinetic rate constants and transport parameters across the blood brain barrier and in the brain tissue obtained by using different techniques support a glucose value of 2-4 mM. One paper, using microdialysis in awake freely moving animals has reported a value of 0.47 mM which is several fold lower than the currently accepted value.

Microdialysis was used to determine the basal concentration of glucose in the striatum of freely moving rats. While there are several approaches to calibrating brain microdialysis probes that subsequently allow determination of the tissue concentration, the zero net flux method at a fixed perfusion flow rate, was used to make such determinations. The basal glucose concentrations were found to vary with variation in perfusion flow rate. The *in vivo* recoveries did not equal *in vivo* deliveries. To probe glucose dynamics in the brain, pharmacological agents such as glucose inhibitors and sodium channel blockers were used. In addition, to determine concentration profiles with the microdialysis probes inserted in tissue, a mathematical model was developed which took into account transport and metabolism of glucose.

In conclusion, the measured basal values of glucose depend on the perfusion flow rate when a zero net flux calibration is performed. The dialysate glucose levels are closely related to neuronal activity. When non linear kinetics dominate in the tissue, *in vivo* recoveries and deliveries are not equal, at least for endogenous glucose. Increases in *in vivo* delivery at higher flow rates could be due to factors such as saturable transport of glucose across the blood brain barrier and its subsequent uptake by neuronal cells.

List of Symbols

Symbols	Meaning
ϕ	Volume fraction
μ	Micro
R_{ecf}	Resistance of the tissue or extracellular space
R_m	Membrane resistance
R_d	Dialysate resistance
k	Rate constant
λ	Tortuosity
EE_r	Extraction efficiency in recovery mode
EE_d	Extraction efficiency in delivery mode
C_d	Concentration in dialysate
C_p	Concentration in perfusate
C_s	Concentration surrounding the probe
C_e	Concentration in the extracellular space/tissue
C_1	Concentration in the blood/plasma
C_i	Intracellular concentration
J	Net transport of glucose across BBB at steady state
V_{max}, K_m	Michaelis Menten constants
K	Partition coefficient
K_o	Average mass transfer coefficient
A	Area of semi-permeable membrane
Q	Perfusion flow rate
P	Permeability
S	Surface area of microdialysis probe
Γ	Concentration depth parameter
k_o, k_1	Modified Bessel functions
K_{m1}	Michaelis-Menten constant for GLUT1
k_e	Rate constant of disappearance of solute

K_{m2}	Michaelis-Menten constant for GLUT3
R	Radial distance of probe infusion in tissue
D_e	Diffusion coefficient of glucose in tissue
D	Diffusion coefficient of glucose in water
C_a	Concentration of glucose near probe surface

Chapter 1

Glucose Transport and Metabolism

1.1 Problem Statement

Two classes of substances exist within the mammalian brain: energetic and informational. Examples of the former are glucose, dissolved oxygen and carbon di oxide while the latter include excitatory amino acids, catecholamines and opiates. The simple ions Na^+ and Cl^- are generally associated with energetic processes while extracellular K^+ and Ca^{2+} tend to be informational in nature.

Glucose is one of the most significant energy substrates in the brain. The brain derives its energy from the oxidation of glucose. In this respect, cerebral metabolism is unique because very few tissues rely on carbohydrate for energy. Its metabolism accounts for nearly all of the brain's oxygen consumption.

Glucose has been implicated in diabetic hypoglycemia and major neurodegenerative disorders such as Alzheimer's and Huntington's disease. In hypoglycemia, it is well known that a fall in blood glucose content, if of sufficient degree, is rapidly followed by aberrations of cerebral function. In studies of insulin hypoglycemia in humans (Kety *et al.*, 1948), it was observed that when arterial glucose levels decreased, oxygen consumption decreased ensuing in deep coma. In such situations, there is no measurable uptake of glucose from the blood into the brain. In Alzheimer's disease, glucose metabolism is decreased and is associated with decreased amounts of glucose transporter (GLUT1) protein of the blood brain barrier (BBB) in the frontal cortex and hippocampus, the regions most affected (Kalaria and Harik, 1989). In Huntington's disease, there is neural degeneration of the basal ganglia. The transporter proteins are decreased, presumably because of the decline in glucose metabolism following destruction of neurons (Gamberinao and Brennan, 1994). Glucose transport also seems to be down regulated during cerebral ischemia (Suzuki *et al.,* 1994), while expression of GLUT1 mRNA is increased in glia and neurons. Brain tumors have been associated with increased glucose utilization.

To study glucose metabolism and utilization in the brain, it is extremely important to determine the basal glucose concentration in the extracellular environment. Surprisingly, the determination of basal glucose levels in the rat brain has been a subject of intense discussion for a long time now. It has turned out that it is not so easy to address this seemingly simple problem. The complexity arises for various reasons: the complex neurochemical environment of the brain, the numerous metabolic pathways in which glucose is implicated, the presence of the blood brain barrier that selectively allows passage of low molecular substances from the blood to the brain, the necessity to simplify the complex system by several assumptions, and the inherent limitations of the analytical methods that are used for such measurements.

Traditionally, it has been accepted that the basal glucose levels in the rat brain range from 2-4 mM. These values fit in very well with the kinetic models developed for glucose transport across the blood brain barrier and its subsequent utilization by the neuronal cells. In the recent past, a paper published by Fellows *et al.*, 1992, has reported a value of 0.47 +/- 0.03 mM. This number is several fold lower than the currently accepted value and, if found true, would cause a major revision of our current understanding of energy metabolism and utilization in the brain. This would cause serious spin-offs in pharmaceutical research for CNS drug discovery, basic neurochemical research and pharmacology.

Verification of the results of Fellows *et al.*, 1992, in the laboratory was one of the objectives of this work. Other issues addressed by this thesis are the role of the analytical methodology employed for such determinations, the use of pharmacological agents to obtain information about the behavior of such systems and development of a mathematical model for understanding of microdialysis sampling processes in the complex neural microenvironment.

This chapter deals with the transport of glucose from the blood into the brain and its subsequent metabolism/utilization. The role of the blood brain barrier (BBB), glucose utilization, glucose transporters, transport inhibitors and the use of neurotoxins to yield valuable information about these systems has been summarized. Several

analytical methods have been employed for the determination of basal glucose concentrations. A brief introduction to these methods and their inherent limitations has also been presented.

1.2 Major components of the brain microenvironment essential for glucose transport and metabolism.

The brain microenvironment is unique to the type of system being studied. The discussion of all the components of the brain microenvironment is beyond the scope of this thesis, but a brief discussion about processes essential for glucose metabolism and transport is necessary.

The major barrier to diffusion of substances from the blood to the brain is called the blood brain barrier (BBB). As discussed further in Section 1.2.1, this barrier consists of an endothelial cell layer covering the blood capillaries.

The entire brain is bathed in a fluid called the extracellular fluid whose composition has been repeatedly studied and its volume has been the subject of some controversy (Davson, 1967, van Harreveld and Malhotra, 1967). Extracellular fluid does not drip from the surface of a freshly isolated brain. Unlike the extracellular fluids of other organs, that of brain is not easily seen, being held in the gel of the matrix. Differences between the composition and potential of plasma and extracellular fluid are maintained by the vascular endothelium.

The different cell types of significance are the neuronal cells, and the glial cells consisting of astrocytes and oligodendrocytes. A striking feature of the neuronal cell is the ability to generate and to conduct pulses of electrical activity called action potentials. They are usually made up of the cell body called an "axon" which contains the nucleus and long protrusions called "dendrites". Information in the form of action potentials can thus, travel long distances through the dendrites. Axons and dendrites emerging from neurons intercommunicate by means of specialized junctional complexes known as synapses. Neurons present before a synapse are called

presynaptic neurons and those present after the synapse are called postsynaptic neurons.

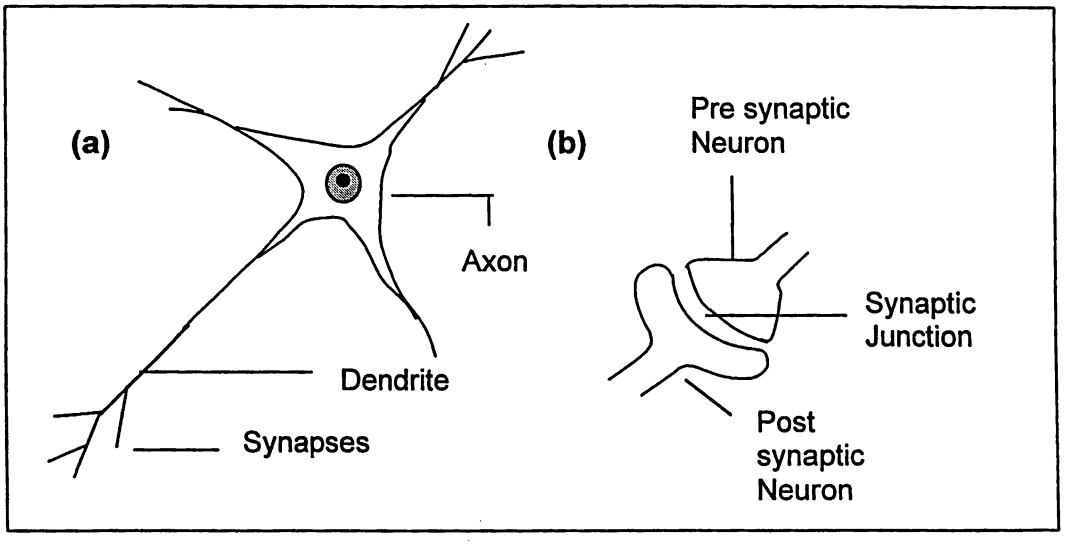

Figure 1.1 The (a) neuronal cell and the (b) synapse

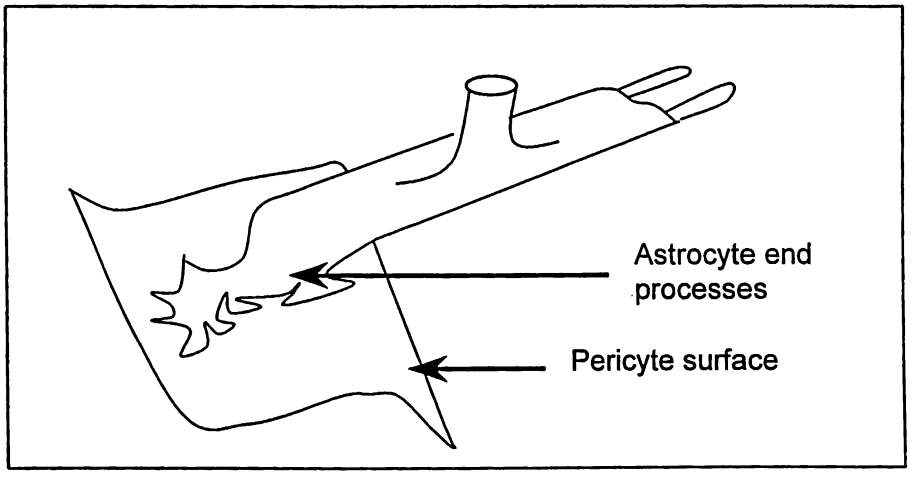

Figure 1.2 Astrocyte end feet processes on the pericyte surface

Glial cells do not have the ability to conduct electrical impulses. Surrounding the capillary endothelial cell is a collagen-containing extracellular matrix, also called the extracellular space. The outer surface of the endothelial cells is covered by the basal lumina. Cells called pericytes, which play a role in differentiation during growth, cover this surface. Foot processes from astrocytes cover the pericytes. As their name

suggests, astrocytes have a star-like appearance, with numerous long arms radiating out from a central cell body. Astrocytes do not line an obvious surface: lacking a clear luminal surface they are bathed by the extracellular fluid of the brain (Watson, 1980). Oligodendrocytes also have a central cell body, with radial arms that tend to be shorter than the astrocytes. They play a role in the functioning of neurons by forming a myelin sheath around axons.

The function of glial cells is speculated to provide structural support and segregation for neurons i.e. function as electrical insulators. They are also thought to play a role in supplying metabolic components but this role is largely unconfirmed (Forsyth, 1996).

1.2.1 BBB and glucose transport via GLUT1

The first study revealing the presence of a diffusion barrier between blood and brain was reported by Ehrlich, (Ehrlich, 1885) nearly a century ago. Ehrlich injected vital dyes systematically into laboratory animals and noted that virtually all organs except the central nervous (CNS) took up the dye. It was recognized by 1930's that brain capillaries were unlike the microvessels in any other organs (Schaltenbrand *et al.*, 1928). First, continuous tight junctions are present between the endothelial cells that prevent trans-capillary movement of polar molecules varying in size from proteins to ions. Second, there are no detectable transendothelial pathways (Takata *et al.*, 1990b). In the past ten years, it has been generally accepted that there are two discrete barrier systems: the BBB and the blood CSF barrier (Pardridge, 1983). The BBB is found at the vast majority i.e. 99% of brain capillaries and the blood CSF barrier is found at the small number of capillaries perfusing the circumventricular organs.

The BBB has been extensively studied (Fishman, 1980, Betz and Glodstein, 1986, Cserr, 1986, Strand, 1988, Dermietzel and Krause, 1991). Crone (1965), using intracarotid injection of labeled glucose in dogs proposed a possible mechanism involving endothelial cells in the brain capillaries for the transport of glucose across the blood brain barrier. A carrier mediated, facilitated passage of glucose across the BBB was observed. Dick *et al.*, 1984 later demonstrated the presence of a 53 kDa

glucose transporter designated as the erythrocyte glucose transporter (GLUT1) through antibody labeling studies.

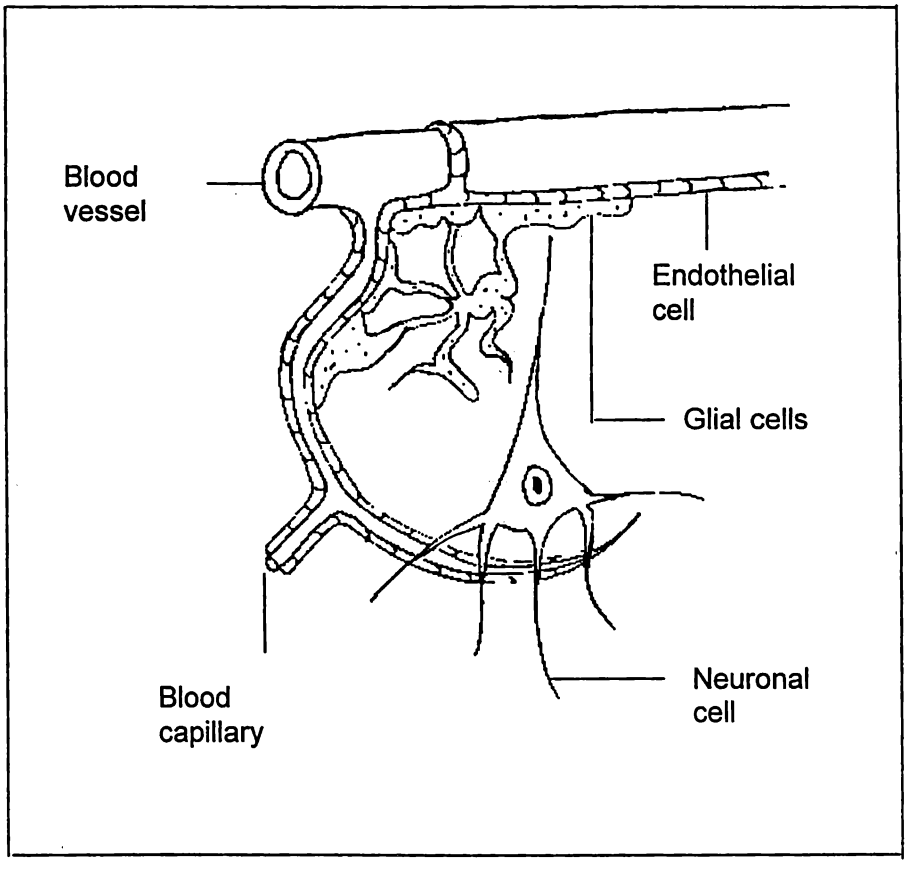

Figure 1.3 Blood brain barrier in the brain microenvironment on a blood capillary. The endothelium covers the blood capillary/vessel and forms an impermeable barrier.

This observation was later confirmed by immunoblotting studies (Kalaria et al., 1988, Gerhart *et al.*, 1989, Pardridge *et al.*, 1990, Takata *et al.*, 1990), Northern blotting (Flier et al., 1987, Boado and Pardridge, 1990) and cytochalasin B (glucose transport inhibitor) binding studies (Kalaria *et al.*, 1988). These studies also established that GLUT1 is the principal glucose transporter isoform mediating glucose transport across the BBB. See Figure 1.4. GLUT1 is localized at both the luminal and contraluminal plasma membranes asymmetrically and is thought to provide the molecular basis for the trans-endothelial transfer of glucose in the BBB. The

asymmetrical distribution of GLUT1 is thought to create a faster rate of glucose transport across the contraluminal membrane compared with that of the luminal membrane, thereby maximizing transfer across the barrier.

Additionally, Figure 1.4 represents the expression of GLUT1 in astrocytes, (Devasker *et al.*, 1991, Lee and Bondy, 1993, Morgello *et al.*, 1995), epithelial cells of the choroid plexus (Takata *et al.*, 1990b, Farrell *et al.*, 1992a) which constitutes the blood-CSF barrier. Whereas GLUT1 of microvessels showed a molecular mass of 54 or 55 kDa, that of astrocytes and choroid plexus showed a molecular mass of 42-45 kDa (Maher *et al.*, 1993). The apparent difference is caused by differential N-linked glycosylation (Kumagai *et al.*, 1994a), the functional significance of which remains to be clarified.

Much less is known about the mechanism of transport regulation for GLUT1. GLUT1 mediated glucose uptake is stimulated by cytokines and oncogenes of interleukin-3 (IL3) and is therefore thought to represent an important regulatory point (Baldwin *et al.*, 1995). Signal transduction mechanisms are not fully understood.

1.2.2 Glucose transporter located on the neuronal cells (GLUT3)

While there are 5 isoforms of the GLUT superfamily, the relevant isoform, GLUT3 has been detected as a protein of 45-50 kDa. Three studies to date have reported GLUT3 protein detection by immunocytochemistry. It was shown to be specifically localized in neurons in the rodent brain (Nagamatsu *et al.*, 1992, 1993a) by Northern blotting, *in situ* hybridization, immunoblotting and immunohistochemical staining (Kayano *et al.*, 1988, Bell *et al.*, 1990) and not in the blood vessels.

GLUT3 is found in the nerve fibers rather than in the cell bodies (Nagamatsu *et al.*, 1992). See Figure 1.4. In contrast, GLUT3 was also reported to be in both the cell body and the nerve fibers (van Bueren *et al.*, 1993). Furthermore, in contrast to immunoblot analysis where GLUT3 is not detectable in white matter regions (Maher *et al.*, 1993, Brant *et al.*, 1993), GLUT3 was detected in white matter regions by

immunohistochemistry (Nagamatsu *et al.*, 1993). Clearly, confirmation of the immunohistochemical studies is required for precise anatomical and cellular localization of GLUT3 protein *in situ*.

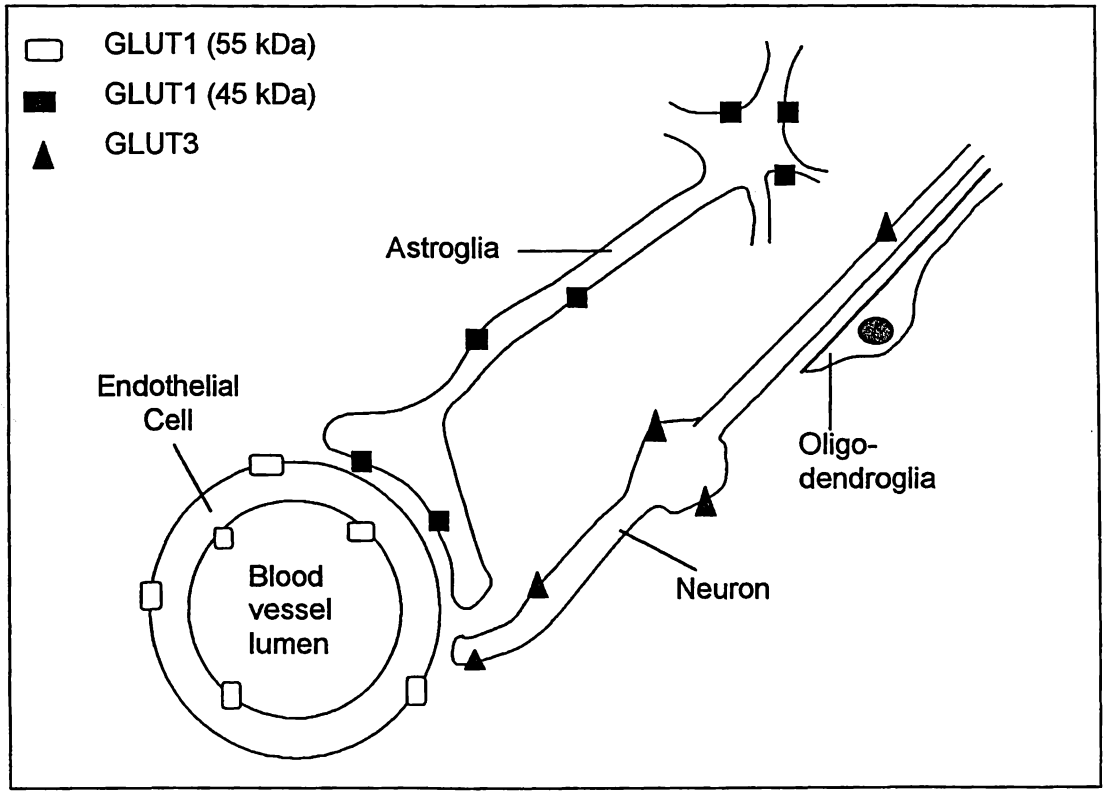

Figure 1.4 Schematic representation of cellular localization of glucose transporters

Table 1.1 GLUT[¶] family of transporters in the brain

Transporter	Site	MW	IC_{50} for Cytochalasin B (μM)	# amino acids
GLUT1	BBB, erythrocytes	54-55 kDa	0.1	492
GLUT3	Neuronal cells	55 kDa	0.1-2	493

[¶] Takata *et* al., 1997

1.2.3 Phosphorylation - Enzyme Hexokinase

The predominant route of glucose metabolism is aerobic oxidation via glycolysis and the tricarboxylic acid (TCA) cycle. The first step in glycolysis is the conversion of glucose to glucose-6-phosphate (G6P), in the presence of enzyme hexokinase (EC 2.7.1.1) and Mg^{2+} and ATP (Lowry *et al.*, 1964). This step is referred to as the phosphorylation reaction.

Hexokinase exists in mitochondrial and cytoplasmic forms. A relatively high amount of mitochondrial hexokinase is found in nerve endings (Kant *et al.*, 1973), which are neuronal elements. Lusk *et al.*, 1980 have reported that over 80% of the total hexokinase exists in the cytoplasmic form, using cultured astrocytes from rat brain. Therefore, cytoplasmic hexokinase is located in the glia, whereas mitochondrial hexokinase is located in the neuron. The molecular weight of brain mitochondrial hexokinase is approximately 98,000 and the enzyme consists of a single polypeptide chain. The enzyme has a single binding site for glucose, for G6P and for phosphate. The K_m for hexokinase is 0.04-0.05 mM. Its kinetics is believed to follow random addition mechanism. It is inhibited by the product G6P. Inhibition of the enzyme by G6P is believed to play a central role in regulation of its activity (Lowry *et al.*, 1964, Colowick, 1973, Ellison *et al.*, 1975).

Table 1.2 Kinetic transport parameters for the important transporters and enzyme

Transporter / Enzyme	K_m (mM)	V_m (μmol/100g min)	Type of transport
GLUT1	20.9+/-2.9[b] 6.9+/-1.5[c] 11.0+/-1.4[d]	0.4[c] 1.42+/-0.14 μmol/g.min[d]	Passive, Facilitated, Saturable
GLUT3	10.6+/-1.3[b] 1.4+/-0.06[c]	-	Passive, Facilitated, Saturable
Hexokinase	0.04-0.05[a]	0.07[a]	Saturable

[a] Lund Anderson, 1979, [b]Using 3-O-methyl glucose, Takata, *et al.*, 1997, [c]Using 2-deoxyglucose, Gould and Holman, 1993, [d]Pardridge *et al.*, 1975

1.3 Use of pharmacological agents that affect glucose transport

One effective method of studying glucose transport is by the use of pharmacological agents. Such agents are either inhibitors or energy decouplers like phloretin or cytochalasin B or compounds that affect glucose uptake by the neuronal cells by blocking the sodium channel. Some of the properties of these agents are discussed in this section.

1.3.1 Glucose Transport Inhibitors - Phloretin and cytochalasin B

The influence of drugs is a major mechanism by which BBB glucose transport is altered. Phloretin (K_i = 16 μM) inhibits BBB glucose transport (Betz *et al.*, 1975, Fritschka *et al.*, 1979). Phloretin inhibits glucose as well as lactate transport (Pardridge *et al.*, 1975). It is a phenol and binds in a competitive and irreversible manner (LeFevre, 1954). The presence of a phenol binding site in the GLUT1 transporter has been speculated (Betz *et al.*, 1975). This phenol is highly soluble in ethanol but practically insoluble in water. This inhibitor has been used in cell preparations and tissue slices but not in intact freely moving animals.

Cytochalasin B (K_i = 7 μM), is a more potent inhibitor of glucose transport than phloretin and effective at low concentrations (Drewes *et al.*, 1977). It is a mold metabolite and soluble in DMSO and DMF and insoluble in water. For a complete review refer to Plageman and Richey, 1974. In contrast to phloretin, this inhibitor behaves in a non competitive, reversible manner. In one study cytochalasin B was used to differentiate between GLUT1 of brain and muscle type glucose transporters by determining the binding affinities (Hellwig and Joost, 1991).

1.3.2 Use of sodium channel blockers -TTX

Tetrodotoxin (TTX) is one of the most poisonous nonprotein substances known. It is a puffer fish poison and acts in a specific manner on one of the most fundamental of all physiological processes: the generation of bioelectricity (Furman, 1986). At rest, the entire cytoplasm in excitable neuronal cells is electrically more negative than the external bathing fluid by 30 to 100 mV. All of this potential drop occurs across extremely thin external cell membrane. In the normal state, the extracellular concentration of sodium is 145 mM and its intracellular concentration is 12 mM. This difference in concentration helps to maintain a membrane potential. This resting membrane potential is -70 mV (by convention, the membrane potential is always reported in terms of "inside" minus "outside", and hence the negative sign). When energy is required by the neuronal cell i.e. when glucose is utilized, extracellular sodium enters the cell by means of voltage gated sodium channels. This causes the membrane to depolarize (Siegel *et al.,* 1994). Depolarization is any effect that causes the resting membrane potential to become more positive.

This fundamental concept can be used to probe glucose behavior. When TTX is introduced into the brain, it blocks the voltage gated sodium channel. This alters normal function. First, extracellular sodium cannot enter the cell when energy is required and the membrane cannot be depolarized, and second, glucose is not utilized. TTX has been used in Chapter 4 to selectively perturb the energy utilization.

1.4 Glucose Transport and Metabolism: Traditional view

Normally, the brain utilizes glucose as its key fuel. In the adult human brain, glucose metabolism is about 30 μmol/100 g per min: the oxygen consumption is approximately equivalent to the glucose utilization (Sokoloff, 1973). The adult subject uses about 110g glucose each day for brain metabolism. In the resting state, approximately 20% of the whole-body glucose utilization provides fuel for the substantial energy requirements of the brain. The brain is unable to metabolize fat, but can utilize ketone bodies during a prolonged fast and in young animals and pre-weaning (Sokoloff, 1973).

The brain is relatively impermeable to the penetration of polar molecules, such as glucose, but the circulation and carrier-mediated transport of glucose (stereospecific, saturable and insulin independent: Pardridge and Oldendorf, 1975, Lund-Anderson, 1979) across the blood brain barrier has long been recognized. In general, there are two substrate-limited pathways of brain metabolism wherein BBB transport is either rate limiting or rate affecting. 1) If the intracellular substrate concentration is so low that the apparent volume of distribution of the substrate (i.e. the brain to plasma ratio) is less than the brain extracellular space (e.g. ~0.15 ml/g), then the transport step is rate limiting. 2) When the brain to plasma ratio is >0.15 ml/g, BBB transport is not rate limiting. In this situation an intracellular enzyme is rate limiting.

A simplified model for description of glucose transport between the blood and the brain under steady state conditions has been presented (Lund-Anderson, 1979) in Figure 1.5. This model has generally been accepted by most researchers, even to this day. Some recent findings have challenged this view and these will be discussed in Section 1.5 of this chapter. The model is composed of a simple, series-coupled three-compartment system. **A** represents the blood circulation, separated from **B**, which represents the brain's aqueous phase (intra- and extracellular space), by the blood brain barrier (BBB). **C** represents the metabolic pool.

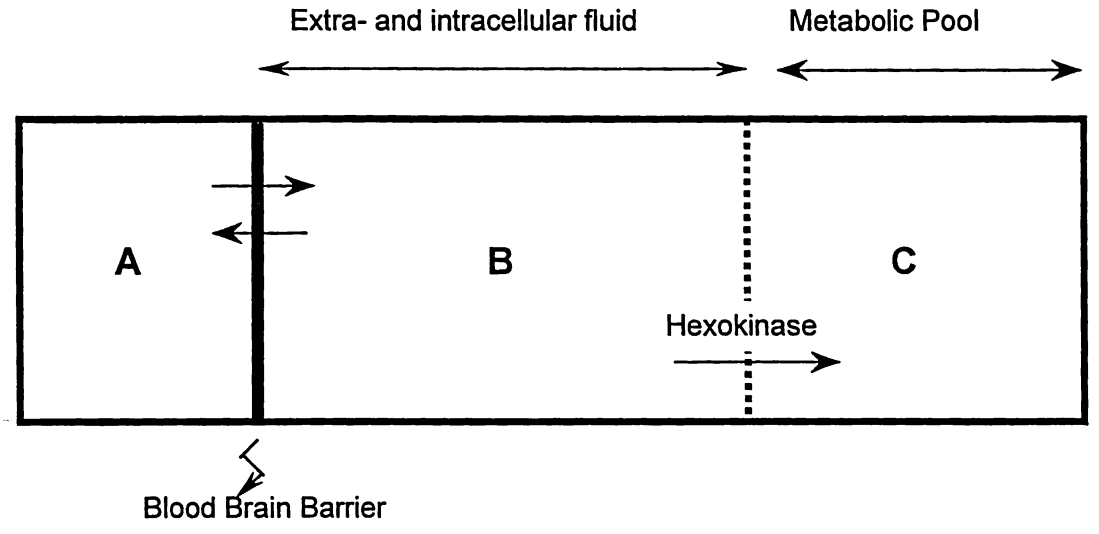

Figure 1.5 Schematic representation of model describing the transport of glucose from blood to brain.

The blood circulation is perceived as a single well-mixed compartment, without regard to changes in glucose and tracer substance concentrations that take place during passage through the capillaries. This is allowable when the transport across the barrier is estimated over longer time intervals.

A single membrane represents the BBB, with a transport mechanism that obeys simple Michaelis-Menten kinetics. This is a considerable simplification, but permissible in terms of a long duration analysis in the steady state. A single well-mixed compartment represents the extra- and intracellular aqueous phases. This is justified by the fact that an inter-capillary distance of 30-40 μm results in no significant concentration in the extracellular space (Diemer, 1968). The size of this space is 77% of the brain's volume. Glucose metabolism, represented by the phosphorylation reaction, acts as a single enzymatic reaction placed in series with the cerebral aqueous space. In this manner, metabolism's sink action in the system is portrayed. Significant regional differences in phosphorylation have been detected (Sokoloff *et al.*, 1977). Glycolysis in brain is normally limited by hexokinase, which has a low K_m (~40 μM) for glucose (Lund-Anderson, 1979). The normal brain glucose concentration is 2-3 μmol/g or 3-4 mM, which greatly exceeds the hexokinase K_m.

Therefore, brain glycolysis is substrate independent under normal conditions. Brain glycolysis, phosphorylation limited in the normal state, can become transport limited in pathological conditions. Betz *et al.*, 1974 , used perfused dog brains and measured unidirectional influx with the indicator dilution technique and net glucose utilization with arteriovenous sampling to show an excellent experimental switch from phosphorylation limitation to transport limitation. These pathological states could be due to hypoglycemia wherein intracellular brain glucose is near zero when plasma glucose level drops (Lewis *et al.*, 1974) or conditions such as seizures, anoxia or salicylate intoxication (Chapman *et al.*, 1977, Kintner *et al.*, 1980, Thurston *et al.*, 1970) which cause an increase in brain glycolysis.

According to this model, the relationship between transport and phosphorylation rates *in vivo* can be estimated from the related values of the extra- and intracellular glucose concentrations. This relationship can be analyzed according to the following rationale, Michaelis-Menten kinetics corresponding to equation 1.1,

$$J = \frac{V_{max}}{C_1 + K_t} C_1 - \frac{V_{max}}{C_e + K_m} C_e \qquad \text{Equation 1.1}$$

where J is the net transport across the barrier corresponding to glucose utilization in steady state, C_1 is the plasma glucose concentration, C_e is the brain extracellular concentration, V_{max} and K_m are the Michaelis-Menten constants. An average value of net transport across the barrier (J) is 0.4 μmol g^{-1} min^{-1} (Lund-Anderson, 1979), corresponding to the glucose utilization in steady state. V_{max} and K_m are assumed to be 1.5 μmol g^{-1} min^{-1} and 5 mM respectively, and assigning a plasma glucose concentration (C_1) of 6 mM, the brain's extracellular concentration (C_e) is calculated to be 2.0 mM. With an extracellular space of 15% (Fenstermacher *et al.*, 1975), a total cerebral glucose content of 1.7 μmol g^{-1} min^{-1} (Lund-Anderson) and a dry content of 20%, the intracellular glucose concentration is calculated to be 2.2 mM. The intra- and extracellular glucose concentrations thus are equally large which implies that under normal conditions, the membrane transport rate is much higher than the phosphorylation rate.

In conclusion, glucose crosses the BBB by facilitated diffusion directly into an extracellular pool estimated to have a glucose concentration of 2.5 mM. When more energy is required, neurons use glucose from this pool and also recruit more blood supply thereby maintaining concentration of glucose in the pool.

1.5 Current understanding of glucose transport and metabolism

Several recently published experimental studies of brain glucose report results that are inconsistent with conventional models of brain glucose uptake and transport (Forsyth, 1996, Hu *et al.*, 1996, 1997, Eyre *et al.*, 1994, Guseinov, 1991). Some reports have demonstrated a brain extracellular fluid glucose concentration that is both low and significantly affected by changes in neuronal activity (Fellows *et al.*, 1992), observations of transient glucose export in certain neurointensive settings (Guseinov, 1991, Eyre *et al.*, 1994). Hu *et al.*, 1997, using biosensors implanted in the brain have reported rapid extracellular changes in basal glucose concentrations. The transient initial rapid decrease up to 20-34% was observed on a time scale (10-13 sec) comparable to that for neurotransmitter release.

Forsyth, 1996 has examined the inability of conventional kinetic models of blood-brain handling to provide satisfactory explanations for the origin of transients of glucose export seen in the recent findings. Numerical modeling was used to show that, for such transients to result from falls in neuronal metabolism, a reservoir for temporary storage of glucose behind the blood brain barrier is required, which is capable of generating net fluxes of glucose into the brain glucose pool exchanging with plasma. The author suggests that considering the neuroanatomy of the astrocytes, neuron and cerebral capillary, plasma glucose may initially exchange with an intracellular astrocytic glucose pool, rather than the brain extracellular fluid. Astrocyte glycogen, mobilized at times of increased neuronal activity, could form the reservoir whose presence is inferred from demonstrations of transient glucose export, but only if glycogenolytic products can be exported from astrocytes such as glucose.

It is important to realize that the above arguments are hypothesis and not actual valid conclusions. The role of astrocytes and glia as nutritional reservoirs, taking up blood-

borne glucose and passing on metabolic substrates to neurons, has not been established unequivocally.

1.6 Methods used to determine basal glucose levels in the rat brain.

A variety of methods have been employed to study brain glucose transport and utilization. In no way complete by themselves, each of the methods have contributed to the development of a coherent picture of glucose dynamics in the brain. This section deals with a review of the different methods that have been used. Principles behind techniques such as the 2-deoxyglucose method, biosensors, *in vivo* NMR and microdialysis will be discussed briefly along with their corresponding results. Some limitations and advantages of these methods are also discussed.

1.6.1 2-deoxy glucose method

The 2-deoxyglucose method was developed for the simultaneous measurement of rates of glucose consumption in the various structural and functional components of the brain *in vivo* (Sokoloff *et al.*, 1977). This method is based on the use of 2-deoxy-D-[^{14}C]glucose ([^{14}C]DG) as a tracer for the exchange of glucose between plasma and brain and its phosphorylation by hexokinase in the tissue.

2-Deoxy-D-glucose (2-DG) differs from glucose only in the replacement of the hydroxyl group on the second carbon atom by a hydrogen atom. The remainder of the molecule is indistinguishable from that of glucose, and is metabolized qualitatively exactly like glucose until a point in the glycolytic pathway is reached where its anomalous structure prevents its further metabolism. Thus 2-DG is transported between blood and brain tissues by the same saturable carrier that transports glucose. In the tissue, it competes with glucose for hexokinase, which phosphorylates both glucose and 2-DG back to their respective hexose-6-phosphates. It is at this point in the biochemical pathway that the further metabolism of the two compounds diverges. Glucose-6-phosphate is converted to fructose-6-phosphate and metabolized further in the tricarboxylic acid and glycolytic pathways. 2-Deoxyglucose-

6-phosphate cannot be isomerized because of the lack of a hydroxyl group on its second carbon and its metabolism ceases at this point in the pathway.

A pulse of [^{14}C]DG is administered intravenously and the arterial plasma [^{14}C]DG and the glucose concentrations monitored for a preset time between 30 and 45 minutes. At the prescribed time, the head is removed and frozen in liquid nitrogen-chilled Freon XII, and the brain sectioned for autoradiography. Local cerebral glucose consumption is calculated by equations on the basis of these measured values. Measurements from several laboratories using similar techniques or biochemical assays on fixed tissues have shown that the average glucose content of the rat brain is 2-4 μmol/g wet weight or 3-4 mM at normoglycemic plasma concentrations (6-8 mM) (Lowry *et al.*, 1964, Lewis *et al.*, 1974a, Gjedde and Diemer, 1983, Evans and Meldrum, 1984). This technique also demonstrated that there exists tight coupling between phosphorylation and glucose influx into the brain via correlation between glucose utilization and regional cerebral blood flow (rCBF).

The method requires brain removal and correction for differences in transport kinetics between glucose and the labeled analogues. Certain assumptions about the labeling of products beyond glucose are necessary for this method to be used successfully.

1.6.2 Biosensors

Biosensors are microelectrodes used in the brain of an anesthetized or freely moving animal, usually specific to the analyte of interest. They typically consist of an enzyme (e.g. glucose oxidase for measurement of glucose) immobilized on a metal surface. For example, a glucose biosensor developed by Hu and Wilson, 1997, consists of a teflon coated platinum-iridium wire with a sensing cavity created by removal of teflon. The cavity is coated with an inner layer, an immobilized enzyme (glucose oxidase) layer and an outer layer. In typical amperometric detection, the enzyme catalyses the conversion of glucose to gluconolactone with the production of hydrogen peroxide. H_2O_2 is oxidized at the platinum electrode, giving rise to a current due to release of electrons at a constant potential. The measured current is correlated back to the concentration of glucose.

Table 1.3 lists the several measured basal glucose values using similar biosensors. These values show slight negligible inter animal variability and are in agreement with the glucose kinetic constants for transport and uptake. Biosensors need to be characterized over a concentration range. They need to be tested for their linearity and sensitivity. Some of the major limitations of biosensors such as interference due to species that are oxidized at the operating potential such as uric acid, ascorbic acid etc. (Lowry *et al.*, 1994) are offset by the specificity and temporal resolution they offer.

Table 1.3 Basal glucose values using biosensors

Basal glucose values (mM)	References
2.6 +/- 0.2	Hu and Wilson, 1997
2.4 +/- 0.13	Silver and Erecinska, 1994

1.6.3 *In vivo* NMR

Mason *et al.*, 1992 have used ^{13}C nuclear magnetic resonance (NMR) measurements to report intracerebral glucose values of 2.8 μmol/g at plasma glucose values of 9.3 mM. In contrast with previous methods, ^{13}C NMR is both non-invasive and allows direct detection of intracerebral glucose following infusion of ^{13}C-labeled glucose.

Briefly, this technique involves the cannulation of the tail vein of the rat for infusion of ^{13}C. The scalp is retracted and a single turn elliptical surface coil is placed on the skull. ^{13}C NMR spectra are obtained with a surface coil double tuned to 1H and ^{13}C frequencies and optimization of field intensities by shimming with water resonance. The authors have shown that ^{13}C NMR can be used for direct detection of the intracerebral glucose concentration in the rat brain. In this particular study, quantitation was based on the postmortem measurement of [3-^{13}C] lactate. However, as the authors suggest, large bore magnets in conjunction with external

concentration standards would allow the procedure to be performed entirely *in vivo*. This was demonstrated for the human brain by Gruetter *et al.*, 1992.

1.6.4 Microdialysis

Microdialysis is a chemical sampling technique that involves the implantation of a dialysis fiber in the tissue of interest. Isotonic buffer solution is pumped inside the probe and is termed as 'perfusate'. Sampling occurs due to the diffusion of analytes across a concentration gradient. Constant flow of the perfusate drives the solution out of the probe and is termed as the 'dialysate'. This technique offers several attractive features. First, the delivery of substances to the site of interest is relatively easy through the perfusate medium. Virtually any inhibitor/pharmacological agent can be delivered. Second, the dialysate samples contain many chemicals such as neurotransmitters, along with the analyte of interest. Simultaneous detection of a number of substances is possible using microdialysis coupled to HPLC or CE. Technically, microdialysis can be attached to any detection system. Third, since the dialysis fiber allows the passage of low molecular weight substances, sample clean up procedures may not be required.

Several approaches are now available for the quantification of extracellular substances in the tissue matrix. Earlier researchers in the field tried to correct *in vivo* data using an *in vitro* calibration factor. It has now been established that such a correction is incorrect, as the tissue environment is different from the hydrodynamic *in vitro* environment. Therefore, empirical calibration methods such as the zero net flux method (Lönnroth, 1986), the variation in perfusion flow rate method (Jacobson 1985) and the very slow perfusion flow rate method (Menacherry *et al.*, 1992) were developed. These approaches allowed the researcher to measure concentration of substances in the extracellular space. These approaches are explained in detail in Chapter 2.

Using the *in vitro* recovery correction factor, Harada *et al.*, 1992, established a brain extracellular glucose concentration of 20.8 +/- 2.8 mg/dl (1.15 mM).

Fellows *et al.*, 1992 used microdialysis with the zero net flux approach to measure the basal glucose concentration in the rat brain. These authors, using a flow rate of 2 μL/min, reported a value of 0.47 +/- 0.13 mM, which is several fold lower that the value reported so far, using the above mentioned techniques. Therefore, verification of their results was one of the objectives of this thesis.

Although microdialysis is rapidly gaining significance in neuroscience research, some calibration issues need to be resolved. For example, the dialysate concentrations need to be corrected for a recovery factor, which is function of flow rate, temperature, time, to name a few. It has now been established that it is incorrect to apply *in vitro* recovery correction factor for *in vivo* data. The temporal resolution is limited by the sample volume necessary for it detection. Even though on line detection systems are being developed, the time resolution is still on the time scale of minutes.

The remainder of this thesis deals with the microdialysis technique and issues related towards the measurement of basal glucose levels in the extracellular space of rat brain.

1.7 References

Baldwin, S. A., Barros, F. L., Griffiths, M. Trafficking of glucose transporters-Signals and Mechanisms. *Bioscience Reports.* **1995**, *15*, 419-426.

Betz, A. L., Gilboe, D. D., Drewes, L. R. Effects of anoxia on net uptake and unidirectional transport of glucose into the isolated dog brain. *Brain Res.* **1974**, *67*, 307-316.

Betz, A. L. Drewes, L. R., Gilboe, D. D. Inhibition of glucose transport by phlorizin, phloretin and glucose analogues. *Biochim. Biophys. Acta*, **1975**, *406*, 505-515.

Boado, R. J., Pardridge, W. M. The brain type glucose transporter mRNA is specifically expressed at the blood brain barrier. *Biochem. Biophys. Res. Commun.* **1990**, *166*, 174-179.

Brant, A. M., Jess, T. J., Milligan, G., Brown, C. M., Gould, G. W. Immunological analysis of glucose transporters expressed in different regions of the rat brain and central nervous system. *Biochem. Biophys. Res. Commun.* **1993**, *192*, 1297-1302.

Chapman, A. G., Meldrum, B. B., Siesjo, B. K. Cerebral metabolic changes during prolonged epileptic seizures in rats. *J. Neurochem.* **1977**, *28*, 1025-1035.

Colowick, S. P. *"The Enzymes"*, P. D. Boyer, ed., 3rd Ed., **1973**, *9*, 1-48.

Davson, H., *Physiology of the cerebrospinal fluid.* **1967**, Churchill; London.

Dick, A. P., Harik, S. I., Klip, A., Walker, D. M. Identification and characterization of the glucose transporter of the blood brain barrier by cytochalasin B binding and immunological reactivity. *Proc. Natl. Acad. Sci. USA*, **1984**, *81*, 7233-7237.

Diemer, K. Capillarization and Oxygen Supply of the Brain. In: *Oxygen Transport in Blood and Tissue*, edited by D. W. Lubbers, U. C. Luft, G. Thews, E. Witzleeb. Stuttgart: Thieme, **1968**, 118-123.

Drewes, L. R., Horton, R. W., Betz, A. L. Cytochalasin B inhibition of brain glucose transport and the influence of blood components on the inhibitor concentration. *Biochim. Biophys. Acta*, **1977**, *471*, 477-486.

Ehrlich, P., *das Sauerstoff-Bedurfnis des Organismus: eine farbenanalytische Studie.* Berlin: Hirschward, **1885.**

Ellison, W. R., Lueck, J. D., Fromm, H. J. Studies on the mechanism of orthophosphate regulation of bovine brain hexokinase. *J. Biol. Chem.* **1975**, *250*, 1864-1871.

Eyre, J. A., Stuart, a. G., Forsyth, R. J., Heaviside, R. J., Bartlett, K. Glucose export from the brain in man: evidence for a role for astrocytic glycogen as a reservoir of glucose for neural metabolism. *Brain Res.* **1994**, *635*, 349-352.

Fellows, L. K., Boutelle, M. G., Fillenz, M. Extracellular brain glucose levels reflect local neuronal activity: A microdialysis study in awake, freely moving rats. *J. Neurochem.* **1992,** *59*, 2141-2147.

Flier, J. S., Mueckler, M., McCall, A. L., Lodish, H. F. Distribution of glucose messenger mRNA transcripts in tissues of rat and man. *J. Clin. Invest.* **1987,** *79,* 657-661.

Forsyth, R. J. Astrocytes and the delivery of glucose from plasma to neurons. *Neurochem. Int.* **1996**, *28(3),* 231-241.

Fritschka, E., Ferguson, J. L., Spitzer, J. J. Increased free fatty acid turnover in CSF during hypotension in dogs. *Am. J. Physiol.* **1979**, *236*, H802-H807.

Furman, F. A. Tetrodotoxin, tarichatoxin, and chiriquitoxin: Historical perspectives. In Tetrodotoxin, saxitotoxin, and the molecular biology of the sodium channel. *Annals of the New York Academy of Sciences*, **1986**, *479*, 1-14.

Gerhart, D. Z., LeVasseur, R. J., Broderius, M. A., Drewes, L. R. Glucose transporter localization in brain using light and electron immunocytochemistry. *J. Neurosci. Res.* **1989**, *22*, 464-472.

Gould, G. W., Holman, G. D. The glucose family transporter: structure, function and tissue-specific expression. *Biochemical Journal.* **1993**, *295*, 329-341.

Gruetter, R., Novotny, E. J., Boulware, S. D., Rothman, D. L., Mason, G. F., Shulman, G. I., Shulman, R. G., Tamborlane, W. V. Direct measurement of brain glucose concentrations in humans by ^{13}C NMR spectroscopy. *Proc. Natl. Acad. Sci. USA.* **1992**, *89*, 1109-1112.

Gueseinov, T. Y. Carbohydrate metabolism of the brain in hypoxia [in Russian]. *Anesteziol. Reanimat.* **1991**, *3,* 14-17.

Harada, M., Okuda, C., Sawa, T., Murakami, T. Cerebral extracellular glucose and lactate concentrations after moderate hypoxia in glucose- and saline-infused rats. *Anesthesiology.* **1992**, *77*, 728-734.

Hellwig, B., Joost, H. G. Differentiation of erythrocyte-(GLUT1), liver-(GLUT2), and adipocyte-type (GLUT4) glucose transporters by binding of the inhibitory ligands cytochalasin B, forskolin, dipyrigamole and isobutylmethylxanthine. *Mol. Pharmacol.* **1991**, *40* , 383-389.

Hu, Y., Wilson, G. S. Rapid changes in local extracellular rat brain glucose observed with an *in vivo* glucose sensor. *J. Neurochem.* **1997**, *68*, 1745-1752.

Jacobson, I., Sandberg, M., Hamberger, A. Mass transfer in brain dialysis devices - a new method for the estimation of extracellular amino acids concentration. *J. Neurosci. Meth.* **1985**, *15*, 263-268.

Kalaria, R. N., Gravina, S. A., Scmidley, J. W., Perry, G., Harik, S. I. The glucose transporter of the human brain and blood brain barrier. *Ann. Neurol.* **1988,** *24*, 757-764.

Kant, J. A., Steck, T. L. Specificity in association of glyceraldehyde 3-phosphate dehydrogenase with isolated human erythrocyte membranes. *J. Biol. Chem.* **1973**, *248*, 8457-8464.

Kety, S. S., Woodford, R. B., Harmel, M. H., Freyhan, F. A., Appel, K. E., Schmidt, C. F. Cerebral flow and metabolism in schizophrenia. The effects of barbiturate semi-narcosis, insulin coma, and electroshock. *Am. J. Psychiatry* **1948**, *104*, 765-770.

Kintner, D., Costello, D. J., Levin, A. B., Gilboe, D. D. Brain metabolism after 30 minutes of hypoxic or anoxic perfusion or ischemia. *Am. J. Physiol.* **1980**, *239*, E501-E509.

LeFevre, P.G. The evidence for active transport of monosaccharides across the red cell membrane. *Symp. Soc. Exp. Biol.* **1954**, *8*, 118.

Lewis, L. D., Ljunggren, B., Norberg, K., Siesjo, B. K. Changes in carbohydrate substrates, amino acids and ammonia in the brain during insulin induced hypoglycemia. *J. Neurochem.* **1974**, *23*, 659-671.

Lönnroth, P., Jansson, P. A., Smith, U. A. A microdialysis method allowing characterization of intercellular water space in humans. *Am. J. Physiol.* **1986**, *253*, E228-E231.

Lowry, O. H., Passonneau, J. V., Hasselberger, F. X., Schulz, D. W. *J. Biol. Chem.* **1964**, *239*, 18-30.

Lowry, J. P., McAteer, K., Satea S. El Atrash, Duff A., O'Neill, R. D. Characterization of glucose oxidase-modified poly(phenylenediamine)-coated electrodes in vitro and in vivo: Homogenous interference by ascorbic acid in hydrogen peroxide detection. *Anal. Chem.* **1994**, *66*, 1754-1761.

Lund-Anderson, H. Transport of glucose from blood to brain. *Physiol. Rev.* **1979**, *59*, 305-352.

Lusk, J. A., Manthorpe, C. M., Kao-Jen, J., Wilson, J. E. Predominance of the cytoplasmic form of brain hexokinase in cultured astrocytes. *J. Neurochem*, **1980**. *34(6),* 1412-1420.

Menacherry, S., Hubert, W., Justice, J. J. *In vivo* calibration of microdialysis probes for exogenous compounds. *Anal. Chem.* **1992**, *64*, 577-583.

Nagamatsu, S., Kornhauser, J. M., Burant, C. F., Seino, S., Mayo K. E., Bell, G. I. Glucose transporter expression in brain cDNA sequence of mouse GLUT3, the brain facilitative isoform, and identification of sites of expression by *in situ* hybridization. *J. Biol. Chem.* **1992**, *267*, 467-472.

Pardridge, W. M. Brain Metabolism: A perspective from the blood brain barrier. *Phsiol. Rev.* **1983**, *63(4)*, 1481-1535.

Pardridge, W. M., Oldendorf, W. H. Kinetics of blood brain barrier transport of hexoses. *Biochim. et Biophys. Acta*, **1975**, *382*, 377-392.

Pardridge, W. M., Boado, R. J., Farrell, C. R., Brain-type glucose transporter (GLUT1) is selectively localized to the blood-brain barrier. Studies with quantitative western blotting and in situ hybridization. *J. Biol. Chem.* **1990**, *265*, 18035-18040.

Plageman, P. G., Richey, D. P. Transport of nucleosides, nucleic acids, bases, choline and glucose by animal cells in culture. *Biochim. Biophys. Acta.* **1974**, *344*, 263-305.

Schaltenbrand, B., Bailey, P., Die pervaskulare Piagliamembran des Gehirns. *J. Physol. Neurol.* **1928**, *35*, 199.

Siegel, G. J., Bernard, W. A., Albers, R. W., Molinoff, P. B. In: Basic Neurochemistry, Raven Press, New York, **1994.**

Sokoloff, L. Metabolism of ketone bodies by the brain. *Ann Rev. of Medicine*, **1973,** *24*, 271-280.

Sokoloff, L., Reivich, M., Kennedy, C., Des Rosiers, M. H., Patlak, C. S., Pettigrew, K. D., Sakurada, O., Shinohara, M. The [14C]deoxyglucose method for the measurement of local cerebral glucose utilization: theory, procedure, and normal values in the concious and anesthetized albino rat. *J. Neurochem.* **1977,** *28*, 897-916.

Takata, K., Kasahara, T., Kasahara, M., Ezaki, O., Hirano, H. Blood-tissue barriers are rich in erythrocyte/HepG2-type (GLUT1) glucose transporter. *J. Cell Biol.* **1990a**, *111*, 65a.

Takata, K., Kasahara, T., Kasahara, M., Ezaki, O., Hirano, H. Erythrocyte/HepG2-type glucose transporter is concentrated in cells of blood-tissue barriers. *Biochem. Biophys. Res. Commun.* **1990b**, *173*, 67-73.

Takata, K., Hirano, H., Kasahara, M. Transport of Glucose across the Blood Tissue Barriers. *Int. Rev. of Cyt.* **1997**, *172*, 1-53.

Thurston, J. H., Pollock, P. G., Warren, S. K., Jones, E. M. Reduced brain glucose with normal plasma glucose in salicylate poisoning. *J. Clin. Invest.* **1970**, *49*, 2139-2145.

van Bueren, A. M., Moholt-Siebert, M., Begley, D. E., McCal, A. L. An immunization method for generation of high affinity antisera against glucose transporters useful in immunohistochemistry. *Biochem. Biophys. Res. Commun.* **1993**, *197*, 1492-1498.

van Harreveld, A., Malhotra, S. K. Extracellular space in the cerebral cortex of the mouse. *J. Anat.* **1967**, *101*, 197-207.

Watson, W. E. In: Cell Biology of Brain. **1976**, John Wiley and Sons, Inc. NY

Chapter 2

Microdialysis: Theory and Quantitative models for Determinations of Tissue Concentrations.

2.1 Basic Principles of Microdialysis Sampling

Microdialysis is a sampling technique that was introduced for *in vivo* analysis almost thirty years ago. Bito used dialysis bags implanted in dogs to sample blood plasma (Bito *et al.,* 1966). This technique gained popularity through the late 1970's and early 1980's. Microdialysis has allowed researchers and clinicians to observe the chemical events that are directly related to the tissue that is sampled in a whole animal rather than in a biological space unrelated to, or removed from the tissue of interest.

In vivo research in animals and humans has mostly been focussed on collection of biological fluids, such as urine, blood, feces, exhaled air etc. to assess disease states or to determine the concentration of drugs or endogenous compounds. While yielding valuable information, the techniques used, like liver perfusion, tissue slices, whole cell studies or the use of subcellular fractions such as liver microsomes, are destructive and may disrupt or destroy the normal physiological state. Microdialysis can be used in anaesthetized or awake intact subjects. It involves implantation of a probe consisting of a dialysis membrane in the tissue of interest, to separate low molecular weight compounds from larger compounds, such as proteins, by diffusion across a concentration gradient. The protein free samples can be directly analyzed using a suitable detection system so that further sample clean-up procedures may not be necessary. The length of such a membrane can vary from 1-5 mm for rodent studies and up to 30 mm for human studies. The membrane lumen is perfused with a saline solution that is isotonic with the tissue of interest.

This chapter gives a brief introduction to the technique of microdialysis along with the detection system used for glucose analysis. The different quantitative methods that allow users to determine the concentrations of compounds *in vivo* are discussed.

2.1.1 Microdialysis Probe

Several probe designs such as linear, loop, concentric or parallel, are employed depending on their intended use and the site of implantation (Figure 2.1).

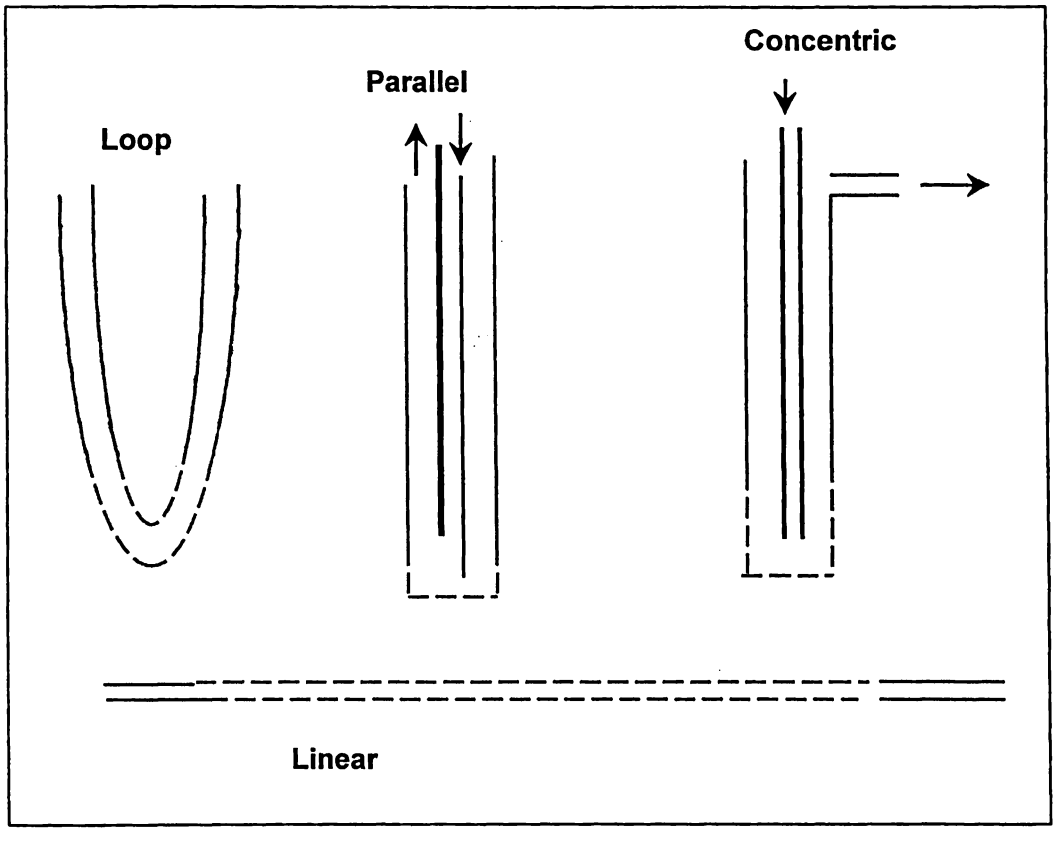

Figure 2.1 Types of probe designs.

Studies that involve implantation of microdialysis probes in the rat brain usually use the concentric design probes. Probes of this design were used throughout the work (Figure 2.2). All the probe designs have a hollow dialysis membrane. The membrane can be made of polymers of different sizes and composition. The commonly used polymers are: polycarbonate/regenerated cellulose also called cuprophan, polyacrylonitrile (PAN) and cellulose acetate. These polymers and their properties are briefly summarized in Table 2.1.

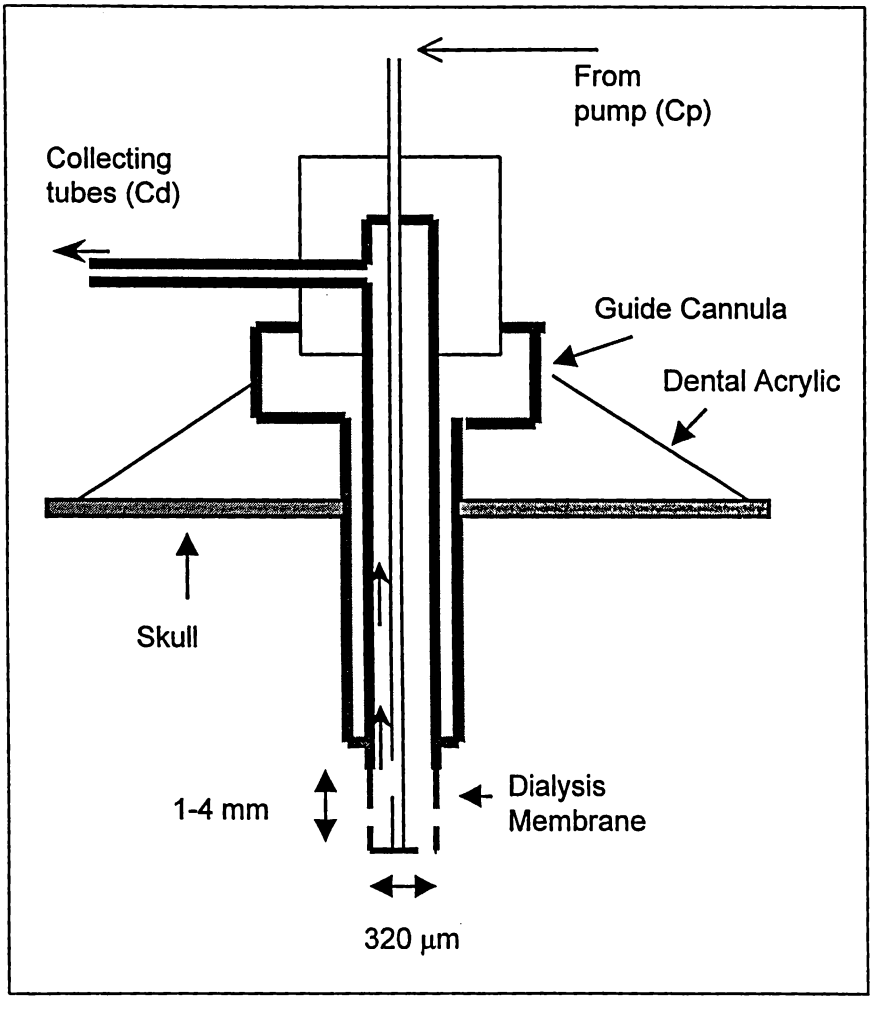

Figure 2.2 Concentric probe design used throughout this work

Table 2.1 Properties of various types of polymers used as membranes

Membrane	MWCO (kDa)	Charge
Cuprophan	~5	Neutral
PAN	~29	Highly negative
Cellulose acetate	~12	Slightly negative

MWCO: Molecular weight cut-off

A typical microdialysis experiment, using concentric design probes, employs perfusing fluids that are isotonic with the brain tissue matrix through the inlet and is usually referred to as the "perfusate". Furthermore, samples are collected through the outlet end of the probe, usually referred to as the "dialysate", and are analyzed by a suitable analytical technique. Since the concentration of dialysate is a function of several factors such as perfusate concentration, flow rate, to name a few, the dialysate samples are converted by mathematical manipulations to yield the "true" tissue values (Benveniste, 1990). Such manipulations basically involve two modes of operation for the probes. They are usually referred to as the recovery mode and the delivery mode. These modes of operations are discussed further in Section 2.1.2.

2.1.2 Modes of Microdialysis Operation

In both modes of operation, the dialysis fiber lumen is perfused with a solution that closely matches the ionic composition of the surrounding tissue space. There is net transport of substances across the dialysis membrane depending on the concentration gradient. Because transport into the dialysis fiber lumen is diffusion based, there is no net loss of fluid from the tissue. This allows the fiber to behave as an artificial blood vessel in which low molecular weight substances can be recovered from or delivered to the tissue.

Both the modes of microdialysis operation are derived from a fundamental equation defined by a term called "Extraction Efficiency (EE)". The EE is defined as,

$$EE = \frac{C_p - C_d}{C_p - C_s} \qquad \text{Equation 2.1}$$

where C_p is the concentration of the analyte in the perfusate, C_d is the concentration of the analyte in the dialysate and C_s is the concentration of the analyte in the surrounding environment. When C_p is zero, the mode of operation of the microdialysis probe is termed the recovery mode (EE_r) or simply "recovery". When C_s

is zero, the operation of the probe is referred to as the dialysate mode (EE_d) or simply "delivery". These two modes are discussed in some detail in the following sections.

2.1.2.1 Recovery

Recovery (Equation 2.2), is defined as the EE when C_p is zero i.e. the perfusion medium does not contain the analyte of interest.

$$EE_r = \frac{C_d}{C_s} \qquad \text{Equation 2.2}$$

The analyte is removed from the surrounding environment by diffusion into the dialysis probe lumen (Figure 2.3 a). It is important to note that microdialysis only samples analytes that are located in the extracellular fluid (ECF) space and not the intracellular fluid (ICF) space. Most researches use the term recovery to indicate relative recovery, which is defined in concentration terms. This is different from mass recovery or the flux, i.e. the amount harvested by the membrane per unit time, which has units of μmoles / cm^2 s. Unlike relative recovery, the mass recovery increases with increase in perfusion flow rate. Mass recovery is a difficult term to work with because in an *in vivo* situation, the total amount of mass of a substance transported across the membrane into the tissue or into the probe, is unknown. In general, during a recovery experiment, the concentration of a substance is zero in the perfusion fluid that enters the microdialysis fiber lumen, but in principle, only needs to be less than the concentration in the sample ECF space in order for net diffusion into the probe to occur.

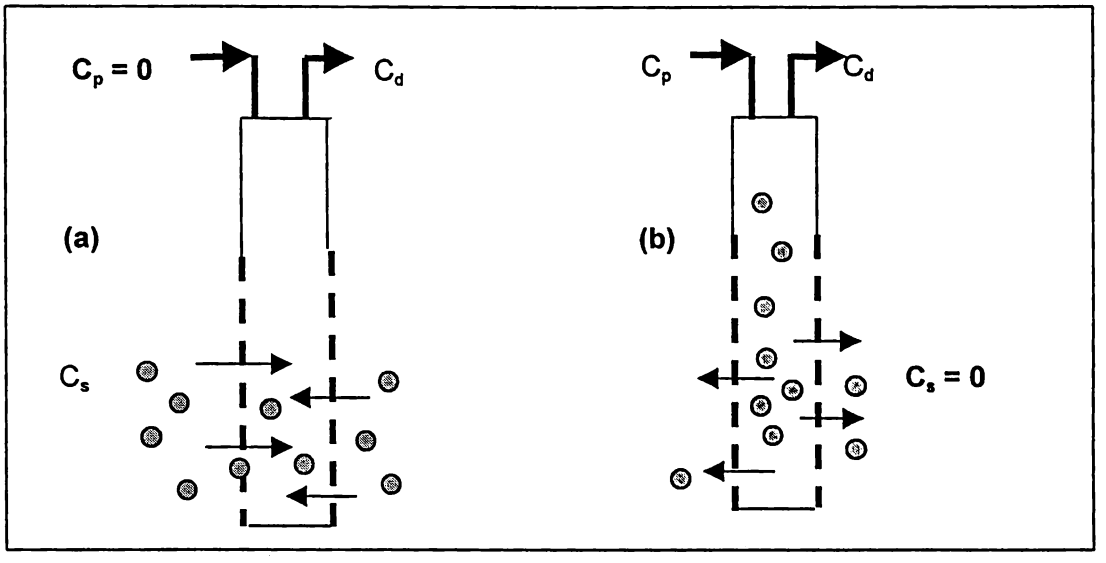

Figure 2.3 The two modes of operation of the microdialysis probes (a) recovery mode, (b) delivery mode

2.1.2.2 Delivery

Delivery is the second mode of operation and is defined as the EE when C_s is zero i.e. the surrounding medium does not contain the analyte of interest.

$$EE_d = \frac{C_p - C_d}{C_p} \qquad \text{Equation 2.3}$$

When the transport of the analyte is in the opposite direction of that in the recovery experiment, the experiment becomes a delivery experiment (Figure 2.3 b). A known concentration of analyte is included in the perfusion medium. The analyte diffuses from across the probe membrane into the ECF space, where it diffuses away from the probe, and is removed from the ECF by local metabolism, transport processes or capillary permeation. In a pharmacological experiment, this is an advantage as a potential toxic chemical can be delivered directly to the tissue space rather than through the circulatory system, which may cause dysfunction of the organs in the subject.

2.1.3 Mass transfer resistance in Microdialysis

The percentage of a substance that enters or leaves the microdialysis probe is a complex function of a variety of factors of which only a few i.e. the concentration in the dialysate and the flow rate, can be experimentally manipulated or measured. The driving force for mass transport is a concentration gradient across the dialysis membrane.

In Figure 2.4, the resistance due to the ECF space is denoted as R_{ecf}, that due to the membrane is R_m and the resistance due to the dialysate is denoted as R_d.

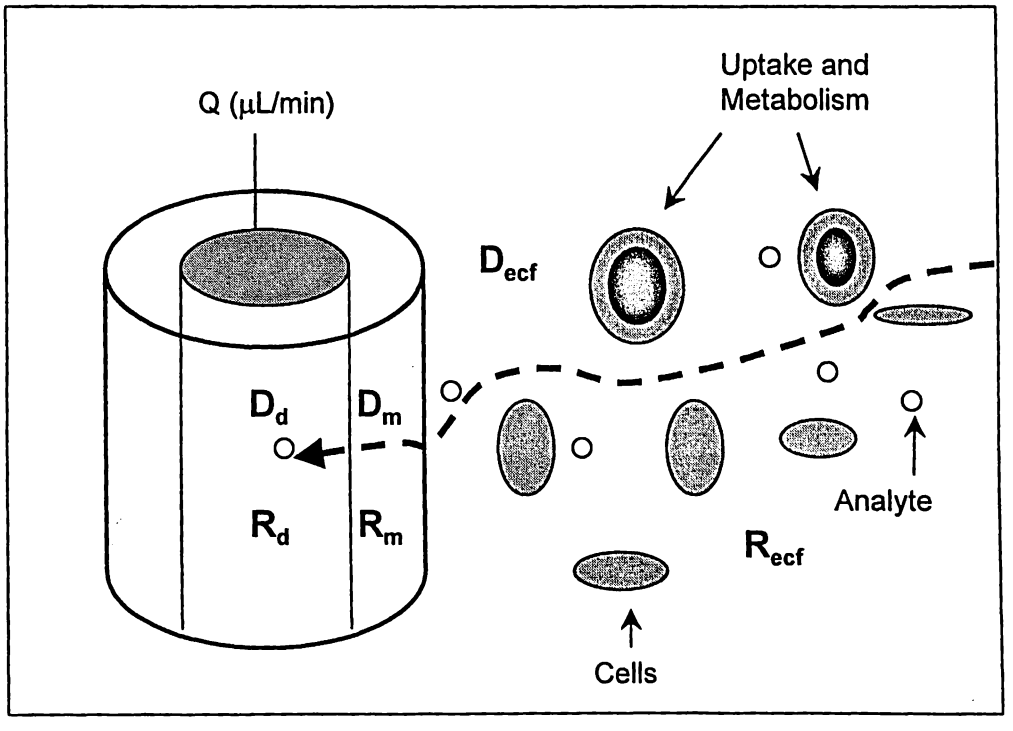

Figure 2.4 Expanded view of the three resistances due to the tissue, membrane and dialysate and their corresponding diffusion coefficients.

Figure 2.4 shows an expanded version of the three distinct mass transfer regions, the extracellular space, the membrane, and the dialysate perfusion fluid. The mass transfer resistance provided by each of these spaces can be understood better by

considering each space as a string of series resistances. In this case, the mass flow experienced by each of the resistances is the same and their effects are additive.

2.1.3.1 Tissue Resistance (R_{ecf})

In the tissue space, the analyte undergoes a tortuous path around the cells and blood vessels to reach the dialysis fiber membrane. This tortuous path increases the distance that the molecule must diffuse and thus reduces the diffusion coefficient by a tortuosity factor that accounts for the increased path length. In brain tissue, this factor is usually considered to have a value of about 1.5 to 1.6 and differs between the various regions of the brain (Nicholson and Phillips, 1981). The diffusion coefficient that is used to describe transport through the tissue space is generally the aqueous diffusion coefficient (D) at 37° C, divided by the square of the tortuosity factor, λ, thus giving an effective ECF diffusion coefficient D_{ecf},

$$D_{ecf} = D / \lambda^2 \qquad \text{Equation 2.4}$$

Equation 2.4 has been verified for inert substances (Nicholson, 1993) but for dopamine, a cation, the use of equation 2.4 to describe its *in vivo* diffusion coefficient was found to be incorrect (Rice *et al.*, 1985). It was suggested that the glycoaminoglycan content in tissue has a hindering effect on the *in vivo* diffusion coefficient of dopamine. This indicates that caution should be exercised when applying *in vitro* diffusion measurements to *in vivo* situations.

2.1.3.2 Membrane Resistance (R_m)

Considering a recovery experiment, the molecule of interest must pass through the dialysis membrane after it has passed through the tissue space. The resistance associated with the membrane is due to the thickness and length of the membrane as well as the diffusion of the analyte through the membrane. Different types of membrane have different properties (Table 2.1), and therefore, different resistances.

For instance, acetaminophen glucoronide (MW 350) is extracted poorly by PAN membranes despite the 29,000 molecular weight cutoff designated to PAN membranes. This is because PAN carries a negative charge due to the cyano groups, thus, hindered diffusion of polar or charged species could be expected with this membrane. This change in the diffusion rate from interaction with the membrane will result in an increased resistance due to the decrease in the diffusion properties.

2.1.3.3 Dialysis Resistance (R_d)

Diffusion coefficient of the analyte in the perfusion medium in the dialysis fiber lumen and to some extent, the perfusion flow rate, contribute to the mass transfer coefficient in the dialysate. The diffusion of the analyte in the aqueous perfusion will be greater than in the membrane or tissue because there will be no tortuosity or volume fraction effects in the dialysate. Therefore, this resistance should, in theory, be the least contributing factor to the overall resistances. An exception to the above would be when the combination of membrane surface area and perfusion flow rate allow for 100 % recovery or delivery of the analyte. For the recovery experiment, it would be an indication of equilibrium. In a delivery experiment, it would indicate the efficiency of the tissue to extract the analyte from the dialysis probe.

2.2 Applications of Microdialysis

Microdialysis has become a standard technique in the field of neuroscience and has been used in blood brain barrier studies (de Lange *et al.*, 1995) and neurotransmitter and neuropeptide sampling (Robinson and Justice, 1991). Microdialysis sampling strategies have also been developed for sampling from the extracellular fluid (ECF) matrix of other tissues such as the skin (Ault *et al.*, 1992, 1994), liver (Scott et al., 1990, 1993), kidney, heart (van Wylen *et al.*, 1992), muscle (Deguchi *et al.*, 1991), and solid tumors (Palsmeier and Lunte, 1994a, 1994b). Microdialysis sampling has been used in humans (Ståhle *et al.*, 1991c, Lönnroth *et al.*, 1986, Bolinder *et al.*, 1989, Stenken, 1995) and has been approved for use in humans for determining

levels of glucose in diabetics in Sweden. In addition to gaining information about the extracellular concentration of a substance in the ECF, this technique has been used to sample and obtain pharmacokinetic information from the blood (Ståhle, 1993) and tissue of an animal (Lunte *et al.,* 1991, Wong, 1993). The technique has demonstrated promise in drug distribution studies (Ståhle *et al.*, 1991a, 1991b, Ljungdahl-Ståhle *et al.*, 1992, van Belle *et al.,* 1995). Even though microdialysis offers sampling of organs in their native environment which preserves the organ integrity and allows the animal to serve as its own control, it is important to note that the insertion of a microdialysis probe causes initial damage to the tissue.

2.3 Review of quantitative *in vivo* calibration models and methods

One of the primary applications of microdialysis is to determine concentrations of substances in the extracellular space of tissue matrix. In the brain, these substances could be endogenous e.g. glucose, lactate, neurotransmitters etc. or exogenously administered drugs such as caffeine, tacrine, acetaminophen etc. A number of mathematical models and methods for quantifying microdialysis data have been proposed. These treatments are necessary because *in vitro* parameters cannot be indiscriminately applied to the *in vivo* situation. Also, experimental limitations do not allow the use of long dialysis membranes or very low perfusion flow rates at which recoveries would be 100%. All models discussed in this section involve continuous perfusion of the probe, which is the key criterion for monitoring extracellular compounds under transient conditions.

Ungerstedt *et al.*, 1982 were the first to recognize the recovery phenomena and the first to try and calculate *in vivo* concentrations. Their theory assumes that *in vitro* recovery measured in a quiescent (non stirred) medium is the same as *in vivo* recovery. Thus by measuring *in vitro* recovery and using the same probe and the same flow rate *in vivo*, the extracellular concentration of a substance C_e can be calculated as,

$$EE_{r1} \text{ (}in\ vitro\text{)} = C_{d1} / C_s \qquad \text{Equation 2.5}$$

$$EE_{r2}(\textit{in vivo}) = C_{d2} / C_e \qquad \text{Equation 2.6}$$

$$C_e = C_{d2} / EE_{r1} \qquad \text{Equation 2.7}$$

where EE_{r1} and EE_{r2} is the *in vitro* and *in vivo* extraction efficiencies in recovery mode respectively, C_{d1} and C_{d2} are the *in vitro* and *in vivo* dialysate concentrations respectively, and C_s is the *in vitro* concentration of glucose surrounding the probe. This approximation is very rough since the diffusion of a solute in a free liquid medium is much more rapid than in a porous matrix such as the brain. The only practical consequence of this model today is that it highlights the importance of measuring *in vitro* recoveries to check for possible disturbances, and the degree and reproducibility of recovery. EE_{r1} should be measured in artificial CSF at pH 7.4 and at 37^0 C. Reproducibility is significant problem especially when reusing the probes, when using new batches of probes or when combining microdialysis with complicated and expensive studies.

It has been demonstrated that *in vivo* recoveries are lower than *in vitro* recoveries, especially for Ca^{2+} (Benveniste *et al.*, 1989, 1990, Benveniste, 1990). The authors concluded that calculations using Equations 2.5 and 2.7 would lead to underestimation of concentrations of extracellular substances and metabolites. To compensate for hindered diffusion *in vivo*, equation 2.7 was rewritten as,

$$C_e = [\, K \lambda C_d \,] / [\phi \, EE_{r1} \,] \qquad \text{Equation 2.8}$$

Here λ is the tortuosity factor correcting for the increased diffusional path, ϕ is the volume fraction related to total brain volume, and K expresses differences in concentrations between inside of a membrane and the outside medium, both *in vivo* and *in vitro*. The volume fraction is defined as the fraction of a brain region that is extracellular. For flow rates above 2.5 μL/min, dialysate concentrations, depending on membrane length, inside the probe approach zero (maximal absolute recovery) and thus, K is given the value of 1. For lower flow rates, K has been empirically estimated as 0.7. Other constants have empirical values, λ = 1.6 (range 1.5-2), ϕ =

0.2 (Nicholson *et al.*, 1979, 1981) for non-pathological conditions. Equation 2.8 has been shown to fit well for extracellular calcium measurements. However, for neurotransmitters (glutamate and dopamine) this method gave rather disperse and unconvincing values. The concept of correcting concentrations for uptake mechanisms by including uptake blockers produces another approximation, additionally increasing the error of such calculations (Beveniste *et al.*, 1990). Large variations of the tissue parameter λ^2 / ϕ (1 for K^+, 12 for Ca^{2+}) results in overweighted influence of this coefficient in Equation 2.8 on the final result.
The most important observation from these measurements was the existence of a drop in the concentration of a substance in the vicinity of the membrane (about 1 mm from the surface). It was shown later that profile of this concentration gradient regulates the diffusion flux, i.e., *in vivo* recovery, and is specific for each substance, or group of substances.

Amberg *et al.*, 1989 attempted to describe *in vivo* recovery (EE_{r2}) as an explicit function of flow rate, the diffusion coefficient, length, diameter and porosity of the membrane. The mathematical analysis is based on the theory of diffusion and mass transfer in fluid systems. The resulting equation for EE_{r2} (Amberg *et al.*, 1989) is an inverse function of the flow rate and corrects for the functions describing the time needed to reach steady state conditions.
This model provides theoretical evidence that perfusion during microdialysis leads to a quasi-steady state between concentrations of a solute diffusing through the membrane. But it does not consider chemo-biochemical differences of molecules in the ECF. For example, the only variable indicating the difference between dopamine and DOPAC is the *in vitro* diffusion coefficient D.

Jacobson *et al.*, 1985 and Lerma *et al.*, 1986 have presented a simple mathematical description of mass transfer in brain dialysis. Considering laminar flow in a hollow cylinder with semipermeable walls (or a flat duct) and ignoring diffusion in the direction of flow, it was shown that,

$$EE_{r2}=C_d / C_e =1-[\exp (- K_o A/Q)] \qquad \text{Equation 2.9}$$

where C_d is the bulk concentration in the probe (or the dialysate), C_e, the uniform extracellular concentration outside the probe, Q, is the flow rate and K_o, the average mass transfer coefficient, A denotes the area of the semi-permeable membrane. Practical calculations are based on measuring several concentrations, C_d, at varying flow rates, which will give a corresponding number of equations. Computer programs make it quite easy to use non linear regression analysis of an experimentally measured curve depicting the function of the concentration C_e on the flow rate Q. Using a least square successive approximation to fit Equation 2.9 to the experimental data, one can obtain the product K_oA and the apparent extracellular concentration C_o. Graphical representation of C_e versus Q gives a slope corresponding to K_oA and C_o is the intercept at zero flow. An important underlying implication of this mathematical description is that the non-linear fit of the asymptotic function to experimental data would give an estimation not only of the product K_oA, but also of C_e, the apparent extracellular concentration. Thus, the use of recovery factors from model dialysis experiments could be avoided. Overall mass transfer is affected not only by the diffusional resistance of the membrane and perfusion fluid but also by the diffusional resistance of the phase outside the dialysis device.

The application of Equation 2.9 to model dialysis data obtained previously (Johnson and Justice, 1983, Sandberg and Lindstrom, 1983, Jacobson and Hamberger, 1984, Ungerstedt, 1984) reveals an excellent fit. However an analysis of the regression residues from the data of Johnson and Justice, 1983, reveal a considerably lower value of the product K_oA at flow rates below 0.3 μL/min. It was shown that the net flux into the probe will increase with increasing flow rate, the upper limit set by the product CK_oA. The increased net flux (or the absolute recovery) has been observed by Jacobson and Hamberger, 1984.

The strength of this method is that it uses more information concerning properties of the dialysis device *in vivo* (Parsons, 1991, Ståhle, 1991, Menachery 1992, Parsons and Justice, 1992). However, it must be emphasized that the extracellular values obtained reflect the concentration in the immediate vicinity of the dialysis probe. Concentration gradients arise in the tissue around the probe due to the draining

effect of continuous sampling. This model assumes that K_o is constant and does not vary within the flow rate regime, which also means that the concentration profiles outside the probe should be constant. Furthermore, the dialysis membrane is supposed to constitute a major diffusion barrier. This is not entirely true.

An expanded version of Jacobson's model in an attempt to further specify the mass transfer coefficient K_o from physical and biochemical processes occurring *in vivo,* was developed by Bungay *et al.,* 1990 and Morrison *et al.*, 1991. A new variable, an overall probe-external medium permeability P (equivalent to K_o) was introduced (Bungay *et al.*, 1990) and defined as

$$K_o = P = \frac{1}{S(R_d + R_m + R_e)} \qquad \text{Equation 2.10}$$

Substitution in Equation 2.9 would give,

$$EE_{r2} = C_d / C_e = 1 - \exp\left(\frac{-1}{Q\,(R_d + R_m + R_{ecf})}\right) \qquad \text{Equation 2.11}$$

Here, *in vivo* recovery is expressed as a function of flow rate Q and the sum of mass transfer resistances of a dialysate, R_d, membrane, R_m, and tissue, R_{ecf}. Parameters R_d and R_m are functions of cannula and membrane dimensions, porosity and diffusion coefficients in the membrane, and free medium. Resistances to solute movement in the tissue, R_{ecf}, is given by

$$R_{ecf} = \frac{(k_o / k_1)\,\Gamma}{S\,D_e\,\phi} \qquad \text{Equation 2.12}$$

where Γ is the concentration profile penetration depth defined as

$$\Gamma = [\,D_e / k_e\,]^{1/2} \qquad \text{Equation 2.13}$$

k_o and k_1 are modified Bessel functions of the second type (tabulated) with argument r_0 / Γ , k_e is the overall rate constant of disappearance of the solute from the extracellular space due to metabolic and exchange processes.

This is the first model that considers active processes in a living body. However, since most of the constants are yet unknown, Equation 2.11 has limited application. Some compromise with empirical measurements is thus necessary. For example, the penetration depth Γ can be measured experimentally using quantitative autoradiography of labeled substances (Dykstra *et al.*, 1990, 1991). This will allow the calculation of R_{ecf}. For most of the compounds and probe membranes thus far examined *in vivo,* the resistances are $R_{ecf} >> R_m >> R_d$. However, during *in vitro* measurement in a well stirred medium, $R_{ecf} = 0$, while R_m and R_d have the same values *in vivo* (Hsiao *et al.*, 1990, Bungay *et al.*,1990). Thus, such an experiment could be used for evaluation of R_d and R_m by the same procedure as in Jacobson's model. In practice, this means that, knowing the concentration profile of a substance (drug or neurotransmitter) around the probe and measuring the membrane and dialysate resistances *in vitro*, an estimation of *in vivo* extracellular concentrations could be made from a single measurement.

Lönnroth *et al.*, 1987 introduced a method that widely came to be known as the no net flux method or the zero net flux method. Calibration of an implanted dialysis fiber was performed by perfusion with four to five different perfusate concentrations of the analyte. Linear regression analysis of the results yielded the tissue concentration of the analyte, which was in equilibrium with the surrounding tissue. This method of calibration has been used in Chapter 3 to determine basal glucose concentrations in the rat brain and is therefore not discussed in any detail in this section.

2.4 Analysis of β-D-Glucose

2.4.1 Sensor Technology

The YSI 2700 SELECT glucose analyzer was used for all the glucose measurements. It is an enzyme based biosensor and the technology is based on the principles conceived by Leland Clark (Clark, 1979). As shown Figure 2.4, each probe is fitted with a three-layer membrane containing immobilized enzyme in the middle layer. The perforated polycarbonate membrane, the enzyme layer and the cellulose acetate membranes are held tightly within an O-ring. The face of the probe, covered by the membrane, is situated in a buffer filled sample chamber into which the sample is injected. Some of the substrate diffuses through the membrane.

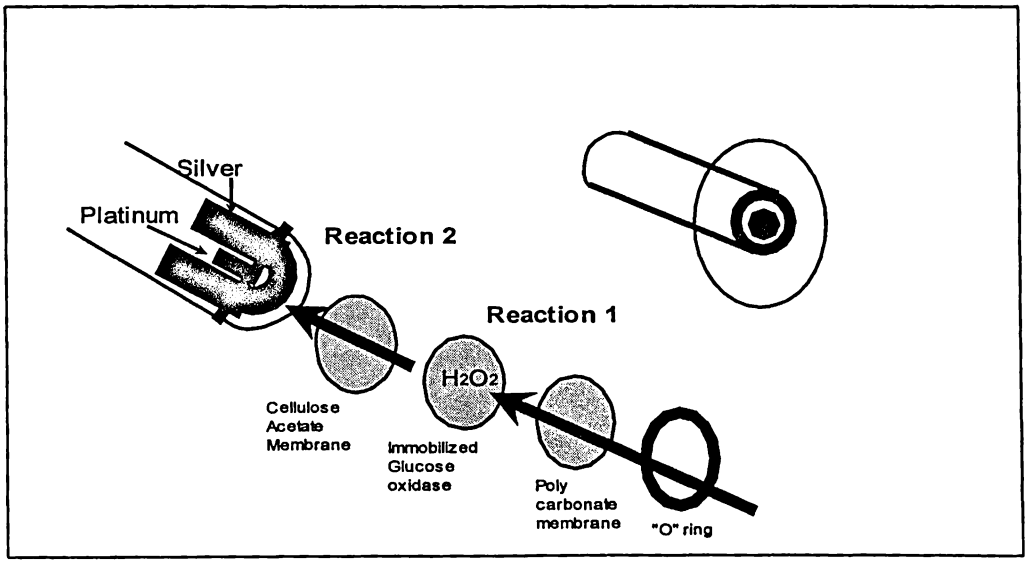

Figure 2.5 Expanded view of the sensor head

When it contacts the immobilized oxidase enzyme, it is rapidly oxidized, producing hydrogen peroxide. See Reaction 2.1,

$$\beta\text{-D-glucose} + O_2 \xrightarrow{GOx} \text{Glucono-}\delta\text{-lactone} + H_2O_2 \qquad \text{Reaction 2.1}$$

The hydrogen peroxide is, in turn, oxidized at the platinum anode, producing electrons (Reaction 2.2)

$$H_2O_2 \xrightarrow{+600\ mV} 2H^+ + O_2 + 2e^- \qquad \text{Reaction 2.2}$$

The platinum electrode is held at an anodic potential (+600 mV) and is capable of oxidizing many substances other than H_2O_2. To prevent these reducing agents from contributing to the sensor current, the membrane contains an inner layer consisting of a very thin film of cellulose acetate. This film readily passes H_2O_2 but excludes chemical compounds with molecular weights above approximately 200. The cellulose acetate film also protects the platinum surface from proteins, detergents, and other substances that could foul it. However, the cellulose acetate film can be penetrated by such compounds as hydrogen sulphide, low molecular weight mercaptans, hydroxylamines, hydrazines, phenols and anilines.

2.4.2 Calibration

To maintain a sample ready status, the analyzer self calibrates. Calibration establishes the sensor's response, in nano-amperes of current, to a known concentration of substrate. The sensor calibration response should be above 5 nA. A response below this range will result in an error. With default calibration settings, the recalibration will occur after every 5 samples or 15 minutes, after a calibration shift of 2% or greater, or after a sample chamber temperature drift of more than 1° C. After every 5 unsuccessful attempts the instrument displays a calibration error message.

2.4.3 Linearity

Under optimal conditions, the sensor depends on diffusional limitation of the substrate. When a substrate can diffuse at a greater rate than the enzyme can turnover product, enzyme kinetics defines the response and non-linearity is a symptom. This occurs as the membrane ages.

The linearity of the analyzer was tested over two ranges of concentration i.e. over 0-1.0mM (Figure 2.6a) and 0-20 mM (Figure 2.6b). Standard solutions of glucose were prepared in distilled water and samples of 15 μL volumes, were injected into the analyzer. Both the curves were linear over the measured range of concentration. Analysis of the residuals did not indicate any particular trends.

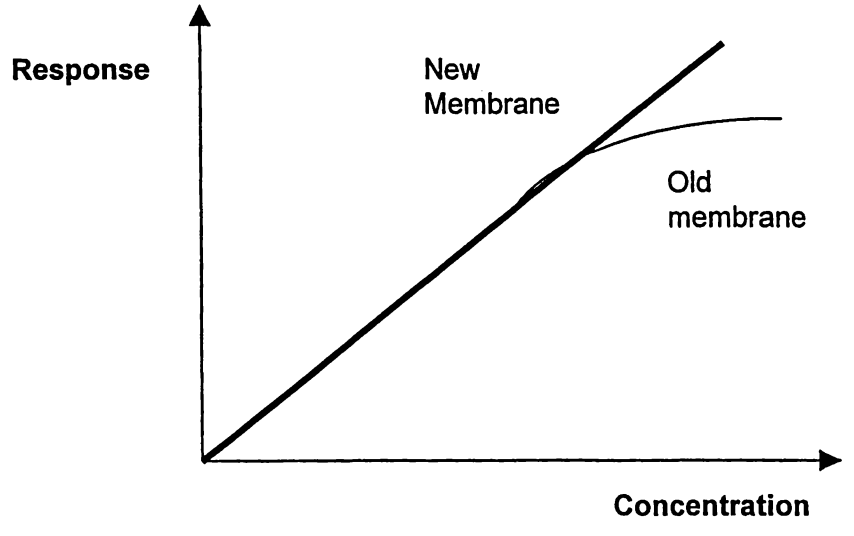

Figure 2.6 Aging Membrane Response

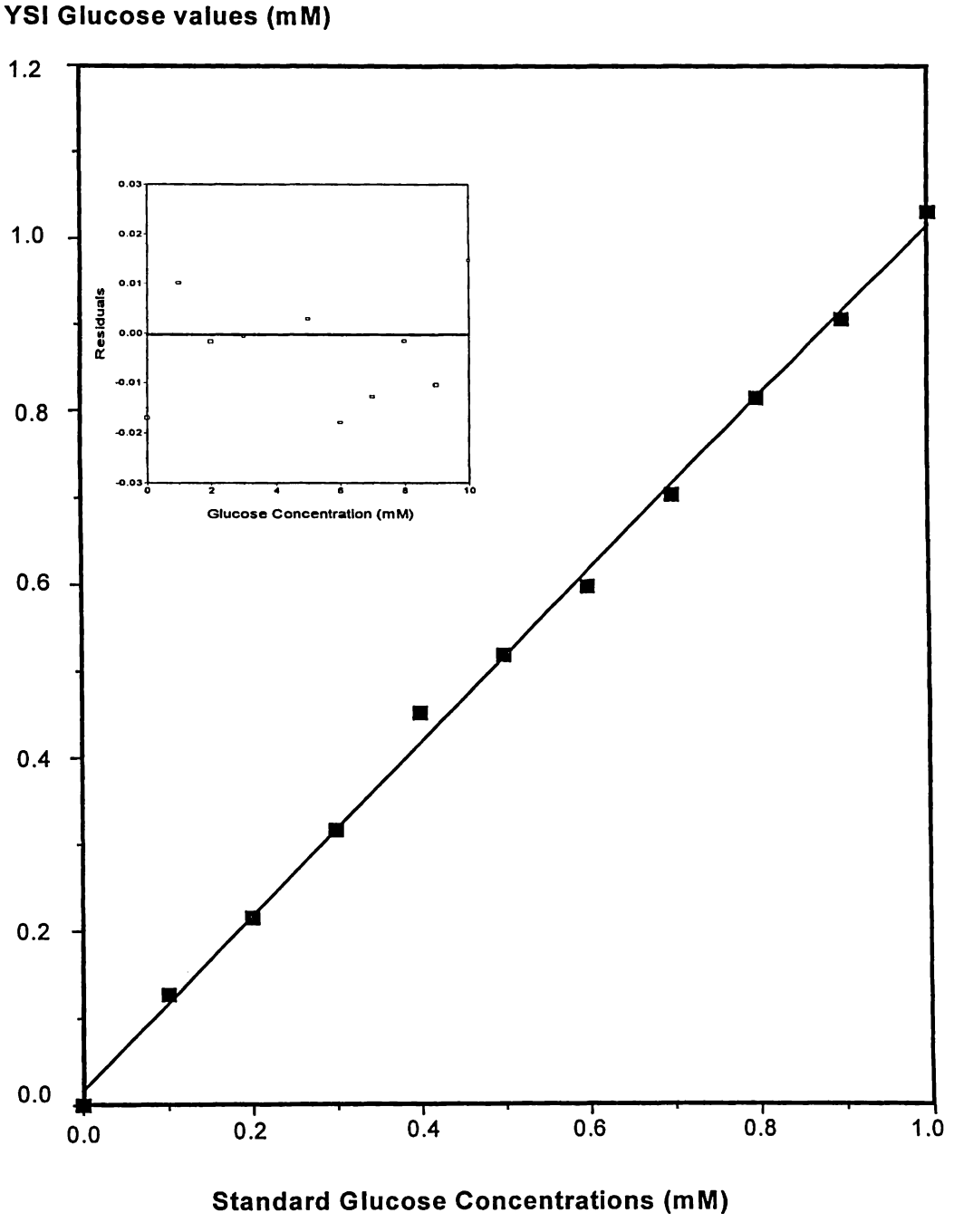
YSI Glucose values (mM)
1.2
1.0
0.8
0.6
0.4
0.2
0.0
0.0
0.2
0.4
0.6
0.8
1.0
Standard Glucose Concentrations (mM)
Residuals
0.03
0.02
0.01
0.00
-0.01
-0.02
-0.03
0
2
4
6
8
10
Glucose Concentration (mM)

(a)

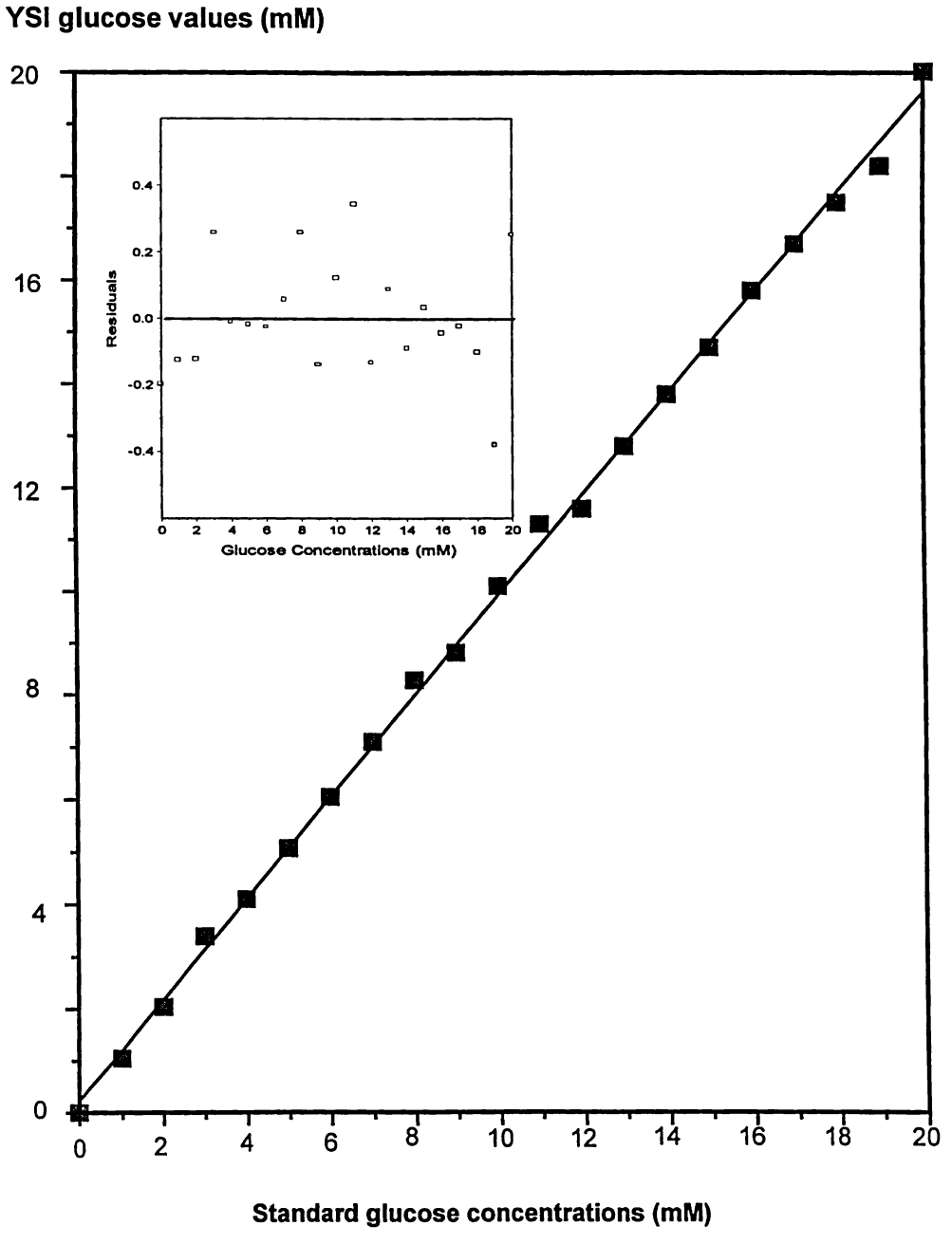

(b)

Figure 2.7 Linear response of the analyzer for different concentration range Curve (a), 0-1 mM: Curve (b) 0-20 mM.

2.5 References

Amberg, G., Lindefors, N. Intracerebral Microdialysis: II. Mathematical studies of diffusion kinetics. *J. Pharmacol. Meth.* **1989,** *22*, 157-183.

Ault, J. M., Lunte, C. E., Meltzer, N. M., Riley, C. M. Microdialysis sampling for the investigation of dermal drug transport. *Pharm. Res.* **1992**, *9*, 1256-1261.

Ault, J. M., Riley, C. M., Meltzer, N. M., Lunte, C. E. Dermal microdialysis sampling *in vivo. Pharm. Res.* **1994**, *11*, 1631-1639.

Benveniste, H., Hansen, A. J. Ottosen, N. S. Determination of brain interstitial concentrations by microdialysis. *J. Neurochem.* **1989,** *52*, 1741-1750.

Benveniste, H., Huttemmeier, P. C. Microdialysis - Theory and application. *Prog. Neurobiol.* **1990**, *35*, 195-215.

Bito, L., Davson, H., Levin, E., Murrey M., Snider, N. The concentrations of free aminoacids and other electrolytes in cerebrospinal fluid, *in vivo* dialysate of brain, and blood plasma of the dog. *J. Neurochem.* **1966**, *13*, 1057-1067.

Bolinder, J., Hagström, E., Ungerstedt, U., Arner, P. Microdialysis of subcutaneous adipose tissue *in vivo* for continuous glucose monitoring in man. *Scand. J. Clin. Lab. Invest.* **1989**, *49*, 465-474.

Bungay, P.M., Morrison, P. F., Dedrick, R. L. Steady-state theory for quantitative microdialysis of solutes and water *in vivo* and *in vitro. Life Sci.* **1990**, *46*, 105-119.

Clark, L. C., Jr. The hydrogen peroxide sensing platinum anode as an analytical enzyme electrode. *Methods in Enzymology*, **1979**, *56*, 448. **1979**

Deguchi, Y., Terasaki, T., Kawasaki, S., Tsuji, A. Muscle microdialysis as a model study to relate the drug concentration in tissue interstitial fluid and dialysate. *J. Pharmacobio-Dyn.* **1991**, *14*, 483-492.

de Lange, E. C. M., Hesselink, M. B., Danhof, M., de Boer, A. G., Breimer, D. D. The use of intercerebral microdialysis to determine changes in blood-brain barrier transport characteristics. *Pharm. Res.* **1995**, *12*, 129-133.

Dykstra, K. H., Hsiao, J. K., Morrison, P. F., Bungay, P. M., Mefford, I. N., Scully, M. M., Dedrick. R. L. Quantitative examination of tissue concentration profiles associated with microdialysis. *J. Neurochem.* **1992**, *58*, 931-940.

Dykstra, K. H., Arya, A., Arriola, D. M., Bungay, P. M., Morrison, P. F., Dedrick. R. L. Microdialysis study of zidovudine (AZT) transport in rat brain. *J. Pharmacol. Exp. Ther.* **1993**, *267*, 1227-1236.

Hsiao, J. K., Ball, B. A., Morrison, P. F., Mefford, I. N., Bungay, P. M. Effects of different semi-permeable membranes on *in vitro* and *in vivo* performance of microdialysis probes. *J. Neurochem.* **1990**, *54*, 1449-1452.

Jacobson, I., Hamberger, A. Veratridine-induced release *in vivo* and *in vitro* of amino acids in the rabbit olfactory bulb. *Brain Res.* **1984**, *299*, 103-112.

Jacobson, I., Sandberg, M., Hamberger, A. Mass transfer in brain dialysis devices- a new method for the estimation of extracellular amino acids concentration. *J. Neurosci. Methods.* **1985**, *15,* 263-268.

Johnson, R. D., Justice, J. B. Jr. Model studies for brain dialysis. *Brain Res. Bull.* **1983,** *10,* 567-571.

Lerma, J.,Herranz, A. S., Herreras, O., Abraira, V., Martin del Rio, R. *In vivo* determination of extracellular concentration of amino acids in the rat hippocampus. A method based on brain dialysis and computerized analysis. *Brain Res.* **1986**, *384*, 145-155.

Lindefors, N., Amberg, G. Ungerstedt, U. Intracerebral microdialysis: I. Experimental studies of diffusion kinetics. *J. Pharmacol. Meth.* **1989**, *22*, 141-156.

Lönnroth, P., Jansson, P. A., Smith, U. A microdialysis method allowing characterization of intercellular water space in humans. *Am. J. Physiol.* **1986**, *253*, E228-E231.

Lunte, C. E., Scott, D. O., Kissinger, P. T. Sampling living systems using microdialysis probes. *Anal. Chem.* **1991**, *63*, 773A-780A.

Menacherry, S., Hubert, W., Justice, J. J. Jr. *In vivo* calibration of microdialysis probes for exogenous compounds. *Anal. Chem.* **1992**, *64*, 577-583.

Morrison, P., Bungay, P., Hsiao, J., Mefford, I., Dykstra, K., Dedrick, R. Quantitative Microdialysis. In: *Microdialysis in the Neurosciences.* In Justice, J., Robinson, T., eds, Techniques in the Behavioral and Neural Sciences. New York: Elsevier; **1991**, 47-80.

Nicholson, C., Phillips, J. M., Gardner-Medwin, A. R. Diffusion from an iontophoretic point source in the brain: role of tortuosity and volume fraction. *Brain Res.* **1979**, *169*, 580-584.

Nicholson, C., Phillips, J. M. Ion-diffusion modified by tortuosity and volume fraction in the extracellular environment of rat cerebellem. *J. Physiol. (Lond).* **1981**, *321*, 225-257.

Palsmeier, R. K., Lunte, C. E. Microdialysis sampling of tumors for the study of of metabolism of antineoplastic agents. *Cancer Bull.* **1994a**, *46*, 58-66.

Palsmeier, R. K., Lunte, C. E. Microdialysis sampling in tumor and muscle: Study of the disposition of 3-amino-1,2,4-benzotriazine-1,4-di-N-oxide (SR4233). *Life Sci.* **1994b**, *55*, 815-825.

Parsons, L. H., Justice, J. B. Jr. Extracellular concentration and in vivo recovery of dopamine in the nucleus accumbes using microdialysis. *J. Neurochem.* **1992**, *58*, 212-218.

Rice, M. E., Gerhardt, G. A., Hierl, P. M., Nagy, G., Adams, R. N. Diffusion coefficients of neurotransmitters and their metabolites in brain extracellular fluid space. *Neuroscience*, **1985**, *15*, 891-902.

Robinson, T. E., Justice, J. B. Jr., eds. *Microdialysis in the Neurosciences.* Elsevier: Amsterdam, **1991**.

Sandberg, M., Lindstrom, S. Amino acids in the dorsal lateral geniculate nucleus of the cat: collection *in vivo*. *J. Neurosci. Methods*, **1983**, *9*, 65-74.

Scott, D. O., Sorenson, L. R., Lunte, C. E. *In vivo* microdialysis sampling coupled to liquid chromatography for the study of acetaminophen metabolism. J. Chromatogr. **1990**, *506*, 461-469.

Scott, D. O., Lunte, C. E. *In vivo* microdialysis sampling in the bile, blood, and liver of rats to study disposition of phenol. *Pharm. Res.* **1993**, *10*, 335-342.

Ståhle, L., Segersvård, S., Ungerstedt, U. A comparison between three methods for estimation of extracellular concentrations of exogenous and endogenous compounds by microdialysis. *J. Pharmacol. Methods*. **1991a**, *25*, 41-52.

Ståhle, L., Segersvård, S., Ungerstedt, U. Drug distribution studies with microdialysis. II. Caffeine and theophylline in blood, brain, and other tissues in rats. *Life Sci.* **1991b**, *49*, 1843-1852.

Ståhle, L., Arner, P., Ungerstedt, U. Drug distribution studies with microdialysis. III. Extracellular concentration of caffeine in adipose tissue in man. Life Sci. **1991c**, *49*, 1853-1858.

Ståhle, L. Microdialysis in pharmacokinetics. *Eur. J. Drug Metab. Pharmacokinet.* **1993**, *18*, 89-96.

Stenken, J. A. Identification and modeling of parameters that influence microdialysis sampling *in vitro* and *in vivo*. *Ph.D. Dissertation*. University of Kansas, **1995**

Ungerstedt, U., Herrera-Marschitz, M., Jungnelius, U., Stahle, L., Tossman, U., Zetterstrom. T. Dopamine synaptic mechanisms reflected in studies combining behavioural recordings and brain dialysis. In: M. Kotisaka (Ed.), Advances in Dopamine Research, Pergamon, New York, **1982**, pp. 219-231.

van Belle, K., Sarre, S., Ebinger, G., Michotte, Y. Brain, liver, and blood distribution kinetics of carbamazepine and its metabolic interaction with clomipramine in rats: A quantitative microdialysis study. *J. Pharmacol Exp. Ther*, **1995**, *272*, 1217-1222.

van Wylen, D. G. L., Schmit, T. J., Lasley, R. D., Gingell, R. L., Mentzer, R. M. Cardiac microdialysis in isolated rat hearts - interstitial purine metabolites during ischemia. *Am. J. Physiol.* **1992**, *262*, H1934-H1938.

Wong, S. L., van Belle, K., Sawchuk, R. J. Distributional transport kinetics of zidovudine between plasma and brain extracellular fluid/cerebrospinal fluid in the rabbit: Investigation of the inhibitory effect of probenecid utilizing microdialysis. *J. Pharmacol. Exp. Ther.* **1993**, *264*, 899-909.

CHAPTER 3

Quantitative Microdialysis Using Zero Net Flux Approach for the Determination of Basal Glucose Levels in the Brain of Freely Moving Rat.

3.1 Introduction

This chapter deals with the issues related to the determination of basal glucose levels in the rat striatum using the zero net flux approach, originally developed by Lönnroth (Lönnroth, *et al.*, 1986). In this study, many factors lead to the choice of this method over others. In their original paper, Fellows *et al.*, 1992, the authors used this approach to determine a basal glucose value of 0.47 mM using microdialysis. As enumerated in Chapter 1, this value is several fold lower than the currently accepted value. Replication of the results of the microdialysis study in the laboratory was one of the goals. Most of the assumptions that are required for the zero net flux technique appeared to fit the brain glucose model known so far. It was an obvious choice over other methods such as the variation in perfusion flow rate technique, developed originally by Jacobson (Jacobson, 1985). The Jacobson technique assumes a constant concentration profile of the substance of interest outside the probe and that membrane transport dominates the mass transfer. Both assumptions are probably not valid. The fact that the probe constantly removes substances from the tissue leads to a reduction in mass transport. Second, because dialysis affects substance concentrations quite far from the probe, the membrane does not constitute the dominant diffusion barrier (Benveniste *et al.,* 1991).

The issues associated with quantifying glucose were explored by performing the ZNF calibration at different perfusion flow rates. The striatum was chosen as the sampling area in the brain tissue because it is larger than the hippocampus and allows the use of longer probes, which improves the overall recovery. The zero net flux approach requires establishment of steady state concentration of glucose in the tissue. This was verified by a series of experiments. For an endogenous substance such as

glucose, this was somewhat easier as the concentration is assumed to be maintained by the normal cellular enzymatic systems of the tissue.

3.2 Materials

D-(+)-Glucose was purchased from Sigma Chemicals, NaCl, $NaHCO_3$, KCl, KH_2PO_4, Na_2SO_4, $CaCl_2.2H_2O$, $MgCl_2.6H_2O$ were purchased from Fischer Scientific, water purified with Barnstead Nanopure II system, 2-bromo-2-chloro-1,1,1-trifluroethane (halothane) was purchased from Aldrich Chemical Company Inc., MO, Xylazine from Bayer Corporation, IO and Ketamine from Fort Worth Laboratories Inc., KS.

3.3 Subjects

Male Sprague Dawley rats (250-350 g) were bred and housed in AALAC approved Animal Care Unit facility of the University of Kansas with free access to food and water. Rats were undisturbed in their home cages prior to the experiment and were housed in groups of three.

3.4 Apparatus

The YSI 2700 SELECT glucose analyzer was used for the measurement of D-glucose. Briefly, the analyzer consists of an enzyme glucose oxidase sandwiched between two cellulose acetate films. This forms the head or the probe. The probe is situated in a buffer filled sample chamber in which the sample is injected using an aspirator. Some of the substrate diffuses through the membrane when it contacts the immobilized enzyme, it is rapidly oxidized producing H_2O_2. Following reaction occurs at the probe head,

$$\beta\text{-D-glucose} + O_2 \xrightarrow{GOx} \text{glucono-}\delta\text{-lactone} + H_2O_2 \qquad \text{Reaction 3.1}$$

$$H_2O_2 \xrightarrow[+600\ mV]{} H_2O + 2e^- + O_2 \qquad \text{Reaction 3.2}$$

H_2O_2 produced in the enzyme reaction is oxidized at a constant applied potential of +600 mV, producing electrons. The electron flow is linearly proportional to the steady state concentration and, therefore, to the concentration of the substrate. The concentration can be easily read through the LCD display panel on the instrument and recorded on paper. The limit of detection is 0.05 mM. The instrument calibrates itself every 30 minutes. The minimum sample volume is 10 μL. Unless otherwise specified, samples of 15 μL were collected for all the experiments. Sample analysis time using the analyzer is 30 sec.

3.5 Microdialysis Probes

The microdialysis probes, made of inert bio-compatible non metallic polymers were purchased from Bioanalytical Systems, Inc., W. Lafeyette, IN. Briefly, the probe had an active length of 2 or 4 mm and an outer diameter of 320 μm. Unless otherwise specified, 4 mm probes were used throughout this work. The membrane, made of polyacrylonitrile (PAN), had a molecular weight cutoff ~29,000. The guide cannula, consisting of a stainless steel stylet and a length of 10 mm, o.d. of 520 μm, were purchased from BAS, Inc. The probes were perfused with artificial cerebrospinal fluid (aCSF) with the following composition: 154.7 mM Na^+, 2.9 mM K^+, 1.1 mM Ca^{2+}, 0.82 mM Mg^{2+}, 139.49 Cl^- at pH 7.4. During perfusion, the inlet was connected to a 500 μL BAS Gastight Syringe and the perfusion flow rate was controlled by a microinjection pump (Model CMA/100). The dialysate was collected from the outlet line into polyethylene microcentrifuge tubes (250μL, Fischer Scientific). The inlet and outlet lines were purchased from BAS (FEP, 0.65 mm o.d., 0.12 mm i.d.) and were connected to a dual channel Teflon lined liquid swivel (BAS, Inc.).

3.6 Surgical Procedure

Male Sprague Dawley rats weighing 250-350 g were anaesthetized briefly with gaseous halothane. A mixture of ketamine and xylazine (150 mL/per kg body weight) was prepared and 0.35 mL was injected IM. If required, more anesthetic was injected, during surgery. Stereotaxic surgery and probe placements were performed using a

standard rat brain atlas (Paxinos *et al.,* 1986) and a lab standard stereotaxic instrument (Stoelting Co., Wood Dale, IL, U.S.A.) The guide cannula was placed in the right striatum (coordinates from bregma: A/P 1.0 mm, M/L 2.5 mm, from dura: -6.0 mm), and secured with skull screws and dental acrylate. Following surgery, the animals were placed in large plastic bowls and allowed to recover for 24 hours. The health of the animals was assessed following recovery in accordance with published guidelines (Morton *et. al.*, 1985). All surgical procedures were performed according to the recommendations of the Animal Care Unit.

3.7 *In vitro* experiments

To characterize the recovery of glucose *in vitro*, the dialysis probe was placed in vials containing different concentrations of glucose (1-5 mM). A dry heat block (Thermolyne Type 17600 Dri Bath) maintained at 37°C controlled the temperature of the glucose solutions. The solution was stirred continuously with a magnetic stirrer and the probe was perfused with aCSF, via a high precision syringe pump (BAS Baby Bee Syringe Drive), for recovery experiments and glucose concentrations (1-5 mM) for delivery experiments, at perfusion flow rates of 0.5, 1.0, 1.5, 2.0 μL/min. Dialysate fractions were collected during 8 to 30 minute time intervals, depending on the flow rate, and the concentration of glucose was determined using the YSI 2700 SELECT glucose analyzer.

3.8 *In vivo* experiments

Glucose solutions of concentrations ranging from 0.5 to 10 mM were prepared with aCSF. After surgery, the rats were allowed to recover for 24 hours. The microdialysis probe was soaked in water for 24 hours before implantation. The *in vitro* probe performance i.e. EE_r and EE_d was determined before the experiment. On the day of the experiment, the rats were divided into groups of three and the probes were carefully inserted into the guide cannula. The probes were perfused with aCSF and allowed to equilibrate for 1.5 hours at a fixed flow rate (0.5, 1.0, 1.5 or 2.0 μL/min) before sample collection began. Each group was then perfused with glucose

solutions ranging from 0.5 to 5 mM and sometimes up to 10 mM concentrations in random order. Only data collected at steady state was used for the zero net flux calculations. The collection intervals depended on flow rate for samples of 15 μL volume. After the experiment, the rats were euthanized and the probes were carefully removed. Their *in vitro* recoveries and deliveries were verified the next day.

3.9 Statistical Data Analysis

The data from the *in vivo* experiments were analyzed by linear regression using STATMOST 2.5 for Windows, DataMost Corporation. The data analysis was performed by graphing C_d - C_p, the difference between the concentration of glucose perfused through the probe (C_p) and that obtained from the dialysate (C_d) versus C_p. (see Figure 3.1). Linear regression of these data yielded a slope (*in vivo* recovery) and an intercept (C_p at C_d-C_p=0). To calculate the extracellular concentration, the linear function, $y = ax + b$ was solved for x at the point of no net flux, that is, when y = 0. Therefore, C_e, concentration external to the probe, is equal to $x_{y=0} = - b/a$, where b is C_d at C_d-C_p = 0.

The equation $SEM_{ext} = [(S_b/b)^2 + (S_a/a)^2]^{1/2}$ was used to calculate the error for the extracellular glucose concentrations, S_b is the standard deviation of the y intercept, S_a is the standard deviation of the slope, b is the Y-intercept and a is the slope. In all cases, error was reported as the standard error of the mean (SEM). Several statistical tests were used to evaluate data from the experiments. All the formulae, tables used were found in any standard statistical textbook (Miller *et al.*, 1993). When a Student's t-Test was used, the null hypothesis was either that the sample means derived from two methods differ significantly from a standard value or that the two means derived from two methods not differ significantly.

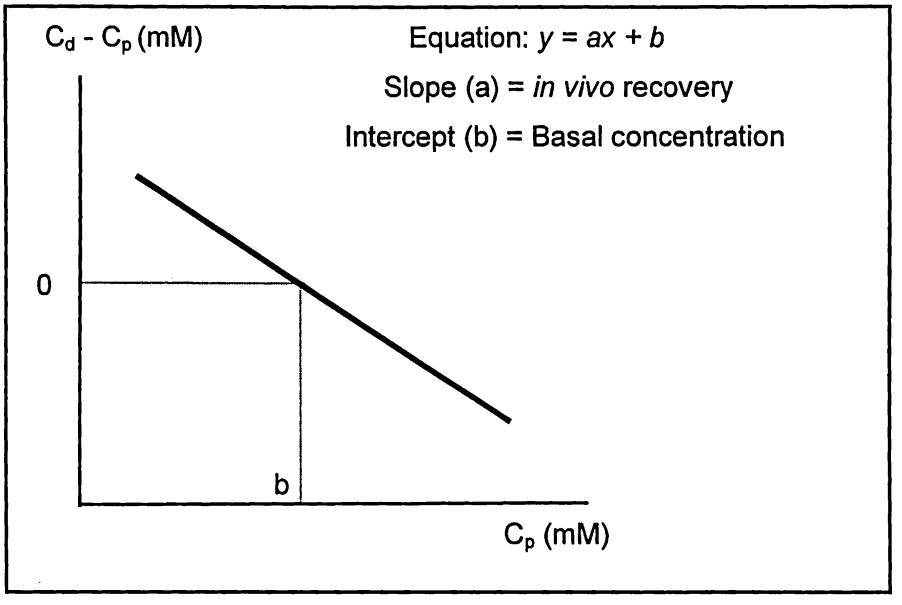

Figure 3.1 ZNF approach for determination of *in vivo* recovery and extracellular concentration

3.10 Results

3.10.1 *In vitro* evaluation of probe function

The factors affecting probe function are concentration, flow rate, temperature, time, diffusion coefficient, size and composition of membrane and the flux or mass recovery (Benveniste *et al.,* 1992). Evaluation of the commercial BAS probes for their concentration, flow rate, temperature and time dependence was performed *in vitro.* Since glucose was the substance of interest, the *in vitro* diffusion coefficient in aCSF is assumed to be the same as in water. Similar probes, from the same manufacturer were used, therefore, the size and composition of the membrane was assumed to be the same. The mass recovery or flux was also evaluated *in vivo.*

3.10.1.1 Concentration dependence

In order to understand the behavior of the microdialysis probes, a series of experiments was conducted. In all cases, probes were calibrated in exactly the same

manner. It has been shown that the extraction efficiency of the probes is independent of concentration (Zhao *et al.*, 1995) and this was tested by determining the EE of three 4 mm BAS probes (Figure 3.2). The concentration range chosen bracketed the estimated concentration of glucose in the rat brain. Standard glucose solutions of 0.5, 2.5 and 5.5 mM were prepared and a series of *in vitro* EE calibrations were done in both the recovery and delivery modes. The probes were randomly selected from different batches.

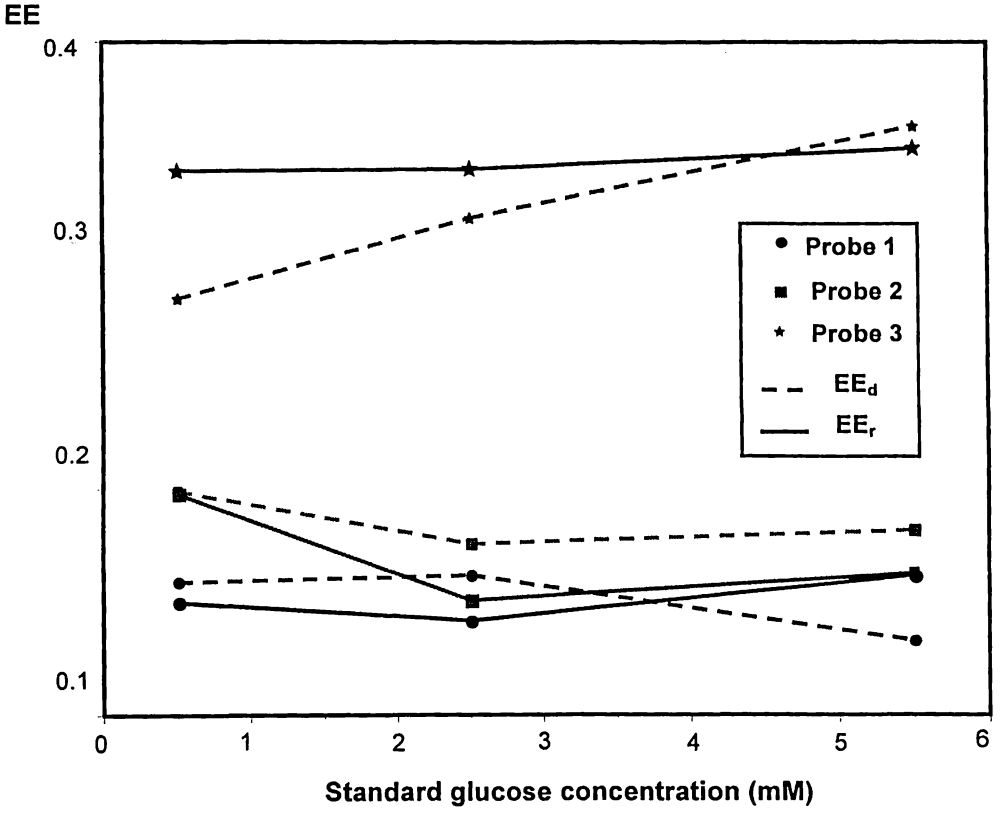

Figure 3.2 Probe performance variation with concentration

Furthermore, it has been shown that *in vitro* calibrations of a microdialysis probe in a stirred, temperature controlled solution are suitable for determining extraction efficiencies (Stenken *et al.*, 1993). A hydrodynamic environment is one where the velocity of a solution flowing past the fiber membrane is sufficiently fast such that the extraction efficiency is determined by diffusion of the analyte through the probe membrane. Therefore, if the extraction efficiency of a probe for a given analyte is

limited only by the diffusive resistance imposed by the membrane, then the extraction efficiency will be independent of extraction mode (i.e. $EE_r = EE_d$).

The statistical analysis of the data in Figure 3.2 is summarized in Tables 3.1 and 3.2. The inter probe variation was 10.5% rsd and the intra probe variation was 1.7% rsd. For this small sample set, the intra probe EE for glucose was independent of concentration and direction. There was significant inter probe variation and this was probably due to the fact that the probes belonged to different batches and the composition of the membrane could have been different from batch to batch. This seems more likely since all the probes were calibrated in exactly the same manner. For this reason, all the probes were first calibrated *in vitro,* before and after every *in vivo* calibration.

Table 3.1 EE_r +/- SEM of 3 probes with different concentrations in the environment surrounding the probe (C_s)

	[Extraction Efficiency]$_r$ +/- SEM in the recovery mode			**T test** intraprobe
C_s	0.5 mM	2.5 mM	5.5 mM	
Probe 1	0.150 +/- 0.020	0.142 +/- 0.032	0.186 +/- 0.041	S
Probe 2	0.198 +/- 0.018	0.151 +/- 0.085	0.163 +/- 0.052	S
Probe 3	0.342 +/- 0.036	0.343 +/- 0.049	0.352 +/- 0.055	S
T test interprobe	D	D	D	

n=3, D = significantly different, S = NOT significantly different, *p=0.005*

Table 3.2 EE_d +/- SEM of 3 probes with different perfusate concentrations (C_p)

	[Extraction Efficiency]$_d$ +/- SEM in the delivery mode			**T test** intraprobe
C_p	0.5 mM	2.5 mM	5.5 mM	
Probe 1	0.159 +/- 0.024	0.162 +/- 0.005	0.133 +/- 0.019	S
Probe 2	0.199 +/- 0.056	0.176 +/- 0.040	0.182 +/- 0.006	S
Probe 3	0.285 +/- 0.008	0.321 +/- 0.061	0.362 +/- 0.021	S
T test interprobe	D	D	D	

n=3, D = significantly different, S = NOT significantly different, *p=0.005*

3.10.1.2 Flow rate dependence

The probes were evaluated for their EE_r at different perfusion flow rates. Briefly, aCSF was perfused through the 4 mm brain microdialysis probe in a calibration vial containing 2.5 mM glucose solution. The temperature of the calibration vial was maintained at 37°C in a heat block. The perfusion flow rate was varied from 0.25, 0.50, 1.0, 1.5, 2.0, 3.0 μL/min and the *in vitro* EE_r was determined. Figure 3.3 illustrates that EE_r increases when the perfusion flow rate declines and theoretically, the EE_r values would reach 100% at zero flow. It has been generally been assumed that higher concentrations in the dialysate i.e. recovery observed immediately after perfusion will result in a traumatic tissue response. In this case, the probe was allowed to equilibrate in the calibration solutions for 40 minutes before sample collection began.

3.10.1.3 Time dependence

In the following experiment, the time profile of EE_r in the initial 50 minutes after introduction of probe in the calibration solution was evaluated *in vitro*, i.e. sample collection began before the probe was allowed to equilibrate with the surrounding

medium. It was found that this initial perfusion was required to allow the probe to equilibrate with the surrounding environment. Probes used had an active membrane length of 2 mm and glucose solutions of 2.86, 8.70, 11.0 mM concentrations were used for calibration. The flow rate was kept constant at 2 μL/min.

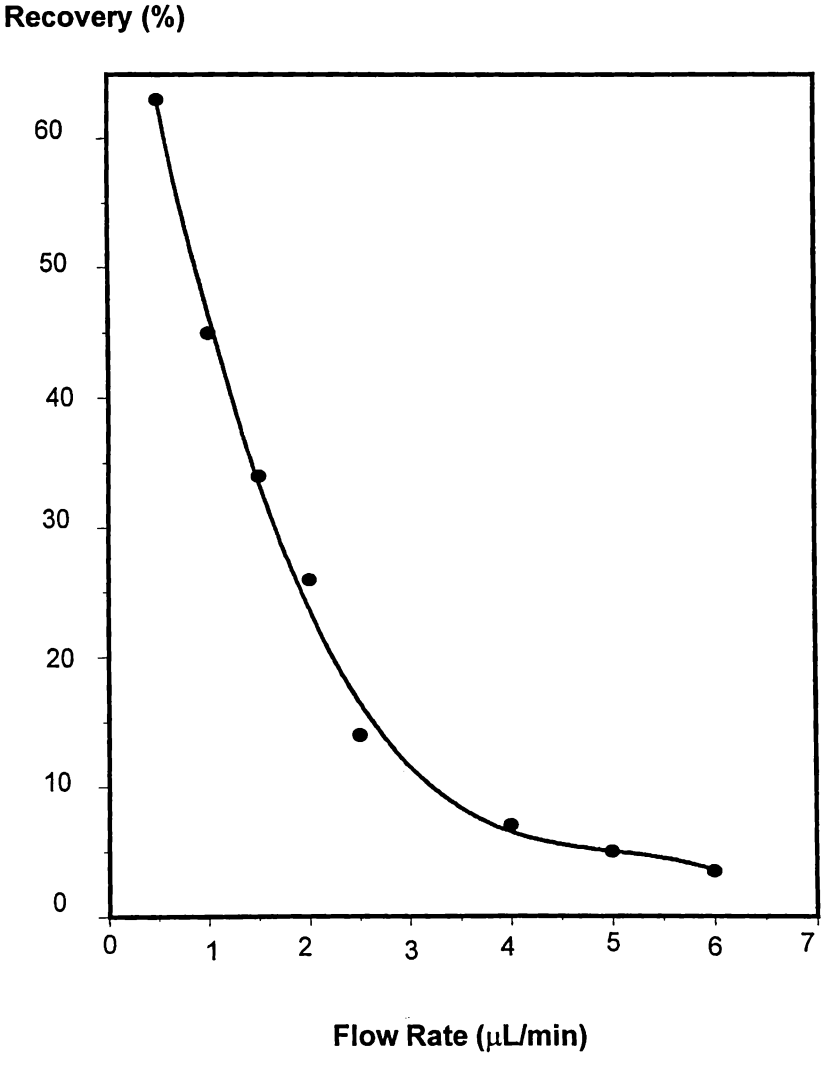

Figure 3.3 Effect of EE_r on perfusion flow rate.

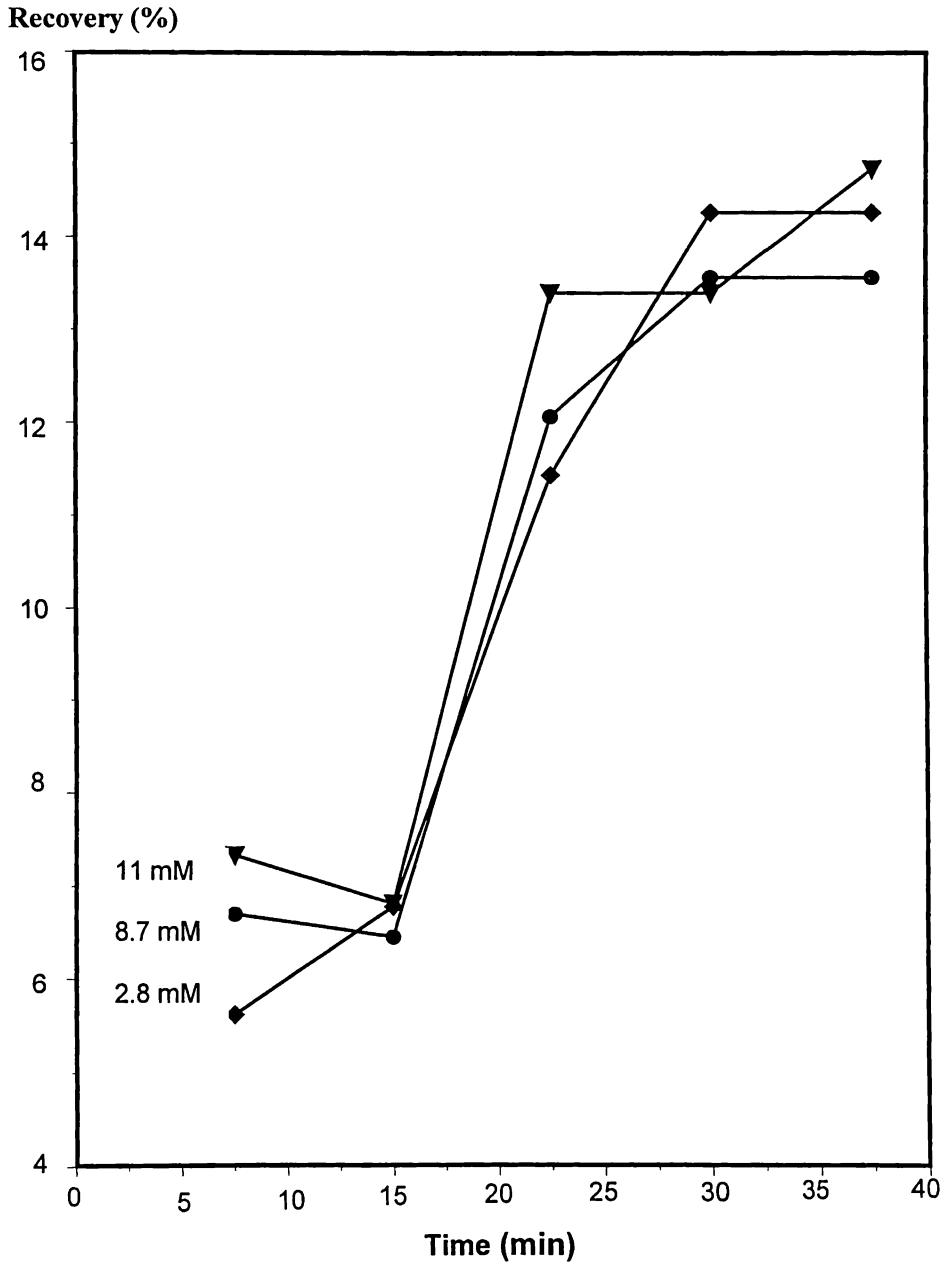

Figure 3.4 Time dependence of EE_r of 2 mm microdialysis probe at constant flow rate of 2 μL/min, (0 min is the time at which probe was introduced into the calibration vial).

Figure 3.4 indicates that EE_r tend to reach constant values after ~30 minutes from the time of immersion of the probe in the perfusion fluid. Therefore, it is important that

in vitro sample collection be started after at least of 30 minutes of continuous perfusion. This phenomenon of time dependence of EE_r can be explained by the presence of a maximal steep concentration gradient across the dialysis membrane initially when the probe is inserted in the medium. The gradient gradually diminishes due to removal of substance.

3.10.1.4 Temperature dependence

The fact that diffusion coefficients increase 1-2% per °C (Bard and Faulkner, 1980) readily explains the temperature dependency of EE_r. Recovery may increase 30 % if the temperature is increased from 23°C to 37°C (Wages *et al.*, 1986, Benveniste, 1989, Lindefors *et al.*, 1989). It is essential to perform the *in vitro* calibration at temperatures identical to *in vivo* conditions (Zetterstrom *et al.*, 1982, Korf and Venema, 1985, van Wylen *et al.*, 1986, Wages *et al.*, 1986, Young and Bradford, 1986, Benveniste *et al.*, 1989)

The EE_r of microdialysis probe was evaluated first, by keeping the calibration vial at 37° C with stirring in a temperature controlled heating block and second, by evaluating the non stirred EE_r at room temperature. The flow rate was kept constant at 2 µL/min and the calibration vial contained 2 mM glucose solution.

Table 3.3 Effect of temperature on EE_r.

	37°C (stirred)	Room Temperature (Non stirred)	% Decrease
EE_r	0.269 +/- 0.023	0.178 +/- 0.034	33.83

As shown in Table 3.3, the EE_r of the probe was significantly lower at room temperature than its corresponding value at 37°C. The % decrease was 33.83%. This observation indicates the importance of maintaining the system at body temperatures i.e. 37° C, while performing *in vitro* calibrations.

3.10.2 *In vivo* calibration of probes using the zero net flux calibration

In order for the zero net flux calibration method to work, several conditions must be satisfied (Morrison *et al.,* 1991).

- Metabolism or transport must be linear (zero or pseudo first order)
- Tissue binding must be rapid and linear.
- No sources or sinks for the analyte exist within the dialysate membrane.
- Tissue diffusion occurs predominantly through extracellular space
- Sampled substance may enter or leave tissue by transport across walls of uniformly distributed microvessels.
- Axial diffusion is minor
- The probe must be operating at steady state.

Initially, these conditions were assumed to be true for glucose.

Certain physiological factors limit the experimental conditions used in this calibration.

3.10.2.1 Tissue response

Microdialysis is an invasive technique and therefore, changes in brain tissue occur after probe implantation. The first change is disruption of the blood brain barrier (BBB). The BBB integrity has been measured after implantation of a microdialysis probe with BBB-impermeable substances such as α-amino-isobutyrate and sodium technitate (Benveniste *et al.*, 1984, Tossman and Ungerstedt, 1986). Despite some degree of brain tissue trauma produced by the insertion procedure, the BBB around the microdialysis probe was intact shortly (30 min to 2 h) after implantation. No reports on BBB integrity in chronic preparations (>1 day) are currently available.

Measurements of local cerebral blood flow (ICBF) have shown that ICBF decreases by approximately 50% within 1 hour after implantation of a horizontally positioned microdialysis probe into the rat hippocampus (Benveniste *et al.*, 1987). The vertical probe design seems to be less invasive (Sandberg and Benveniste, 1989), because implantation of this type of probe into one hippocampus did not evoke changes in ICBF (evaluated after 2 hours), and the local glucose consumption was only

moderately increased (approx. 50% of values obtained by the horizontal probe). By 24 hours after probe implantation, ICBF and local glucose consumption (CMR_{glu}) were near normal in all brain regions. (Benveniste *et al.,* 1987). Therefore, all calibrations were carried out 24 hours after surgery.

It is well established that tissue reactions are unavoidable in the vicinity of implants and lesions (Del Rio Hotega and Penfield, 1972, Collias and Manuelidis, 1957, Stansaas and Stensaas, 1976). Inflammatory changes resulting in gliosis and fibrosis may change local brain metabolism and blood flow, as well as tissue diffusion characteristics. Astrocyte growth begins to surround the probe (Benveniste and Diemer, 1988, Hamberger and Nystrom, 1984) 48 - 72 hours after probe implantation. Since the EE of a microdialysis probe is dependent on the biochemical properties (e.g. metabolism, uptake, etc.) of the tissue and since each cell type exhibits its own unique biochemistry, the calibration experiment should be designed to occur within a time frame where the normal biochemical properties of the tissue exist. As the astrocyte is a cell type different from than the normal paranchymal cells present in the hippocampus, it is not unreasonable to assume that once the probe is surrounded by astrocytes, the neurochemical environment will not be the same as in normal tissue, and therefore, the EE of the microdialysis probe for a given compound would change. This limits the window of time acceptable for *in vivo* calibration experiments in the normal tissue to less than 48 hours after surgery.

3.10.2.2 Establishment of steady state

Steady state is achieved when the concentration of a substance is independent of time. To reach a preliminary estimate about the length of time steady state is maintained and the time required for the next steady state to be attained, the following experiment was designed. aCSF minus glucose, was perfused through the brain of freely moving animals for ~3.5 hours and then the glucose concentration was stepped up to 2.5 mM. Glucose perfusion, at 2 μL/min, was carried out for a period of ~3 hours. The objectives of this experiment were two fold, first, to approximate the duration at which steady state is maintained and second, to determine the time required for the next steady state to be reached. Figure 3.5 illustrates that attainment

of the next steady state, on perfusion with 2.5 mM glucose was rapid, on the time scale of ~15 minutes. The experiment also indicated that glucose levels remain steady for at least 3 hours.

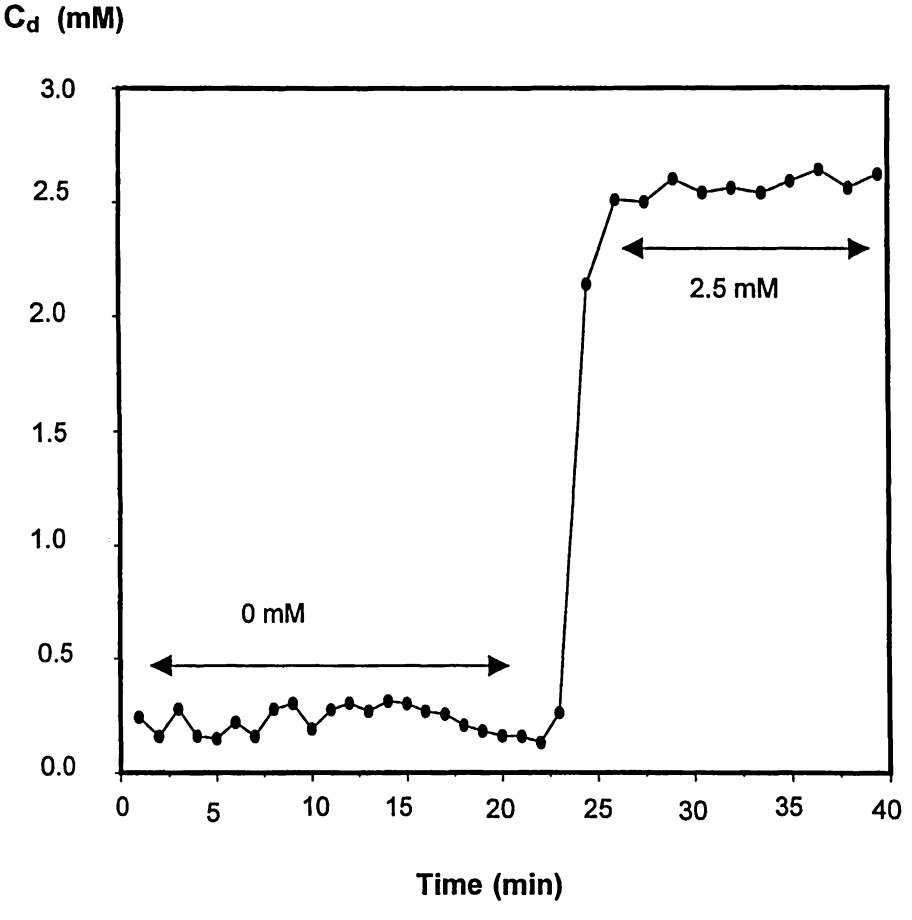

Figure 3.5 Glucose concentration time profile at 0 mM glucose and 2.5 mM glucose added to the perfusion media.

Next, the effect of continuous aCBF perfusion along with stepped increases in glucose concentrations in the perfusate was studied. As shown in Figure 3.6, the time profile reveals that achievement of steady state is rapid. Only data at steady state were selected for ZNF calibration.

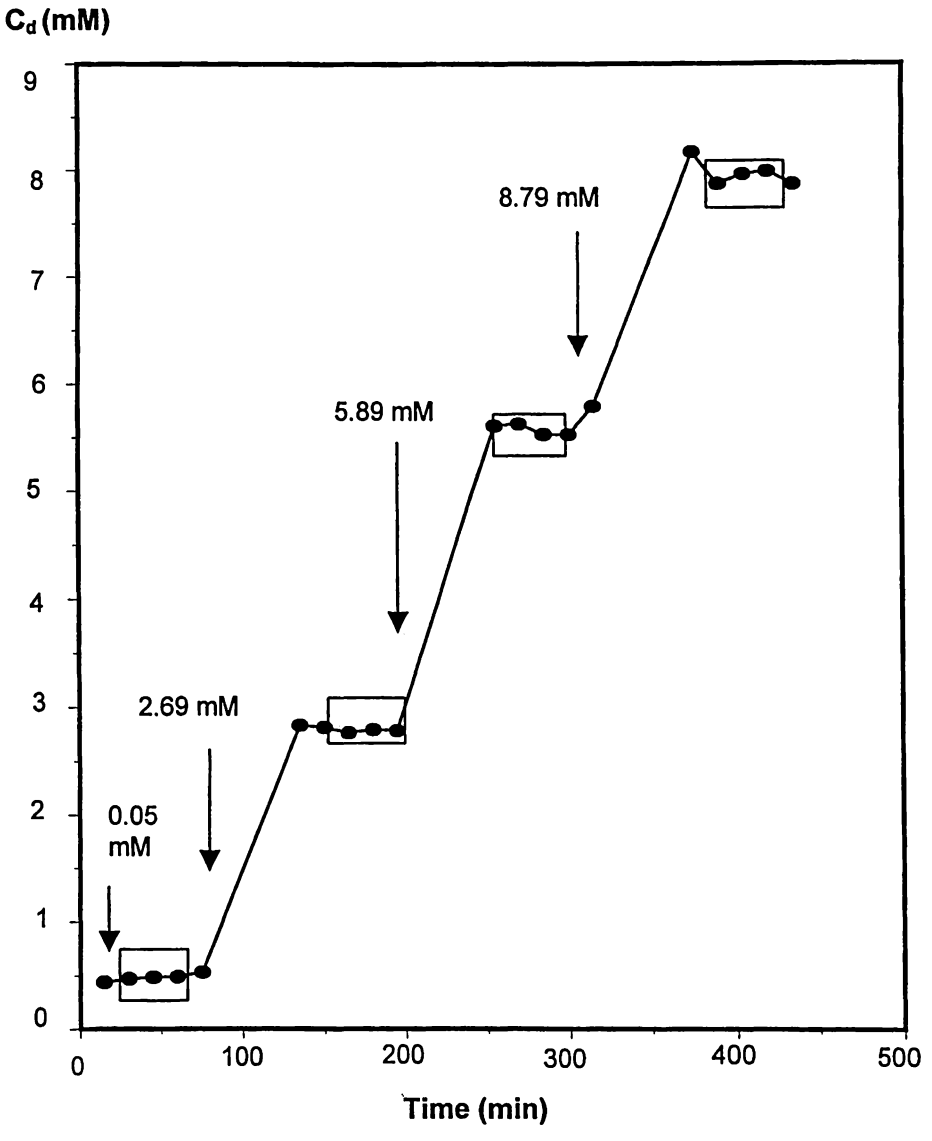

Figure 3.6 Time profile of glucose concentration from a ZNF experiment at 1.0 μL/min perfusion flow rate. The boxed regions represent the concentrations used to determine the Y axis in the ZNF plot.

3.10.2.3 Measurement of dialysate glucose levels

The basal glucose concentrations, as detected in the dialysate dropped significantly on succeeding days (Figure 3.7). Thus 72 hours after probe implantation, the dialyste glucose concentration was reduced to 13% of the levels observed at 24 hours. On

this basis, all subsequent experiments were performed 24 hours after probe implantation.

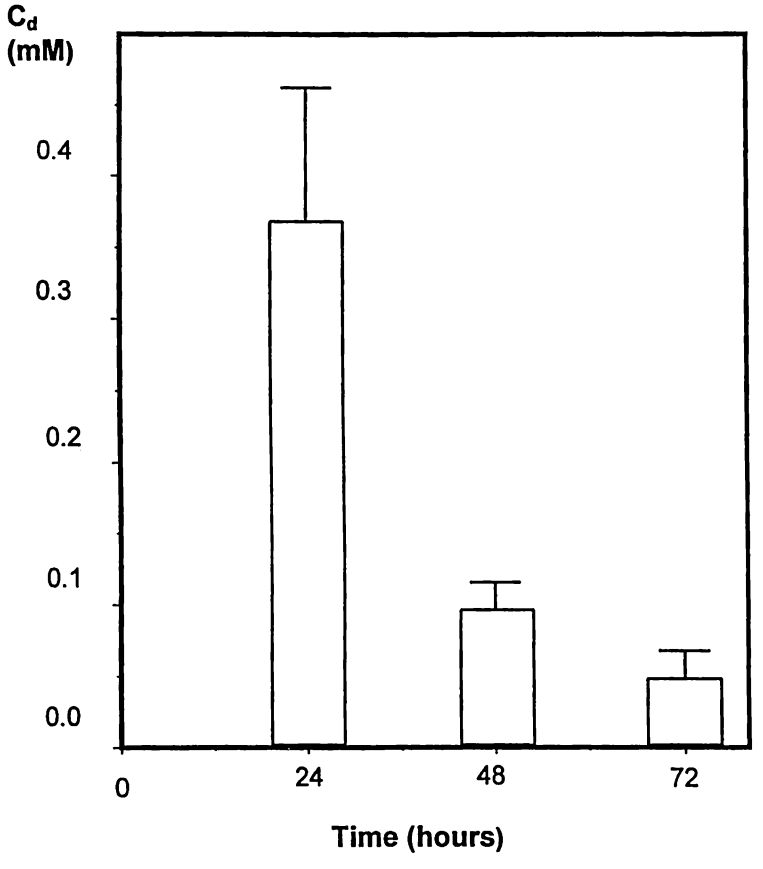

Figure 3.7 Concentration of dialysate glucose levels over 3 days. Measurements were made in the same animals following implantation of probe, *n= 3.*

3.10.2.4 Evaluation of probe function pre and post ZNF calibration

The EE (both in the recovery as well as delivery modes) of the probes before and after each ZNF calibration was performed at all the flow rates under consideration.

Table 3.4 EE_r of the probes before the ZNF calibration

Flow Rate (μL/min)	[Extraction Efficiency]$_r$ +/- SEM of the probes before ZNF calibration			Average +/- SEM
0.5	0.645+/-0.012	0.635+/-0.008	0.682+/-0.012	0.654+/-0.027
1.0	0.440+/-0.015	0.450+/-0.002	0.403+/-0.012	0.431+/-0.044
1.5	0.325+/-0.003	0.319+/-0.014	0.316+/-0.007	0.320+/-0.048
2.0	0.200+/-0.026	0.248+/-0.009	0.258+/-0.003	0.235+/-0.135

n=3, SEM = standard error of the mean

Table 3.5 EE_d of the probes before the ZNF calibration

Flow Rate (μL/min)	[Extraction Efficiency]$_d$ +/- SEM of the probes before ZNF calibration			Average +/- SEM
0.5	0.625+/-0.005	0.62+/-0.001	0.670+/-0.013	0.638+/-0.019
1.0	0.425+/-0.020	0.407+/-0.006	0.411+/-0.013	0.414+/-0.058
1.5	0.306+/-0.049	0.312+/-0.008	0.314+/-0.006	0.310+/-0.165
2.0	0.179+/-0.015	0.282+/-0.004	0.234+/-0.019	0.231+/-0.117

n=3, SEM = standard error of the mean

Table 3.6 EE_r of the probes after the ZNF calibration

Flow Rate (μL/min)	[Extraction Efficiency]$_r$ +/- SEM of the probes after ZNF calibration			Average +/- SEM
0.5	0.579+/-0.011	0.606+/-0.007	0.598+/-0.032	0.594+/-0.089
1.0	0.387+/-0.008	0.426+/-0.009	0.381+/-0.003	0.398+/-0.028
1.5	0.319+/-0.000	0.278+/-0.010	0.287+/-0.012	0.294+/-0.055
2.0	0.158+/-0.003	0.230+/-0.014	0.239+/-0.001	0.209+/-0.064

n=3, SEM = standard error of mean

Table 3.7 EE_d of the probes after ZNF calibration

Flow Rate (μL/min)	[Extraction Efficiency]$_d$ of the probes after ZNF calibration			Average +/- SEM
0.5	0.770+/-0.010	0.591+/-0.003	0.692+/-0.026	0.684+/-0.038
1.0	0.380+/-0.002	0.411+/-0.003	0.358+/-0.002	0.383+/-0.000
1.5	0.312+/-0.000	0.290+/-0.000	0.258+/-0.006	0.286+/-0.023
2.0	0.145+/-0.006	0.252+/-0.008	0.210+/-0.012	0.202+/-0.005

n=3, SEM = standard error of mean

To test for significant differences between the EE before and after *in vivo* ZNF calibrations, T test was performed on the averages.

Table 3.8 The EE_r and EE_d, before and after each ZNF experiment

Flow Rate (μL/min)	[Extraction Efficiency]$_r$			[Extraction Efficiency]$_d$		
	Before	After	T test	Before	After	T test
0.5	0.654 +/- 0.024	0.594 +/- 0.089	D	0.638 +/- 0.019	0.684 +/- 0.038	S
1.0	0.431 +/- 0.044	0.398 +/- 0.028	S	0.414 +/- 0.058	0.383 +/- 0.000	S
1.5	0.320 +/- 0.048	0.294 +/- 0.055	S	0.310 +/- 0.165	0.286 +/- 0.023	S
2.0	0.233 +/- 0.135	0.209 +/- 0.064	S	0.311 +/- 0.117	0.202 +/- 0.005	S

S=NOT significantly different, D=significantly different, n=3, *p=0.005*

In Table 3.8, the significant difference in the EE_r before and after ZNF calibration could be attributed to factors such as adhesion of tissue macromolecules to the membrane surface after it was removed from the brain tissue. In Table 3.9, the significant difference between EE_r and EE_d after the ZNF calibration was attributed to the fact that the temperature of the heat block used to hold the calibration vial could not be held constant, at least on one particular day, due to power fluctuations.

Otherwise, for all the probes tested, there was no significant difference between the probes before and after the ZNF calibration or between the [EE] in the recovery and delivery modes.

Table 3.9 The EE_r and EE_d, before and after each ZNF experiment

Flow Rate (μL/min)	Before ZNF calibration			After ZNF calibration		
	$[EE]_r$	$[EE]_d$	**T test**	$[EE]_r$	$[EE]_d$	**T test**
0.5	0.654 +/- 0.024	0.638 +/- 0.019	S	0.594 +/- 0.089	0.684 +/- 0.038	D
1.0	0.431 +/- 0.004	0.414 +/- 0.058	S	0.398 +/- 0.028	0.383 +/- 0.000	S
1.5	0.320 +/- 0.048	0.310 +/- 0.165	S	0.294 +/- 0.055	0.286 +/- 0.023	S
2.0	0.235 +/- 0.135	0.231 +/- 0.117	S	0.209 +/- 0.064	0.202 +/- 0.005	S

S=NOT significantly different, D=significantly different, n=3, *p=0.005*

3.10.2.5 Linear regression analysis

12 animals were divided in groups of 3 and each group was perfused at a constant flow rate of either 0.5, 1.0, 1.5, 2.0 μL/min. Glucose concentrations were stepped up at different concentrations in a random order within a group. The perfusate concentrations (C_p) were plotted on the x-axis and the difference between the dialysate concentration (C_d) and the perfusate concentration (C_p) i.e. [C_d-C_p] was plotted on the y-axis. The data points collected at steady state glucose levels were made to fit a linear regression curve as shown in Figures 3.7, 3.8, 3.9, 3.10 at different perfusion flow rates. The slope of the lines is defined as the "*in vivo* recovery".

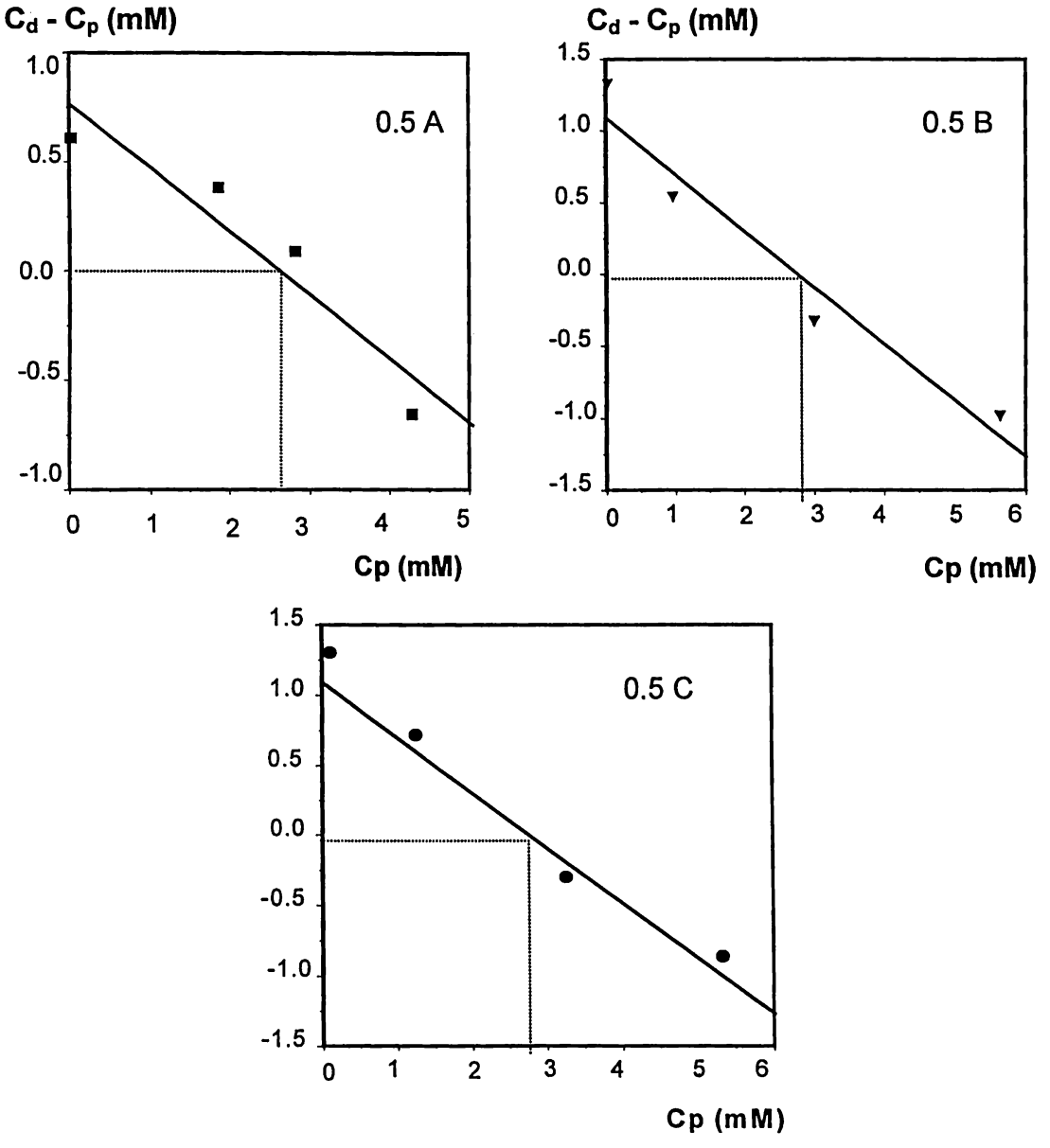

Figure 3.8 Linear regression lines, 0.5A, 0.5B, 0.5C at flow rate 0.5 μL/min

Table 3.10 Regression analysis statistics at perfusion flow rate of 0.5 μL/min

Subjects	Slope	Y intercept (mM)	Basal Glucose (mM)	r^2
0.5A	0.291	0.765	2.62	0.92
0.5B	0.395	1.092	2.75	0.94
0.5C	0.390	1.121	2.81	0.98
Av. +/- SD	0.358 +/- 0.031	0.992 +/- 0.197	2.72 +/- 0.09	0.94 +/- 0.03

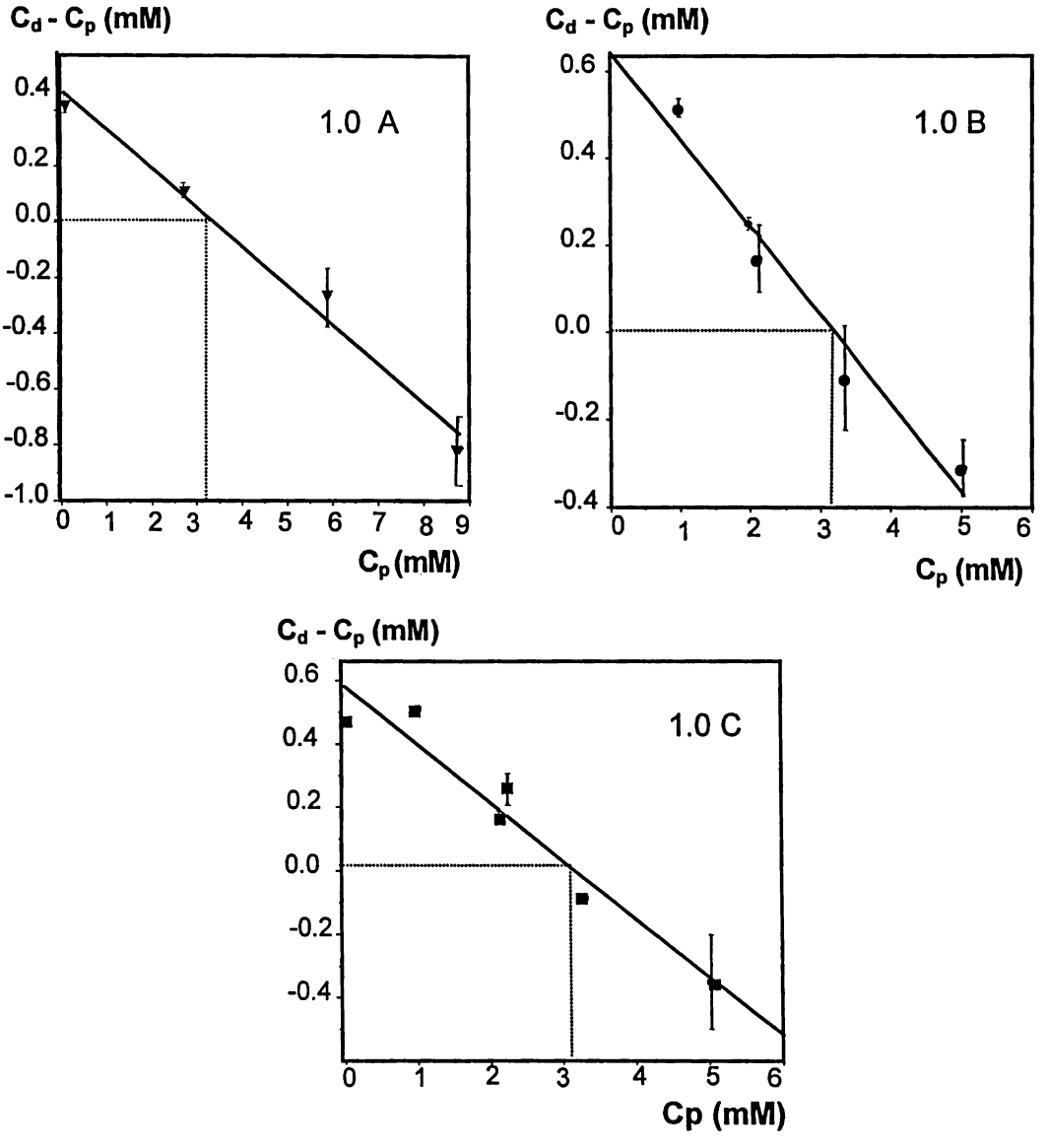

Figure 3.9 Linear regression lines, 1.0A,1.0B, 1.0C, at flow rate 1.0 μL/min

Table 3.11 Regression statistics at perfusion flow rate of 1 μL/min

Subjects	Slope	Y intercept (mM)	Basal Glucose (mM)	r^2
1.0A	0.140	0.472	3.36	0.99
1.0B	0.201	0.648	3.22	0.98
1.0C	0.183	0.581	3.17	0.93
Av. +/- SD	0.175 +/- 0.031	0.567 +/- 0.088	3.25 +/- 0.098	0.96 +/- 0.03

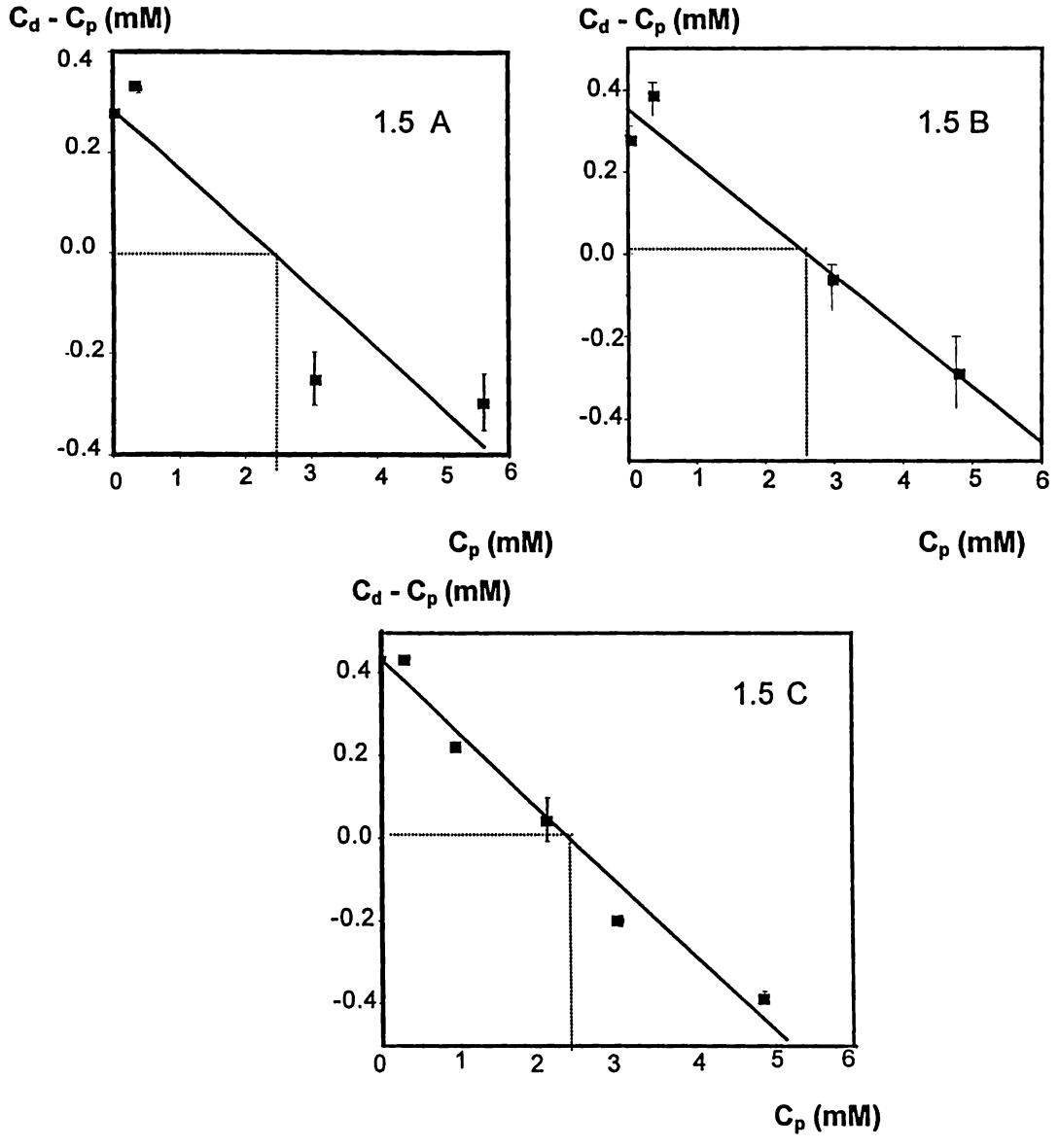

Figure 3.10 Linear regression lines 1.5A, 1.5B, 1.5C at flow rate of 1.5 μL/min

Table 3.12 Regression analysis statistics at perfusion flow rate of 1.5 μL/min

Subjects	Slope	Y intercept mM	Basal Glucose (mM)	r^2
1.5A	0.114	0.263	2.29	0.86
1.5B	0.135	0.353	2.60	0.95
1.5C	0.179	0.429	2.39	0.97
Av. +/-SD	0.143 +/- 0.033	0.348 +/- 0.083	2.42 +/- 0.15	0.92 +/- 0.05

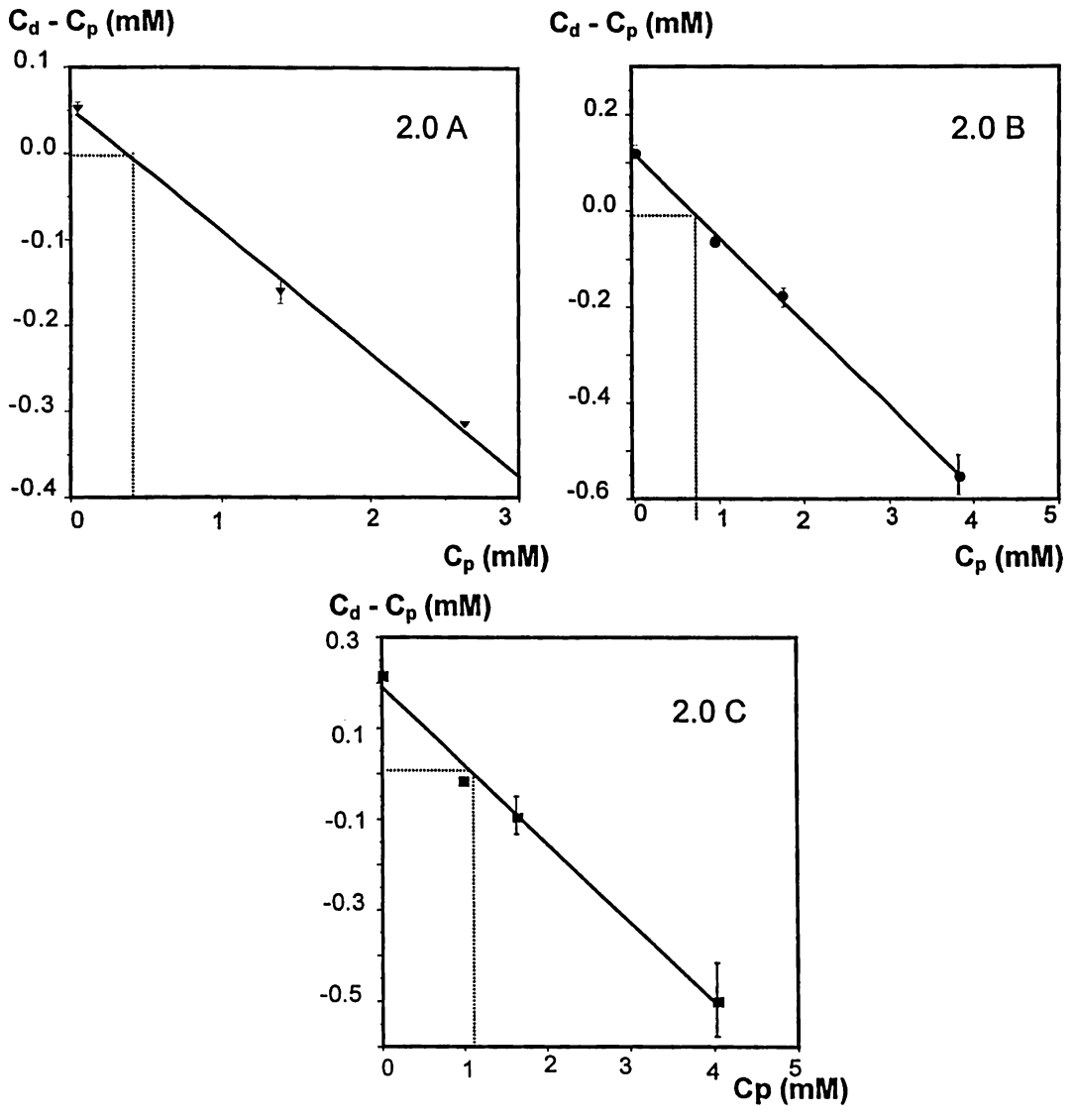

Figure 3.11 Linear regression lines, 2.0A, 2.0B, 2.0C, at flow rate of 2 μL/min

Table 3.13 Regression statistics at perfusion flow rate of 2.0 μL/min

Subjects	Slope	Y intercept (mM)	Basal value (mM)	r^2
2.0A	0.143	0.052	0.36	0.99
2.0B	0.174	0.119	0.68	0.99
2.0C	0.203	0.203	1.06	0.99
Av. +/- SD	0.173 +/- 0.030	0.125 +/- 0.075	0.70 +/- 0.35	0.99 +/- 0.00

3.10.2.6 Mass recovered

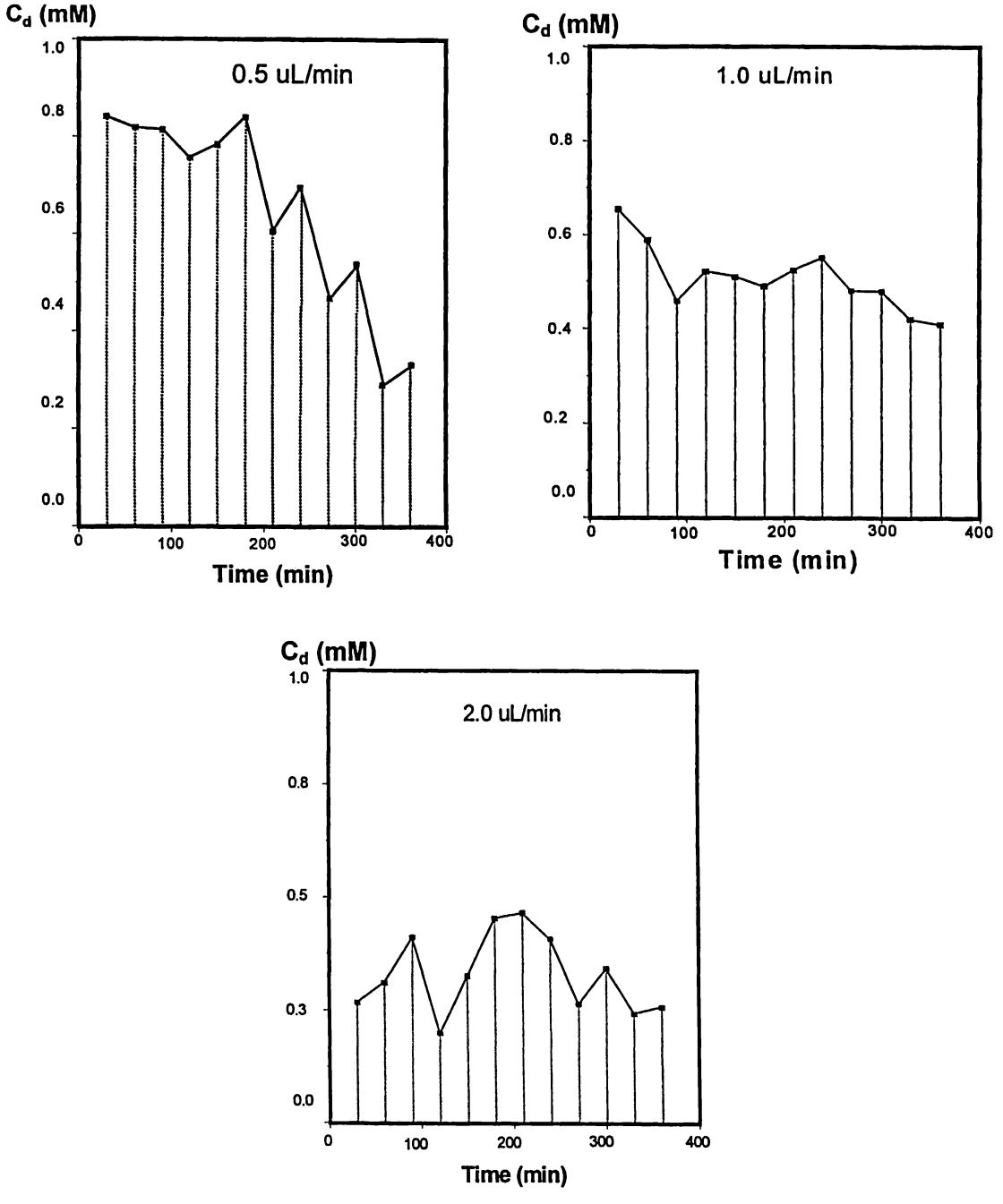

Figure 3.12 Concentration versus time profiles at 0.5, 1.0, 2.0 μL/min perfusion flow rates. The area under the curves was calculated as $_0\int^t$ C (t) dt, see Equation 3.1

The mass recovery or the flux is defined as the net transport of material per unit membrane area per time. Beneveniste *et al.*, 1993 have shown that the flux tends to increase with increasing flow rates and levels off at flow rates higher than 5 μL/min. This particular observation was examined *in vivo* for three perfusion flow rates of 0.5, 1.0 and 2 μL/min. Animals were divided into groups of three and each group was infused with aCSF without glucose for the same total time interval. Samples were collected at intervals of 30 minutes for each of the flow rates. The corresponding dialysate concentration was plotted against time to generate time Vs. concentration profiles, Figure 3.12. The area under the curve was integrated as $_0\int^t C(t)\,dt$ and the total mass recovered M_{tot} was calculated as,

$$M_{tot} = 0.18\,Q \;\; {}_0\int^t C(t)\,dt \qquad \text{Equation 3.1}$$

Q is the perfusion flow rate, dt is the change in time over the entire concentration profile, C (t) is the dialysate concentration measured over time and 0.18 is the conversion factor for glucose. As was expected, it was found that the mass recovered increased as the perfusion flow rate increased.

Flux J was calculated using the using the following equation,

$$J = Q\,C_d / A \qquad \text{Equation 3.2}$$

Where Q is the perfusion flow rate, C_d is the dialysate concentration and A is the area of the probe.

Table 3.14 Changes in the recovered mass and the flux with increase in the perfusion flow rate.

Flow Rate (μL/min)	Mass recovered (μg)	Flux (μmoles/min.cm^2)
0.5	1.618	0.769×10^{-5}
1.0	3.047	1.513×10^{-5}
2.0	3.871	1.959×10^{-5}

3.11 Discussion

This study was primarily undertaken to determine the basal glucose concentration in the striatum using microdialysis in awake freely moving rats. The expectation was that the slopes of the regression lines would change when the flow rate was varied. Specifically, a decrease in the *in vivo* EE_r as the flow rate was increased, was expected. But essentially, the point of zero net flux would remain unchanged i.e. the basal glucose concentration would remain constant. The striatum was chosen as the site of implantation because it is larger in size than the hippocampus. A larger area means that longer probes can be used. This means that the recovery of the probes would improve. Larger values of recovery would translate to steeper slopes for the ZNF linear regression lines. Statistically, the slope of the linear regression line needs to be as steep as possible to minimize the error in determining the intercept.

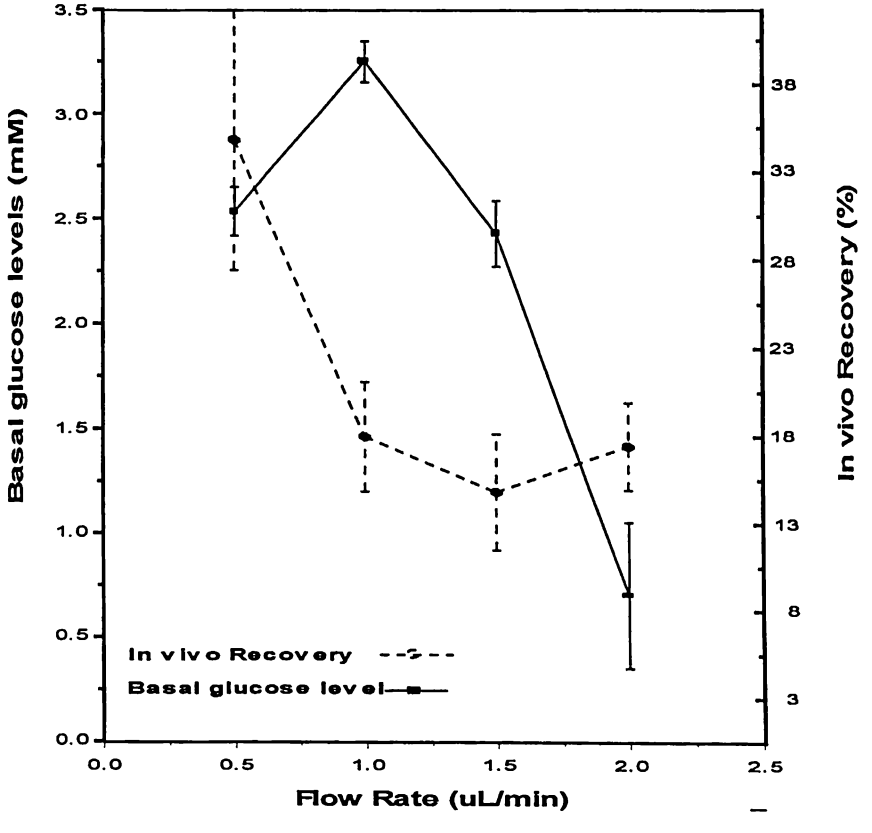

Figure 3.13 Changes in basal glucose concentrations and *in vivo* recovery EE_r versus flow rate, n=3

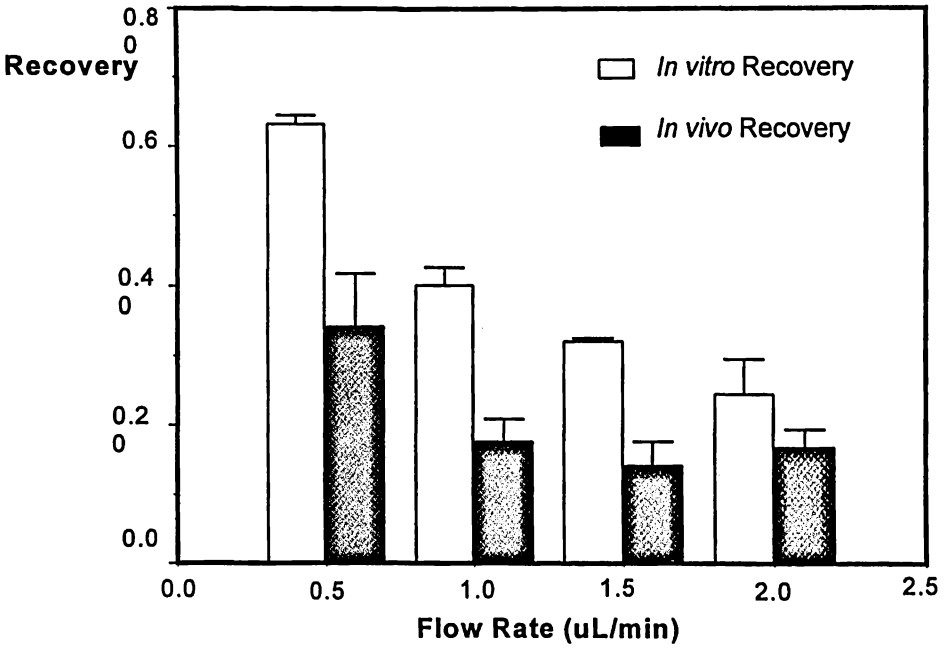

Figure 3.14 Comparison of *in vitro* and *in vivo* recovery

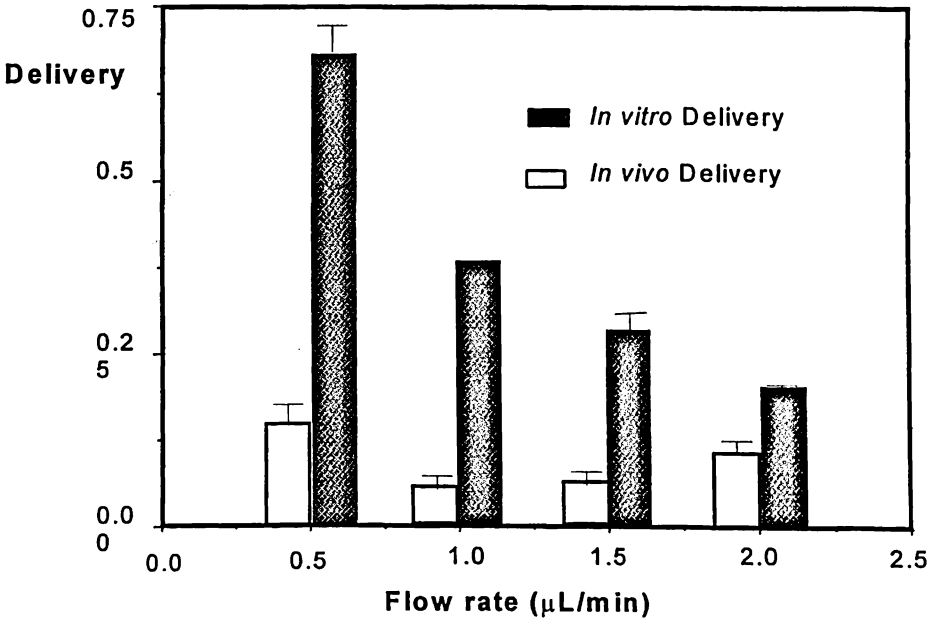

Figure 3.15 Comparison of *in vivo* and *in vitro* delivery

The results from the ZNF experiments indicated that when the flow rate was increased, the slope, defined as the *in vivo* recovery, along with the basal glucose levels changed, and in no apparent linear fashion. Particularly, at higher flow rates of 2 μL/min, the basal levels measured were the lowest. Refer to Figure 3.13.

Comparison of *in vitro* EE with the corresponding *in vivo* EE show that, the *in vitro* EE, at all perfusion flow rates has been consistently greater than the *in vivo* EE. Refer Figure 3.13 and Figure 3.15. This is expected because of the tortuosity factor in the tissue. In a hydrodynamic environment such as the *in vitro* case, the major resistance to diffusion is the membrane. In tissue environment, it has been shown that the major impediment to diffusion is resistance due to the tissue (Benveniste, 1991).

Certain compounds such as dopamine, adenosine (Baranowski *et al.,* 1994, Menacherry *et al.*, 1992) and tacrine (Hadwiger, 1995) have exhibited greater *in vivo* recoveries than their corresponding EE_r *in vitro*. The common factor associated with these compounds was rapid uptake from the cellular interstitium. In the case of dopamine, it was shown that cellular uptake of dopamine in the rat brain interstitium caused the unusual behavior. (Menacherry *et al.*, 1992). When either cocaine or GBR-12909 (inhibitors of dopamine uptake enzymes) were added to the perfusion fluid, *in vivo* EE_r for dopamine decreased roughly by 50% (Smith and Justice, 1994). Like dopamine, EE_r for adenosine was also attributed to cellular uptake from the renal interstitium, although, this was not validated. Furthermore, when reviewing the work of Baranowski *et al.*, it was interesting to note that the *in vivo* EE_r determined for adenosine with a ZNF calibration was approximately five times greater than its *in vitro* EE_r (Baranowski *et al.,* 1994). For tacrine in brain, the higher EE_r has been speculated to be due to the high affinity binding protein or a combination of enzyme systems (Hadwiger, 1995)

This does not seem to be the case for glucose as the *in vivo* EE_r have been consistently lower than *in vitro,* both pre and post ZNF calibration (Figure 3.14). Similar observation holds true for the EE_d (Figure 3.15). These observations are consistent with the tortuosity argument. In a tissue environment, a substance has to

diffuse through a tortuous path defined by the tortuosity factor λ (Benveniste et al. 1992), in contrast to a hydrodynamic in vitro environment. The resistance to diffusion is due to the tissue, *in vivo* whereas *in vitro*, the major resistance is due to the membrane. Also, the concentration of glucose in the extracellular space is a balance between not one, but at least four functions, namely, the cerebral blood flow, the uptake of glucose from the plasma via GLUT1 across the BBB, the uptake of extracellular glucose by the neuronal cells via GLUT3 and the subsequent utilization of glucose by the enzyme hexokinase. For a detailed review, refer Chapter 1 of this work.

An *in vivo* EE different from *in vitro* EE can result from both physical and physiological reasons. Some possibilities are interaction of glucose with the fiber membrane, hydrostatic or osmotic pressure differentials between the fiber lumen and the extracellular matrix, elimination of membrane resistance due to probe failure or a change in the charge (i.e. ionic state) of the analyte.

If the fiber membrane, rather than being a resistance to diffusion was actually a sink for glucose, then the PAN membrane would function like a chromatography column. Glucose would be retained in the fiber membrane until it was eluted off by aCSF or until the capacity of the membrane was exceeded. If this were true, the membrane would have to be saturated with glucose before diffusion into the brain could occur. The practical consequences of this would be that, prior to saturation of the fiber membrane, the amount of glucose trapped in the membrane would be fairly large and the resulting dialysate concentration would be fairly low yielding a high EE_d value. This does not hold true in the present study as repeated measurements of the EE_d yielded fairly reproducible values that were not significantly different from the EE_r *in vitro*. See Tables 3.4 and 3.5.

It has been reported that loss of fluid due to hydrostatic pressure gradients occurs at perfusion flow rates of 10 μL/min. At these flow rates, the probe was observed to "sweat" indicating loss of fluid from the perfusate (Kuipers and Korf, 1993). Due to this, the *in vivo* sampling perfusion flow rates were kept well below 10 μL/min. Also, if

the loss of perfusion solution were to occur due to formation hydrostatic pressure gradient, then the volume of dialysate recovered would decrease. This was not observed to occur as the volume of dialysate recovered was verified. The formation of osmotic gradient between the perfusion fluid (aCSF) and the brain CSF is unlikely as the composition of aCSF was chosen from a list of possible recipes all of which are isotonic with the brain CSF.

The extraction efficiencies of the probes in the delivery mode, were calculated for all the flow rates under consideration using equation 3.3,

$$EE_d \text{ (}in\ vivo\text{)} = \frac{C_p - C_d}{C_p} \qquad \text{Equation 3.3}$$

where C_p is the concentration of glucose perfused in the brain, C_d is the corresponding dialysate concentration. The slope of the ZNF plots was defined as the *in vivo* recoveries.

At this point, the reasons for the discrepancy in the measured values of basal glucose with change in the flow rate can be speculated to be due to Michaelis Menten kinetics of glucose transport and metabolism. GLUT3 has a K_m of 1.44 mM and would be saturated when glucose solutions are delivered during ZNF. Therefore, its transport is not linear. Metabolism, as described by the hexokinase (K_m = 0.04 mM) reaction is not linear either.

One good check on the accuracy of the ZNF calibration is to calculate the basal glucose values using Y intercept and the *in vivo* EE_r. Using the equation,

$$EE_{r\,(\text{in vivo})} = \frac{\text{Y intercept}}{C_{cal}} \qquad \text{Equation 3.4}$$

where C_{cal} is the calculated basal glucose concentration.
Rearranging the equation 3.4,

$$C_{cal} = \frac{\text{Y intercept}}{EE_{r\,(\text{in vivo})}} \qquad \text{Equation 3.5}$$

As seen in Table 3.15, there is a very good correlation between the experimentally determined basal glucose values and the calculated values. This means that the ZNF calibrations performed have been fairly accurate.

Table 3.15 Comparison of experimental and calculated basal glucose values

Flow Rate (μL/min)	$C_{exp.}$ (mM)	C_{cal} (mM)
0.5	2.693 +/- 0.091	2.679 +/- 0.011
1.0	3.268 +/- 0.097	3.014 +/- 0.276
1.5	2.432 +/- 0.158	2.025 +/- 0.597
2.0	0.705 +/- 0.347	0.708 +/- 0.129

Table 3.14 reveals that the mass recovered and the flux is higher at higher flow rates. (Benveniste *et al.*, 1992) have shown that the flux of substances (net transport of substances per unit membrane area per time) increases with flow rate until it levels off at flow rates above 5-10 μL/min. This is probably due to a diffusion limitation when the maximal concentration gradient across the membrane is attained. The stagnant flux could also be explained, however, by transport in the opposite direction mediated by filtration due to a positive hydrostatic pressure gradient (Johnson and Justice, 1983). This explanation seems unlikely because filtration or net fluid exchange (in both serial and parallel probe designs) was less than 0.1% at flow rates of 2 μL/min and of 10 μL/min (Lindefors *et. al.*, 1989). This means that, at higher flow rates, there is more depletion of glucose levels in the area surrounding the probe. At 2 μL/min, the higher flow rate could be instrumental in depleting the tissue of glucose in the recovery mode and hence, lower values are measured.

Fleck and others, using hippocampal brain slices have shown that reducing extracellular glucose concentration (0.2 mM) reduced glutamate release, enhanced aspartate release and reduced AMPA / kainate receptor mediated responses more than NMDA receptor-mediated responses (to 7% and 34% of control, respectively) (Fleck *et al.*, 1993). This finding shows importance in the present study in light of the fact that the calibration method infuses both low and high glucose concentrations in the perfusate. The authors conclude that whatever the source, decrease in glucose

should decrease glutamatergic and increase aspartatergic transmission. In a separate microdialysis study, Justice *et al.* have shown that infusing glucose into the brain tissue causes no apparent change on the lactate and pyruvate levels. But, the time scale of the microdialysis study must be borne in mind. The authors have reported no change in the lactate and pyruvate levels over a period of 30 minutes of glucose infusion. But a typical ZNF experiment can last anywhere from 6-8 hours. Whether the ZNF calibration method by itself causes a change in the levels of other substances (those that are intimately linked to glucose metabolism and need glucose as a precursor) is not known.

The zero net flux method of calibration of brain microdialysis probes is an empirical method. It involves removal and infusion of the substance being studied for extended periods of time. Even though this method is preferred over other calibration methods for determination of basal levels of endogenous substances, it is important to understand the nature of the endogenous substance and the physiology of the tissue being studied. This is especially true in cases such as glucose, wherein the transport and metabolism are defined by non linear, Michaelis-Menten kinetics. Indiscriminate use of this method for all and any analytes is ill advised. The dialysate glucose concentration measured under such conditions are not true representations of tissue concentrations. Therefore, the ZNF calibration, under such conditions, would give erroneous results.

3.12 Conclusions

The present study indicates that the basal glucose concentrations as measured by the ZNF calibration change significantly with variation in perfusion flow rates. Specifically, the values average to 2.7 +/- 0.4 mM at 0.5, 1.0, 1.5 μL/min, but drop to 0.7 +/- 0.3 mM at 2 μl/min perfusion flow rate.

The *in vivo* EE have been consistently lower than the corresponding *in vitro* EE. This is expected because an *in vitro* hydrodynamic environment does not account for factors such as tortuosity, which play an important role in the *in vivo* environment.

Also, since Michaelis-Menten kinetics describes the rates of transport and metabolism in the tissue, *in vivo* recoveries and deliveries do not match.

An explanation for the different basal glucose values measured at different flow rates can be sought by comparison of the *in vivo* recovery and delivery. The kinetics of GLUT3 transporter could get saturated depending on the amount of glucose that is being perfused in the tissue which, in turn, depends on the perfusion flow rate. Also, this high flow rate could be instrumental in depleting the tissue of glucose, in the recovery mode, and hence a lower value is measured. Even though a good correlation exists between the experimentally determined basal glucose values and the calculated values, the ZNF calibration if performed at 2 μL/min, is not a suitable technique for measurement of extracellular glucose in the rat brain.

Along with glucose, other substances like glutamate and aspartate and the catecholamine neurotransmitters are also removed. This may affect the basal glucose values obtained.

3.13 References

Baranowski, R., Westenfelder, C. Estimation of renal interstitial adenosine and purine metabolites by microdialysis. *Am. J. Physiol.* **1994**, *267*, F174-F182.

Bard, A. J., Faulkner, L. R. Electrochemical methods, Wiley and Sons, New York, **1980,** 153.

Benveniste, H. Brain Microdialysis. *J. Neurochem.* **1989**, *52*, 1667-1679.

Benveniste, H., Diemer, N. H. Early postischemic ^{45}Ca accumulation in rat dentate hilus. *J. Cereb. Blood Flow Metab.* **1988a**, *8*, 713-719.

Benveniste, H., Diemer, N. H. Cellular reactions to implantation of a microdialysis tube in the rat hippocampus. *Acta Neuropathol. (Berl.)* **1988b**, *74,* 234-238.

Benveniste, H., Drejer, J., Schousboe, A., Diemer, N. H. Evaluations of extracellular concentrations of glutamate and aspartate in rat hippocampus during transient cerebral ischemia monitored by intracerebral microdialysis. *J. Neurochem.* **1984,** *43,* 1369-1374.

Benveniste, H., Drejer, J., Schousboe, A., Diemer, N. H. Regional cerebral glucose phosphorylation and blood flow after insertion of a microdialysis fiber through the dorsal hippocampus in the rat. *J. Neurochem.* **1987**, *49*, 729-734.

Benveniste, H., Hansen, A. J., Ottosen, N. S. Determination of brain interstitial concentrations by microdialysis. *J. Neurochem.* **1989a**, *52*, 1741-1750.

Benveniste, H., Jorgenson, M. B., Sandberg, M., Christensen, T., Hagberg, H., Diemer, N. H. Ischemic damage in hippocampal CA1 is dependent on glutamate release and intact neuron innervation from CA3. *J. Cereb. Blood Flow Metab.* **1989b**, *9,* 626-639.

Benveniste, H., Hansen, A. J. Practical aspects of using microdialysis for the determination of brain interstitial concentrations. In: Microdialysis in the Neurosciences, In Justice, J., Robinson, T., eds, Techniques in the Behavioural and Neural Sciences. New York: Elsevier; **1991**, 47-80.

Bungay, P.M., Morrison, P. F., Dedrick, R. L. Steady-state theory for quantitative microdialysis of solutes and water in vivo and in vitro. *Life Sci.* **1990**, *46*, 105-119.

Collias, J. C., Manuelidis, E. E. Histopathological changes produced by implanted electrodes in cat brains. Comparison with histopathological changes in human and experimental puncture wounds. *J. Neurosurg.* **1957**, *14*, 302-328.

Del Rio Hotega, P., Penfield, W. Cerebral cicatrix: The reaction of neuroglia and microglia to brain wounds. *Bull. Johns Hopkins. Hosp.* **1972**, *41*, 278-303.

Fellows, L. K., Boutelle, M. G., Fillenz, M. Extracellular brain glucose levels reflect local neuronal activity: A microdialysis study in awake, freely moving rats. *J. Neurochem.* **1992**, *59*, 2141-2147.

Fleck, M., Henze, D. A., Barrionuevo, G., Palmer, A. M. Aspartate and glutamate mediate excitatory synaptic transmission in area CA1 of the hippocampus. *J. Neurosci.* **1993,** *13(9),* 3944-3955.

Hadwiger, M. Development of total microdialysis sampling systems: Analytical and Sampling considerations for Quantitative Microdialysis, *Ph.D. Diss.* University of Kansas, 1995.

Hamberger, A. Nystrom, B. Extra and intra cellular amino acids in the hippocampus during the development of hepatic encephalopathy. *Neurochem. Res.* **1984,** *9,* 1181-1192.

Jacobson, I., Sandberg, M., Hamberger, A. Mass transfer in brain dialysis devices- a new method for the estimation of extracellular amino acids concentration. *J. Neurosci. Methods.* **1985**, *15,* 263-268.

Johnson, R. D., Justice, J. B. Model studies for brain dialysis. *Brain Res. Bull.* **1983,** *10,* 567-571.

Korf, J., Venema, K. Amino acids in rat straital dialysate: Methodological aspects and changes after electroconvulsive shock. *J. Neurochem.* **1985,** *45*, 1341-1348.

Lindefors, N., Amberg, G., Ungerstedt, U. Intracerebral microdialysis: I. Experimental studies of diffusion kinetics. *J. Pharmacol. Methods.***1989**, *22*, 141-156.

Lönnroth, P., Jansson, P. A., Smith, U. A microdialysis method allowing characterizationof intercellular water space in humans. *Am. J. Physiol.* **1986**, *253*, E228-E231.

Menacherry, S., Hubert, W., Justice, J. J. . *In vivo* calibration of microdialysis probes for exogenous compounds. *Anal. Chem.* **1992**, *64*, 577-583.

Morton, D. B., Griffiths, P. H. M. *Vet. Rec.* **1985**, *116*, 431-436.

Morrison, P., Bungay, P., Hsiao, J., Mefford, I., Dykstra, K., Dedrick, R. Quantitative Microdialysis. In: *Microdialysis in the Neurosciences.* In Justice, J., Robinson, T., eds, Techniques in the Behavioral and Neural Sciences. New York: Elsevier, **1991**, 47-80.

Paxinos, G., Watson, C. *The Rat Brain in Stereotaxic Coordiantes*, 2nd edition, **1986**, Academic Press, New York.

Sandberg, M., Benveniste, H. Blood flow and glucose phosphorylation in the rat hippocampus after implantation of a dialysis probe. 7th ESN, June 12-17,**1989,** Gothenburg, Sweden.

Smith, A., Justice, J. J. The effect of inhibition of synthesis, release, metabolism and uptake on the microdialysis extraction fraction of dopamine. *J. Neurosci. Meth.* **1994,** *54,* 75-82.

Stansaas, S. Stensaas, L. The reaction of the cerebral cortex to chronically implanted plastic needles. *Acta Neuropathol. (Berl.)* **1976**, *35,* 187-203.

Stenken, J., Topp, E., Southard, M., Lunte, C. Examination of microdialysis sampling in a well characterized hydrodynamic system. *Anal. Chem.* **1993**, *65*, 2324-2328.

Tossman, U., Ungerstedt, U. Microdialysis in the study of extracellular levels of amino acids in the rat brain. *Acta Physiol. Scand.* **1986,** *128*, 9-4.

van Wylen D. G. L., Park, T. S., Rubio, R., Berne, R. M. Increases in cerebral interstitial fluid adenosine concentration during hypoxia, local potassium infusion, and ischemia. *J. Cereb. Blood Flow Metab.* **1986**, *6*, 522-528.

Wages, S. A., Church, W. H., Justice, J. B. Jr. Sampling considerations for on line microbore liquid chromatography of brain dialysate. *Anal. Chem.* **1986**, *58*, 1649-1655.

Young, A. M. J., Bradford, H. F. Excitatory amino acid neurotransmitters in the corticostriate pathway: Studies using intracerebral microdialysis *in vivo*. *J. Neurochem.* **1986,** *47,* 1399-1404.

Zetterstrom, T., Vernet, L., Ungerstedt, U., Tossman U., Jonzon, B., Fredholm, B. B. Purine levels in the intact rat brain. Studies with an implanted hollow fibre. *Neurosci. Lett.* **1982**, 29, 111-115.

Zhao, Y., Liang, X., Lunte, C. Comparison of recovery and delivery *in vitro* for calibration of microdialysis probes. *Anal. Chim. Acta.* **1995**, *316*, 403-410.

Chapter 4

Effects of Pharmacological Agents on Brain Glucose Levels and Development of a Mathematical Model to Describe Extraction Efficiencies

4.1 Introduction

In the previous chapter, it was observed that *in vivo* delivery increases at 2 μL/min perfusion flow rate, instead of showing the expected decrease. The reasons for this behavior are not known. It can only be speculated that factors such as uptake of glucose by neuronal cells, the blood brain barrier, resistance due to tissue etc. may play a role. The solution to this problem could be tackled by two approaches, first, the use of pharmacological agents to modulate the above mentioned processes and second, by mathematically modeling the biological system.

Pharmacological agents could be defined as substances that specifically act on the biological system under consideration and alter it in a specific way so that variation in the resulting levels of analytes yield specific information. In this case, glucose dynamics were studied by the use of two pharmacological agents, the glucose transport inhibitors and sodium channel blockers. As detailed in Chapter 1, Section 1.3, glucose inhibitors like cytochalasin B and phloretin act by binding to glucose transporter, GLUT1. These inhibitors could be used to block glucose transport into the brain via the BBB. The resulting dialysate levels could reveal the extent to which the BBB affects basal glucose levels. The sodium channel blocker - TTX and its role regarding neuronal activity is discussed further in this chapter.

Microdialysis was initially developed for, and has been primarily used, as a method for assessing local concentrations of various solutes of interest. However, reliable, quantitative interpretation of solute levels measured in the dialysate requires an understanding of the factors affecting the transport of the analyte of interest through the tissue to the probe. Mathematical modeling of such a system forces the researcher to identify all the variables and be able to look at the system in a detailed

manner. Models are used to predict certain outcomes of events that may be impractical to determine through experimentation.

4.2 Effect of sodium channel blockers

To examine the relationship between neuronal activity and local extracellular glucose levels, the sodium channel blocker TTX was added to the perfusion medium. Briefly, one group of rats, n=2, was stereotaxically implanted with the guide cannula and allowed to recover for 24 hours. On the day of the experiment, microdialysis probes were carefully implanted in the striatum, with the same co-ordinates as those in Chapter 3, Section 3.5. Each animal served as its own control. After the probe had equilibrated in the tissue, aCSF was perfused for 60 minutes. TTX, at concentration of 1 μM in aCSF was applied locally through the probe. The drug does not interfere with glucose detection.

The effect of TTX infusion is shown in Figure 4.2. The glucose efflux was maximally increased to 316% of baseline at 30 minutes following drug application and returned slowly to baseline values despite continuous infusion of the drug. The animals exhibited no behavioral effects with the application of the drug.

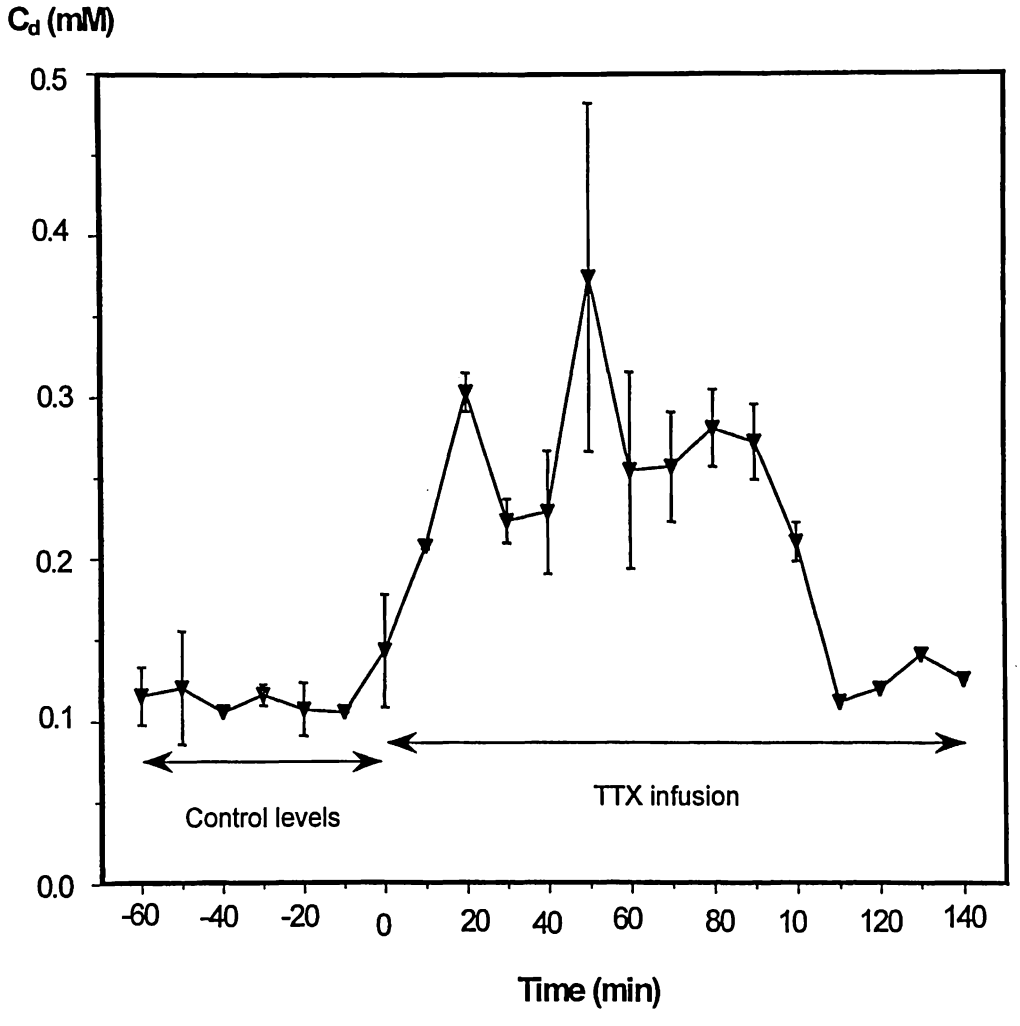

Figure 4.2 Effects of TTX perfusion on dialysate glucose levels, n=2

4.3 Effect of glucose inhibitors

Phloretin is a phenol, with a molecular weight of 274, and a competitive inhibitor of glucose transporters. It is believed to bind irreversibly to a phenol binding site in the GLUT family of glucose transporters (Betz *et al.*, 1975). It has limited solubility in aqueous solutions (0.25 mM) and has a K_I of 16 μM (LeFevre *et al.*, 1959).

Two groups of animals, n=2, were stereotaxically implanted with the guide cannula in the striatum and allowed to recover for 24 hours. On the day of the experiment,

microdialysis probes were carefully implanted in the cannula, and the first group was perfused with aCSF for initial 30 minutes at flow rate of 0.5 μL/min and the second group perfused at 2 μL/min. Samples were collected for 2 hours to establish baseline dialysate glucose levels, after which the perfusate was switched to aCSF containing 0.2 mM phloretin. Phloretin does not interfere with glucose detection. As seen in Figure 4.3, the glucose levels increased to 163% of baseline for ~1 hour. After this time period, the dialysate glucose levels dropped back to baseline despite continuous phloretin infusion. Figure 4.2, on the other hand shows negligible variation between control and infused values.

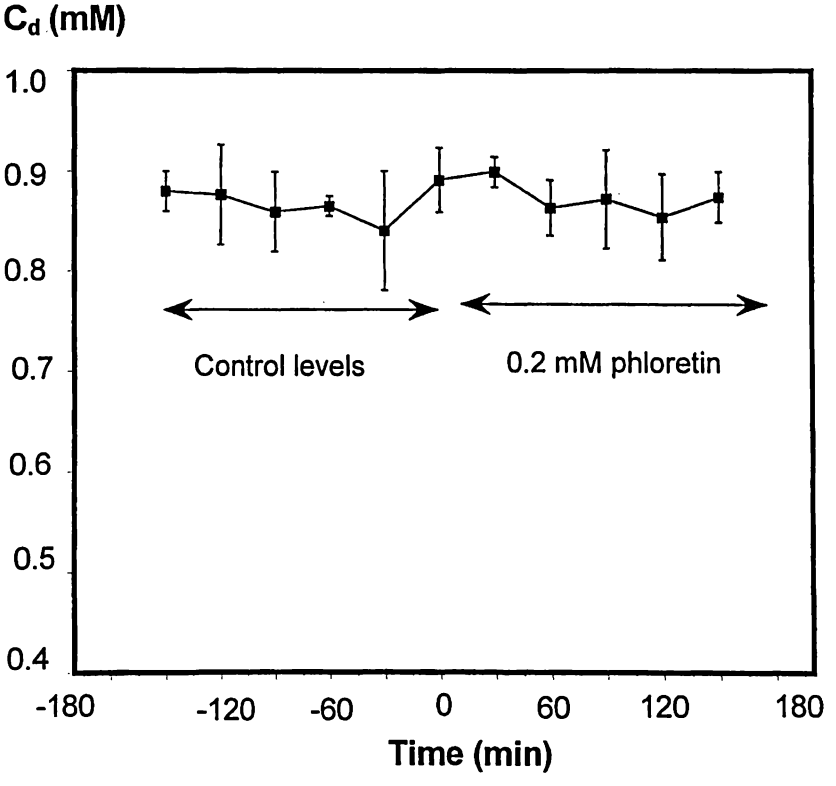

Figure 4.2 Effect of glucose transport inhibitors on dialysate glucose levels at perfusion flow rate of 0.5 μL/min, n=2

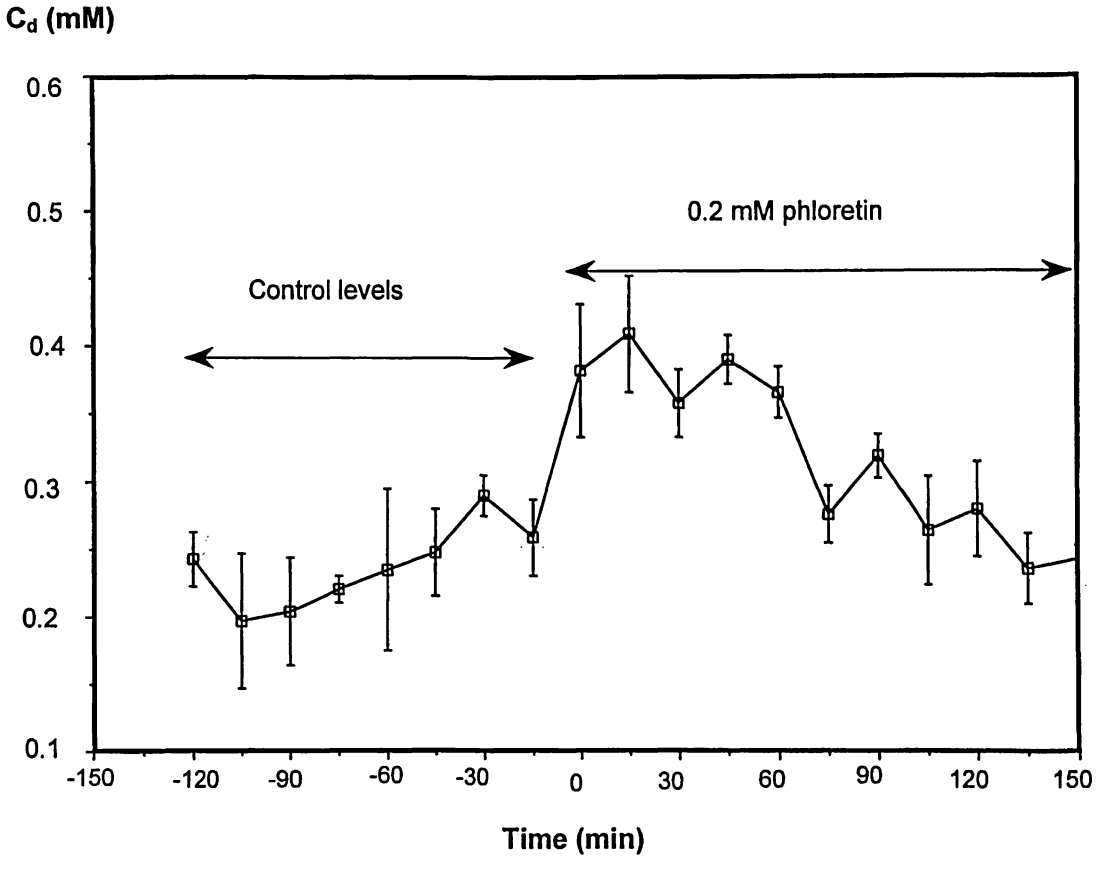

Figure 4.3 Effect of glucose transport inhibitors on dialysate glucose levels at perfusion flow rate of 2 μL/min, n=2

4.4 Development of a model to describe microdialysis experiments

Model building is a cyclical process that first begins with the formulation of a problem which describes the information that is sought by the model creator. The next step involves outlining the model. This involves hypotheses of a quantitative relationship between the input or independent variable and output or dependent variable. This relationship is the expression of the controlling process which is assumed to critically link the stimulus (input) with the response. It also involves identifying variables that are too difficult to model and formulation of necessary assumptions. The third step

involves deciding if the model is useful. In this case, it must be decided if the needed data for the model are available to make predictions. Finally, the model is tested against data and common sense. All these steps can be repeated if the data and the model do not agree or the model creator wishes to incorporate some neglected variables back into the model (Bender, 1978, Rubinstein and Firstenberg, 1995).

Various theoretical descriptions of microdialysis have shown that, for most solutes, tissue transport characteristics are much more important in determining microdialysis behavior than the characteristics of microdialysis probe (See Chapter 2, Section 2.3). In the present situation, model building was undertaken to determine concentration profiles of glucose under recovery and delivery conditions. Variables or parameters that would most affect the concentration profiles could then be identified.

A theoretical framework for describing steady-state and transient microdialysis behavior has been described by Bungay *et al.*, 1990 and Morrison *et. al.*, 1991a, b. For small solutes, the *in vivo* performance of a microdialysis probe in brain was shown to depend primarily on the behavior of the solute in tissue, and only to a small degree on the dialysate and membrane properties. The discussion to follow will therefore focus on this tissue.

4.5 Model Equations and Assumptions

The model is valid only if the following assumptions hold true. 1) The microdialysis probe is a cylinder and is assumed to have intimate contact with the surrounding tissue. Liquid layers, fibrotic layers or protein adsorption on the outer membrane are considered not to influence mass transport even if they exist. 2) Even though the concentration just outside the probe is a function of three mass transfer resistances, dialysate resistance, membrane resistance and tissue resistance, encountered by the analyte, only effects of mass transport of analyte through tissue on the concentration profile are taken into account. 3) Although axial diffusion is physically possible, it is assumed to be negligible as compared to radial diffusion. This is because the the concentration difference is greater radially. 4) Convective processes are ignored and

mass transport is considered to occur by diffusion alone. 5) Diffusion constant remains constant throughout the tissue. 6) Diffusion is considered to occur through the extracellular space. 7) The system is allowed to behave transiently. 8) Blood capillaries are considered to be evenly spaced in the tissue space, i.e. the positioning of the probe with respect to the capillaries is considered unimportant as the probe diameter is greater than the capillaries. 9) Metabolic processes, such as the hexokinase reaction are not considered. This assumption even though untrue, is justified because the K_m for hexokinase is 0.04 mM. This means that the enzyme is always saturated and therefore metabolism is considered constant. 10) Transport processes are considered to follow saturable, Michaelis-Menten kinetics.

Mass balance for the glucose model will essentially be,

$$\text{Concentration profile} = \begin{bmatrix} f(\text{transport of glucose across BBB}) + \\ f(\text{diffusion profile due to probe}) + \\ f(\text{neuronal cell uptake by GLUT3}) \end{bmatrix} = 0$$

Solving the mass balance for diffusion and reaction processes in the tissue (Bird *et al.*, 1960, Robinson *et al.*, 1986) will be

$$\frac{\partial C_e}{\partial t}(r,t) = \frac{\phi K_{m1} (C_1 - C_e)}{(C_1 + K_{m1})(C_e + K_{m1})} + \phi D_e \frac{1}{r} \frac{\partial}{\partial r}\left(r \frac{\partial C_e}{\partial r}\right) + \frac{\phi K_{m2} (C_i - C_e)}{(C_e + K_{m2})(C_i + K_{m2})}$$

Equation 4.1

In a system of ordinary differential equations there can be any number of unknown functions, but all these functions must depend on a single independent variable, which is the same for each function. Partial differential equations involve two or more independent variables, in this case, space and time. A similar equation is found in Morrison's model (Morrison *et al.*, 1991). Equation 4.1 states that the change in concentration in the extracellular fluid C_e, with respect to time, is a function of the following parameters: ϕ, the volume fraction of the extracellular space, typically considered to be 0.2 for most tissues (Nicholson, 1988), K_{m1}, the Michaelis-Menten constant for GLUT1 (K_{m1} = 7 mM, Gould and Holman, 1993), C_1 is the plasma

glucose concentration, ~8 mM, K_{m2}, the Michaelis-Menten constant for GLUT3 (K_{m2} = 1.44 mM, Gould and Holman, 1993), C_i is the intracellular glucose concentration, 2 mM. R = 1000 μm from the outer surface of the probe (Benveniste *et al.*, 1990). D_e is the diffusion constant in the extracellular space obtained by,

$$D_e = D / \lambda^2 \qquad \text{Equation 4.2}$$

Typical values of λ, the tortuosity, are 1.5 - 2 (Nicholson, 1988), D is the diffusion coefficient of glucose in water (5.6 X 10^{-6} cm^2/s).

Boundary conditions:

1) For t = 0, C_e = 2.5 mM , all r = 0 → R
2) For t > 0, $C_e = C_a$, at all r → ∞, where C_a is the concentration near the probe surface

4.5.1 Mass balance equation for recovery

In a recovery experiment, when there is no glucose added in the perfusion medium, concentration of glucose at t > 0, would be a minimum near the surface of the probe. The probe removes glucose from the tissue at a rate that is dependent on the perfusion flow rate. In such a situation, the mass balance equation is the same as Equation 4.1

4.5.2 Mass balance equation for delivery

In a delivery experiment, when 5.8 mM glucose is added to the perfusion medium, the concentration of glucose at t > 0, would be at a maximum near the surface of the probe. The probe would keep infusing glucose into the tissue at a rate that is dependent on the perfusion flow rate. The mass balance can be modified to represent the following equation,

$$\frac{\partial C_e}{\partial t}(r,t) = \frac{\phi\, k_{m1}\,(C_1 - C_e)}{(C_1 + K_{m1})(C_e + K_{m1})} + \phi D_e \frac{1}{r}\frac{\partial}{\partial r}\left(-r\frac{\partial C_e}{\partial r}\right) + \frac{\phi\, k_{m2}\,(C_i - C_e)}{(C_e + K_{m2})(C_i + K_{m2})}$$

Equation 4.3

The mathematical model derived here has several advantages and disadvantages. If the kinetic rate values are known along with *in vivo* diffusion coefficients, this model can be used instead of/along with the zero net flux method. It is simple and the solution can be obtained using standard, easily available software packages. This model allows researchers to determine which factors, such as diffusion coefficients, kinetic rate constants or uptake/metabolism will affect microdialysis dialysate values the most. In its simplest form, it allows determination of tissue concentration profiles.

As Rice *et al.*, 1985, have pointed out, there is a discrepancy of an order of magnitude for dopamine and norepinephrine associated with the calculation from *in vitro* values of the diffusion coefficient in the tissue. Therefore, it is important to determine the value of glucose diffusion coefficients in the tissue. Another parameter that will affect the concentration profiles is the volume of extracellular space ϕ. Another limitation of this model is fitting it to experimental observations. Special techniques such as autoradiography (Dykstra *et al.*, 1992, 1993) would be needed. Otherwise, any combination of diffusion coefficients or rate constants could produce model output. Confirmation by experimental output is difficult as the only parameters that can be readily measured are perfusion flow rate and dialysate concentration. It should be intuitively realized that errors in perfusion flow rate, volume fraction and *in vivo* diffusion coefficient will affect the output of the model most.

4.6 Discussion

The establishment and maintenance of ion gradients constitute a considerable proportion of the brain's energy metabolism. TTX prevents generation of action potentials by blocking the voltage gated sodium channel (Catterall, 1984). In synaptosomal preparations, TTX causes a substantial decrease in oxygen consumption (Edwards *et al.*, 1989). Also, local application of 1 μM TTX leads to a

depression of between 55 to 70% in basal dopamine and GABA levels in the striatum (Osborne *et al.*, 1991).

TTX application, which leads to a decrease in local energy requirements, resulted in an increase in extracellular glucose concentration. As the uptake of glucose across the BBB is thought to be closely linked to, if not solely determined by the rate of glucose phosphorylation, this result is surprising. This in turn implies that the link between uptake and utilization is not close as has been suggested, at least over the short duration of study (Figure 4.2). The enzyme hexokinase has a low K_m of 0.04 mM and would be saturated at brain glucose concentrations of 2.5 mM. Therefore, utilization kinetics are saturated in normal brain. TTX-induced increase in extracellular glucose slowly diminished over time, returning to baseline ~100 minutes after the drug was first applied, despite continuous infusion of the drug. As the glucose sampled by the microdialysis probes reflects a balance between supply by the BBB and uptake by the neuronal cells, changes in local cerebral blood flow might also play a role in fluctuations seen with TTX. This suggests that in the present experiments, extracellular glucose is predominantly being affected by changes in local neuronal metabolic demands, which in turn reflect the intensity of local neuronal activity. This could lead to estimates of basal glucose levels that are much higher than expected.

Glucose transport inhibitors provide another means to perturb the system selectively. Phloretin is thought to bind the phenol binding site in the GLUT family of transporters. The experiments using phloretin were carried out for two perfusion flow rates flow rates of 0.5 μL/min and 2 μL/min. As shown is Figure 4.2, there is no significant change between control and infused dialysate glucose levels at 0.5 μL/min. But when the same experiment is carried out at higher flow rate of 2 μL/min, the glucose levels upon infusion of phloretin increase to 163 % of control values and remain steady for a period of ~1 hour, followed by a return to baseline despite continuous infusion of phloretin.

This particular result can be understood by considering the tissue physiology. Neuronal cells are closest to the probe and GLUT3 transporters would be the first to be inhibited by phloretin. This prevents glucose in the extracellular space from entering the cells. Therefore, glucose levels increase immediately upon phloretin perfusion. After about 1 hour, the GLUT1 transporters on the blood vessel, which are at some distance away from the probe as compared to GLUT3, are inhibited. No more glucose enters the brain via the BBB and therefore, there is a return to control values, at least within the time frame of the experiment. At a perfusion flow rate of 0.5 μL/min, the changes are not so dramatic. One reason could be due to the amount of phloretin being infused into the tissue at 0.5 μL/min is less than the amount being infused at 2 μL/min, as the mass EE of the probe is lower at lower flow rates. This indicates that slower flow rates do not perturb the system significantly.

The two pharmacological agents illustrate that glucose levels in the brain are very closely related to neuronal cell uptake and transport via the BBB. Both these processes are saturable and follow non linear Michaelis-Menten kinetics. When a microdialysis probe in inserted in such a system, the major resistance to mass transfer is from the tissue. The ZNF calibration involves infusion of glucose, whose concentration is higher than that of the brain tissue. This is the delivery part of the ZNF plot. At faster flow rates, the mass EE is higher and therefore, more glucose is infused into the tissue as compared to the mass infused at slower flow rates. Due to this reason, depending upon the total glucose mass in the brain during a delivery experiment, which in turn depends upon the perfusion flow rate, some of the transport processes may get saturated and would therefore be perturbed. When glucose is being delivered, the highest concentration of material will be nearest to the dialysis probe. If this concentration is greater than one tenth of the value of the Michaelis constant K_m, then kinetics in that region will be non linear (Stenken, 1995). However, the kinetics will approach the linear limit further away from the probe as the concentration decreases. The argument for recovery is the opposite, the kinetics near the probe will approach the linear limit whereas at a distance from the probe, the kinetics would be non-linear. These non linearities would affect the recovery and delivery terms. This would indicate that when Michaelis-Menten describe the rates in

the tissue, the values of *in vivo* recoveries may not match *in vivo* deliveries. This is precisely what was experimentally observed in Chapter 3. Therefore, the inequality in *in vivo* recoveries and deliveries may be attributed to the non linear kinetics of glucose transport and metabolism.

The objective of this thesis was to determine the levels of glucose in the extracellular space of a freely moving rat. It is concluded that the ZNF method does not work reliably for endogenous glucose in the brain at faster flow rates due to non linear transport kinetics. At slower flow rates, the system is not significantly perturbed as demonstrated by experiments involving infusion of pharmacological agents, and therefore the ZNF method of calibration provides reasonable results. Also, since, the brain glucose levels obtained by other methods such as biosensors, *in vivo* NMR and 2-deoxyglucose are similar to those obtained by microdialysis using the ZNF calibration at flow rates lower than 2 μL/min, the brain extracellular levels are reported to average at 2.79 +/- 0.42 mM at perfusion flow rates below 2 μL/min.

4.7 Further work

The model needs to be solved using numerical techniques such as implicit finite difference method or by using commercially available software such as MATLAB 5.0. Autoradiographic techniques could be used to obtain experimental data which can then be fitted to the model. The absolute recoveries and deliveries change with perfusion flow rate. Therefore, the model needs to take into effects of perfusion flow rate.

4.8 Conclusions

The present work indicates that extracellular dialysate levels glucose levels are predominantly affected by changes in neuronal metabolic demands, which in turn reflect the intensity of local neuronal activity.

The brain microenvironment does not seem to be affected significantly at perfusion flow rates slower than 2 μL/min. Therefore, the ZNF calibration could be used in this flow regime. The basal glucose levels using this approach are reported to be 2.79 +/- 0.42 mM.

The mathematical model developed here could be used in *lieu* of the zero net flux calibration method if all parameters such as *in vivo* diffusion coefficients, kinetic rate constants and experimental data fitting could be done.

4.9 References

Bender, E. A. *An introduction to mathematical modeling*. John Wiley & Sons: New York, **1978**.

Benveniste, H., Huttemmeier, P. C. Microdialysis - Theory and application. *Prog. Neurobiol.* **1990**, *35*, 195-215.

Betz, A. L., Drewes, L. R., Gilboe, D. D. Inhibition of glucose transport into brain by phlorizin, phloretin and glucose analogues. *Biochim. Biophys. Acta*. **1975**, *406*, 505-515.

Bird, R. B., Stewart, W. E., Lightfoot, E. N. Transport phenomena, John Wiley and Sons, New York. **1960**.

Catterall, W. A. The molecular basis of neuronal excitability. *Science*. **1984**, *223*, 653-661.

Edwards, R. A., Lutz, P. L., Baden, D. G. Relationship between energy expenditure and ion channel density in the turtle and rat brain. *Am. J. Physiol.* **1989**, *257*, R1354-R1358.

Fox, P. T., Raichle, M. E., Mintun, M. A., Dence, C. Non-oxidative glucose consumption during focal physiologic neural activity. *Science*, **1988**, *241*, 462-464.

Gould, G. W., Holman, G. D. The glucose family transporter: structure, function and tissue-specific expression. *Biochemical Journal*. **1993**, *295*, 329-341.

LeFevre, P. G., Marshall, J. K. The attachment of phloretin and analogues to human erythrocytes in connection with inhibition of sugar transport. *J. Biol. Chem*. **1959**, *234*, 3022-3026.

Lowe, A. G., Walmsley, A. R. The kinetics of glucose transport in human red blood cells. *Biochem. Biophys. Acta*. **1986**, *857*, 146-154.

Morrison, P., Bungay, P., Hsiao, J. K., Mefford, I., Dykstra, K., Dedrick, R. Quantitative Microdialysis. In: *Microdialysis in the Neurosciences*. In Justice, J., Robinson, T., eds, Techniques in the Behavioral and Neural Sciences. New York: Elsevier; **1991**, 47-80.

Morrison, P., Bungay, P. M., Hsio, J. K., Ball, B. A., Mefford, I. N., Dedrick, R. L.Quantitaive microdialysis: Analysis of transients and application to pharmacokinetics in brain. *J. Neurochem*. **1991**, *57*, 103-119.

Nicholson, C. Issues involved in the transmission of chemical signals through the brain extracellular space. *Acta Morphol. Neerl.-Scand*. **1988**, *26*, 69-80.

Osborne, P. G., O'Conner, W. T., Kehr, J., Ungerstedt, U. *In vivo* characterization of extracellular dopamine, GABA and acetylcholine from the dorsolateral stiatum of awake freely moving rats by chronic microdialysis. *J. Neurosci. Methods*.**1991**, *37*, 93-102.

Rice, M. E., Gerhardt, G. A., Hierl, P. M., Nagy, G., Adams, R. N. Diffusion coefficients of neurotransmittors and their metabolites in brain extracellular fluid space. *Neurosci.* **1985**, *15*, 891-902.

Robinson, P. J., Rapoport, S. I. Glucose transport and metabolism in the brain. *Am. J. Physiol.* **1986**, *250*, R127-R136.

Rubinstein, M. F., Firstenberg, I. R. *Patterns of problem solving*, 2nd edition. Prentice Hall: Englewood Cliffs, New Jersey, **1995**.

T443

THE UNIVERSITY OF KANSAS
PERMISSION TO COPY MASTER'S THESIS FORM

This form must be completed and returned along with a copy of the thesis title page and abstract and the required two copies of the master's thesis to the Graduate Division of your school.

Please type or print legibly

PERSONAL DATA

1. Full name VRUSHALI TEMBE
   Last name
   VRUSHALI MADHAV
   first name middle name
2. Year of birth NOV 15, 1970
3. Author's permanent mailing address
   9945 LURLINE AVE, #205
   CHATSWORTH, CA 91311

MASTER'S DEGREE DATA

4. Department CHEMISTRY
5. Abbreviations for degree awarded M.S.
6. Date degree awarded 5/17/98

TITLE DATA

7. Title of Thesis Methodological Considerations of Microdialysis sampling for determination of cerebral basal Glucose Concentration in extracellular space of freely Moving rat.
8. Language of text (if other than English)

PERMISSION TO COPY MASTER'S THESIS

The award of the degree is not any way dependent upon the signing of this form.

In presenting this thesis in partial fulfillment of the requirements for a master's degree at the University of Kansas, I understand that the Library shall make its copies freely available for inspection.

By signing this form I give permission for partial or full copying of this thesis in addition to that allowed under the "fair use" provisions of the Copyright Act of 1976 (sec. 107). This permission to copy may be evoked at any time by me as author, upon proper notice to the University Libraries Interlibrary Services Department.

By not signing this form I do not give permission for partial or full copying of this thesis beyond that allowed under the "fair use" provisions of the Copyright Act of 1976 (sec. 107).

Author's Signature Vtembe Date Feb 20, 1998